

# Dissolution Testing of Powders for Inhalation

Dissertation

zur Erlangung des Grades des Doktors der Naturwissenschaften

„doctor rerum naturalium“

der Naturwissenschaftlichen Fakultät III

Chemie, Pharmazie, Bio- und Werkstoffwissenschaften

der Universität des Saarlandes

von

Sabine May

Saarbrücken

2013

Tag des Kolloquiums:	09.12.2013
Dekan:	Prof. Dr. Volkhard Helms
Vorsitzender:	Prof. Dr. Claus Jacob
Berichterstatter:	Prof. Dr. Claus-Michael Lehr Prof. Dr. Marc Schneider
Akad. Mitarbeiter	Dr. Martin Frotscher

*Lernen ist wie rudern gegen den Strom.  
Sobald man aufhört treibt man zurück.*

Benjamin Britten



---

**Table of Contents**

1. Summary / Zusammenfassung.....	2
1.1. Summary.....	2
1.2. Zusammenfassung.....	3
2. Introduction .....	6
2.1. Introduction .....	6
2.2. Background and Significance .....	8
2.2.1. The respiratory tract and the deposition of particles .....	8
2.2.2. What is dissolution? .....	10
2.2.3. State of the art: Dissolution techniques for powders for inhalation.....	10
2.3. Aim of the thesis.....	14
3. Material and Methods .....	16
3.1. Substances and surfactants .....	16
3.1.1. Budesonide .....	16
3.1.2. Substances A.....	16
3.1.3. Fenoterol HBr.....	16
3.1.4. Alveofact®.....	17
3.1.5. Dipalmytoylphosphatidylcholine .....	17
3.1.6. Tween® .....	17
3.1.7. Sodium dodecyl sulfate .....	18
3.2. Methods .....	19
3.2.1. High performance liquid chromatography .....	19
3.2.2. Solubility measurements .....	20
3.2.3. Scanning Electron Microscopy (SEM) .....	21
3.2.4. Dynamic light scattering .....	22
3.2.5. Laser diffraction.....	23
3.2.6. Budesonide-Respirose blend and determination of homogeneity .....	24
3.3. Dose collection methods .....	24

---

3.3.1.	Andersen Cascade Impactor .....	24
3.3.2.	Airbrush.....	27
3.3.3.	Aerosol generator.....	27
3.3.4.	Important pretests -Fine particle dose on membrane.....	28
3.4.	Membrane classification .....	28
3.4.1.	Contact angle measurement .....	28
3.4.2.	Membrane permeation test.....	30
3.5.	Dissolution techniques .....	32
3.5.1.	$\mu$ Diss Profiler™ .....	32
3.5.2.	Flow through cell .....	35
3.5.3.	Franz Cell.....	40
3.5.4.	Transwell® Dissolution System .....	43
3.5.5.	Paddle Apparatus.....	47
3.5.6.	Dissolution model.....	51
3.6.	Data Treatment .....	56
3.6.1.	Evaluation of Dissolution Tests .....	56
3.6.2.	Comparison of dissolution profiles.....	56
4.	Results and Discussion .....	60
4.1.	Pre - test Results.....	60
4.1.1.	Determination of LoQ, solubility and micelle size.....	60
4.1.2.	Substance classification .....	61
4.1.3.	Dose collection.....	64
4.1.4.	Membrane classification.....	67
4.2.	$\mu$ Diss Profiler™ .....	70
4.3.	Flow Through Cell .....	72
4.3.1.	Diffusion pre-tests .....	72
4.3.2.	Dissolution testing .....	73
4.4.	Franz Cell.....	80
4.4.1.	Diffusion test .....	80
4.4.2.	Dose collection and dissolution testing.....	81

---

4.5.	Transwell® Dissolution System .....	87
4.5.1.	Addition of a dissolution layer on the membrane .....	87
4.5.2.	Stirring.....	90
4.5.3.	Comparison of the two different polycarbonate membranes .....	95
4.5.4.	Surfactants.....	97
4.6.	Paddle Apparatus.....	101
4.6.1.	Stirring speed.....	101
4.6.2.	Influence of FPD on the dissolution process of Budesonide and Fenoterol ...	102
4.6.3.	Comparison of different membrane materials .....	102
4.6.4.	Equipment change .....	105
4.6.5.	Best dose collection method.....	106
4.6.6.	Comparison of different membrane holder types .....	109
4.6.7.	Influence of temperature on the dissolution process.....	111
4.6.8.	Influence of lactose .....	111
4.6.9.	Dissolution medium containing surfactants.....	113
4.7.	Dissolution Model.....	119
4.7.1.	Influence of particle mass on the membrane .....	119
4.7.2.	Influence of particle shape.....	120
4.7.3.	Influence of solubility .....	121
4.7.4.	Influence of diffusion layer thickness .....	121
4.7.5.	Influence of particle size distribution.....	122
4.7.6.	Comparison of experimental and modeled data .....	123
5.	General Discussion .....	128
5.1.	General Points .....	128
5.1.1.	Comparison of dissolution profiles with MDT and “fit factors” .....	128
5.1.2.	Wettability and Dissolution .....	128
5.2.	Is a comparison of the dissolution techniques possible? .....	129
5.2.1.	Similarities.....	129
5.2.2.	Handling.....	130
5.2.3.	Duration of experiment.....	131

---

5.2.4. Amount of dissolution medium .....	131
5.2.5. Reproducibility, discrimination power and validity .....	131
6. Summary and Outlook.....	136
7. Appendix .....	138
HPLC Methods .....	138
8. List of bibliography .....	140
<b>Scientific output</b> .....	149
<b>Curriculum vitae</b> .....	150
<b>Acknowledgements</b> .....	151

**List of abbreviations**

aACI	abbreviated Andersen cascade impactor
ACI	Andersen cascade impactor
ACN	acetonitrile
API	active pharmaceutical ingredient
BCS	biopharmaceutical classification system
cAMP	cyclic adenosinmonophosphate
CMC	critical micelle concentration
COPD	chronically obstructive pulmonary disease
DPPE	dipalmytoylphosphatidylcholine
EMA	European Medicines Agency
FDA	Food and Drug Administration
FPD	fine particle dose
FPF	fine particle fraction
HH	HandiHaler® generation 2.6 used in this thesis
HPLC	high performance liquid chromatography
ICH	International Conference on Harmonisation (of technical requirements for registration of pharmaceuticals for human use)
ICS	inhaled corticosteroid
IPC	Isopore™ polycarbonate membrane
LoQ	limit of quantification
mACI	abbreviated Andersen cascade impactor with stage extension and modified filter stage
MDT	mean dissolution time
NGI	next generation impactor
PBS	phosphate buffered saline
PC	Transwell® polycarbonate membrane
PCS	photon correlation spectroscopy
PE	polyester membrane
PEEK	polyether ether ketone
Ph.Eur.	European Pharmacopoeia
RC	regenerated cellulose membrane
RP	reversed phase
RSD	relative standard deviation
SD	standard deviation
SDS	sodium dodecyl sulfate
SE	stage extension
SEM	scanning electron microscopy
SIP	sample induction port
USP	United States Pharmacopoeia
UV	ultraviolet

**List of symbols**

$\rho$	density
$\eta_{\text{water}}$	dynamic viscosity of water at 37°C
$C_s$	solubility of drug
$C_t$	concentration of the drug in the solution at time t
$D$	diffusion coefficient of substance in the solvent
$d_{\text{aero}}$	aerodynamic particle diameter
$d_{\text{geo}}$	geometric particle diameter
$dm$	mass of solid material at time t
$dt$	time interval
$f_1$	difference factor
$f_2$	similarity factor
$h$	diffusion (boundary) layer thickness
$\bar{t}_i$	midpoint of the time interval between two sampling times
$k$	shape factor
$m$	amount of drug released
$N_e$	number of particles in a particle size fraction
$r$	radius
$R_t$	mean percent drug released at each time point for reference product
$S$	the surface area of the particles
$S_e$	the surface area of each particle size fraction
$t$	time
$T_t$	mean percent drug released at each time point for test product
$V$	volume
$V_M$	van der Waals volume
$X_e(0)$	the amount of undissolved drug in a particle size group
$X_e(t)$	the amount of undissolved drug in a particle size group e
$X_{\text{sum}}(t)$	total amount of undissolved drug at time t
$\Delta M_i$	dissolved amount of drug in the time interval

# Chapter 1

## Summary / Zusammenfassung

## 1.1. Summary

Especially for local treatment of lung diseases the respiratory tract is the target for inhalation medicines. In the future the lungs could also be entrance for inhalation therapies for systemic diseases.

Besides a tendency in development of active pharmaceutical ingredients (API) to poorly soluble substances, there is also interest in producing controlled released inhalation dosage forms. Thus, for quality control or decision support in development *in vitro* dissolution measurement would become mandatory. Therefore, appropriate dissolution techniques need to be established.

Aim of this thesis was the evaluation of different dissolution techniques and the determination of impact factors on the dissolution process. For the experiments different poor and one good soluble API as model substances were used.

It could be shown that the membrane material for dose collection of the fine particles has to be chosen carefully. For achieving a mono layer and homogenous particle distribution on the membrane different dose collection systems were tested. The most suitable is a modified Andersen cascade impactor with a stage extension allowing particle sedimentation.

Each of the tested dissolution techniques showed individual advantages and disadvantages. In summary the modified flow through cell was not appropriate, the  $\mu$ Diss and the modified Franz cell showed only a limited usability. As most suitable techniques a modified Transwell® system and the paddle apparatus with membrane holder were identified.

## 1.2. Zusammenfassung

Die Lunge dient vor allem bei Erkrankungen der unteren Atemwege als lokaler Applikationsort inhalativer Wirkstoffe. In Zukunft kann die Lunge auch als Eintrittspforte für inhaltive Arzneiformen mit systemischer Wirkung in den Fokus rücken.

Schlecht lösliche Arzneistoffe, aber auch Formulierungen mit verzögerter Wirkstofffreisetzung werden den Einsatz von *in vitro* Dissolution Techniken zur Qualitätskontrolle, aber auch während der Entwicklung erforderlich machen. Dafür ist jedoch die Etablierung geeigneter Techniken erforderlich.

Ziel dieser Arbeit war die Bewertung verschiedener Dissolutionmethoden und die Untersuchung möglicher Einflussfaktoren auf den Auflösprozess. Mit Hilfe schlechtlöslicher und einem gut löslichen Wirkstoff sollten die Techniken untersucht und die Stärken und Schwächen analysiert werden.

Es konnte gezeigt werden, dass das Membranmaterial, auf dem der Feinanteil abgeschieden wird, sorgfältig ausgewählt werden muss. Zum Erreichen einer gleichmäßigen einschichtigen Partikelbelegung wurden verschiedene Systeme untersucht. Es wurde ein modifizierter Andersen Kaskaden Impaktor mit einer Stageverlängerung, die das Sedimentieren der Partikel ermöglicht, als am geeignetsten identifiziert.

Jede der getesteten Dissolutionmethoden wies Vor- und Nachteile auf. Zusammenfassend ist festzuhalten, dass die modifizierte Durchflusszelle ungeeignet ist und  $\mu$ Diss und modifizierte Franz Zelle nur bedingt einsetzbar sind. Das Transwell® System und die Paddleapparatur mit Membranhalter haben sich als sehr gut geeignet erwiesen.



## Chapter 2

### General Introduction

## 2.1. Introduction

In the past inhalation medicine has focused on the treatment of lung diseases, like chronic obstructive pulmonary disease (COPD) or asthma as the only target [1]. The systemic effect of inhalation medicine has been reserved for anaesthetic gases [2] over years. A few years ago a paradigm shift to inhalation therapy for systemic diseases has been started [3]. The first break through for treatment of a chronic systemic disease due to oral inhalation was the inhaled insulin (Exubera®, Pfizer, New York, USA) [2] which was available on the US - market from 2006 to 2007 [4].

The respiratory tract offers optimum conditions for systemic delivery of medicine due to a large surface area with a good epithelial permeability, optimum blood perfusion, low concentration of drug metabolizing enzymes and the avoidance of the first pass effect [2,5,6]. Furthermore, the lung as systemic entry to the human body is useful if the API is not bioavailable after e.g. oral dosing or due to rapid onset of action [7].

Over the years development of inhaler and powder technology has been advanced and a reproducible pulmonary deposition, also in the deeper lungs is possible [4,8]. Consequently, *in vitro* tests for inhaled formulations focused on the aerodynamic size of inhaled particulate formulations containing active pharmaceutical ingredient and excipients so far [9,10]. However, the fate of substance particles after deposition is still unclear [11]. It is evident, that small hydrophobic molecules are absorbed very fast and the solute is transported across the epithelium with usually good bioavailability [11,12]. But very low water soluble substances may have decreased absorption [11] due to delayed dissolution. However, for bioavailability of active pharmaceutical ingredients (API), either local or systemic, it is necessary that the particles are dissolved in the small volume of aqueous fluid (10 - 20 ml/100 m<sup>2</sup>) in the respiratory tract [13,14]. Furthermore, the development of new pharmaceutical actives tends to poorly soluble substances [15]. In addition, the idea of local treatment of lung diseases like tuberculosis, pulmonary aspergillosis or cancer with controlled released drugs, requires knowledge about the dissolution processes [3,4,16,17]. Therefore, *in vitro* dissolution testing of inhalation powders could be used as meaningful selection tool in inhalation substance development and for quality control. Thus, despite other factors, dissolution of particles in the lung might be different from those of the bulk material during a dissolution test [11]. Nevertheless, the *in vitro* dissolution test might help to understand how the substance might dissolve following deposition in the respiratory tract [18].

In all pharmacopeias *in vitro* dissolution testing of solid and semi-solid dosage forms are standardized test methods [19]. It is well established for quality control testing as well as for prediction of *in vivo* drug release [20]. In some special cases even a correlation between *in vitro* dissolution profiles and *in vivo* pharmacokinetic data [21] and an abbreviated new drug

approval is possible [21,22]. Presently, no pharmacopoeia or other regulatory requirements for dissolution test method for powder for inhalation exist [20]. An evaluation of *in vitro* dissolution tests for inhalation dosage forms was performed by the *Ad Hoc* Advisory Panel of the USP in 2008. They concluded that there is no evidence that dissolution was “kinetically and/or clinically crucial for currently approved” inhalation dosage forms [13]. Nevertheless, in recent years there has been an academic as well as an industrial interest in the development of a suitable *in vitro* dissolution test for determining dissolution of powders for inhalation [20,23].

If local or systemic treatment with low water soluble substances should be also successful in the future, it is necessary to know not only about the aerodynamic particle behavior but also about their dissolution *in vitro* as well as *in vivo*.

## **2.2. Background and Significance**

### **2.2.1. The respiratory tract and the deposition of particles**

#### **2.2.1.1. Anatomy**

The respiratory tract's main function is exchange of oxygen from the alveolar gas into the pulmonary capillary blood and carbon dioxide exchange vice versa [24].

The respiratory tract could be separated into two main parts, the upper and lower lung. All together the lung could be splitted into 23 generations from the trachea to the alveoli. The upper part is divided into the head airway region with nose, mouth, pharynx and larynx, and the tracheobronchial region from the trachea to the terminal bronchioli. Its main functions are warming and humidifying of air, and to retain foreign material to protect the lower lung. The lower lung is the pulmonary or alveolar region where the gas exchange takes place. [24-26]. The respiratory tract is characterized by a thin epithelium, large surface area ( $> 100 \text{ m}^2$ ), low enzymatic activity, and a rich blood supply [27]. In the respiratory tract numerous cell types are existent. The airway epithelium is pseudostratified and mainly contains ciliated cells, goblet cells and Clara cells [28]. The alveolar epithelium in contrast shows a different morphology. It consists of pneumocyte cells type I and II [26,28]. The type II cells produce lung surfactant. The type I cells create due to their structure the large surface area of the respiratory region [26]. The pH of the respiratory tract depends on the health conditions of the human lungs and a link between pH and airway function and disease was found. In healthy humans the pH of the airway surface liquid is described to be between 6.6 [29] and 7.1 [30]. Humans who are suffering on chronic bronchitis or other diseases have an increased average tracheobronchial pH of 7.7 [29].

#### **2.2.1.2. Particle deposition**

Fate of particles after inhalation either as medicine or as environmental aerosol depends on the particle properties [6,26,31], airway geometry, and inhalation velocity [6,31]. More than 90% of particles with an aerodynamic diameter larger than  $10 \mu\text{m}$  are deposited in the oropharynx [32]. The critical aerodynamic diameter for reaching the lungs is supposed to be  $< 5 \mu\text{m}$  [33]. The most important particle deposition mechanisms are impaction, sedimentation, and diffusion (Figure 2.1). A minor part plays interception and electrostatic deposition [25,31,32].

Crucial for deposition of aerosol particles  $> 3 \mu\text{m}$  is the incapability of following the change of direction of the airstream at the crotches. Due to their inertia these particles follow a short distance their primary direction and impact on the airway walls. Particles contacting the airway walls are trapped and could not reenter the airstream [25,31,32]. For lung disease treatment the most desirable deposition mechanism is settling due to gravitation in the bron-

chiols and alveols [31]. The relevant diameter for settling is depending on literature between 0.5 – 4  $\mu\text{m}$  [25,31,32]. For the smallest particles (< 1  $\mu\text{m}$ ) diffusion in all room directions takes place due to Brownian molecular motion [34].

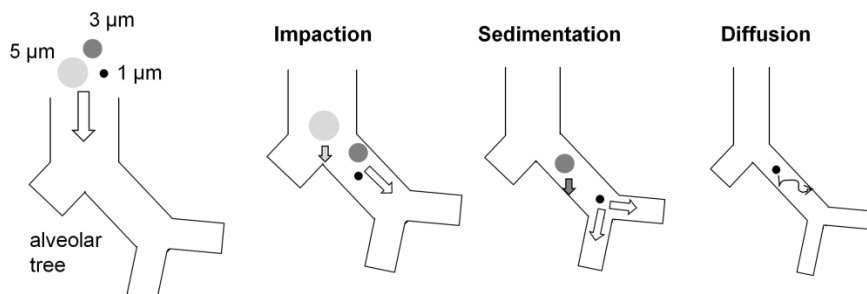


Figure 2.1: Schematic drawing of the most important particle deposition mechanisms in the lung modified from [35]. Impaction takes place for particles > 3  $\mu\text{m}$ , sedimentation for particles with a diameter of 0.5-4  $\mu\text{m}$ , and diffusion for particles < 1  $\mu\text{m}$ .

### 2.2.1.3. Defense mechanisms of the lungs and consequences for substances

The human respiratory tract is a highly complex organ with the function of filtering the inhaled air [7]. Therefore, the lungs have very effective defense mechanisms against aerosol hazards [25] like medicinal particles, pollutants, and dusts. These clearance mechanisms are interacting with the deposited particles and reducing the time for drug dissolution. The epithelium cells in the upper lung are covered with a thick mucus layer (8-15  $\mu\text{m}$ ) [11]. This viscoelastic layer is on top of the beating cilia [36,37] which transport the mucus and entrapped particles with a continuous flow of 3-35 mm/min out of the lungs. Then, the transported mucus and particles are swallowed at the larynx [26,37]. In the human respiratory tract 30-65% of epithelium is covered with ciliated cells [6]. The cilia are hair-like appendages with a central axoneme. This cytoskeletal structure consists of a bundle of microtubules, which are moved due to ATP depletion [6]. The resulting beating or movement of the cilia is coordinated and rhythmic [38]. Moreover, the mucus layer could be divided into an upper gel layer and lower few micrometers thick periciliary layer, with a low viscosity [6,26]. The mucus, a complex fluid of 3% mucus glycoprotein in 90-95% water [6,26], is continuously secreted by goblet cells and subepithelial adenocytes [24,26]. It acts as a chemical and physical barrier to particle diffusion [11] and hinders penetration [39]. Furthermore, the mucus distribution over the respiratory tract is heterogeneous especially concerning the thickness and surface coverage [6,38]. The time frame for particle dissolution before clearing is quite short in the upper lung. The maximum clearance time described in literature for the upper lung is around 24 h [40]. Only particles which are deposited at the edge of the mucus layer undergo the elimination [6].

In the lower or peripheral lung instead of the mucus coverage an ultra thin film of alveolar lining fluid covers the cells. After particle deposition and dislocation a so called lung opsonisation takes place: the particles are coated with lipids and surfactant proteins for enticement of macrophages [36,40-42]. The macrophage are very flexible in "site of operation" due to amoeboid movement [26]. Hence, in the lower lung phagocytosis by macrophages is the predominant clearance mechanism [11,26]. The clearance time in the peripheral lungs takes place in between days, weeks or even month [40].

However, in literature are also descriptions of the failure of the lung defense mechanisms. For a sufficient amount of inert ultra fine charcoal particles inflammation of interstitium and bronchial epithel is described, due to the low water solubility of the charcoal [32]. Furthermore, the shape plays an important role for phagocytoses by macrophages. A very popular example are asbestos fibers which could reach the alveoli but due to the long fibers macrophages can not phagocytose them [32]. Hence, the fiber stays in the alveoli resulting in chronic lung diseases or lung cancer [43].

### **2.2.2. What is dissolution?**

There are several possible formulations to define dissolution. In the most simple one „Dissolution is the process by which a solid substance enters the solvent phase to yield a solution” [44]. More detailed, dissolution is a minimum two step process with heterogeneous interactions between the phases. In the first step molecules from the solid phase are removed and form solvated (in the case of water hydrated) molecules at the solvent-solid phase. In a second diffusion / convection controlled step, these solvated molecules are transported to the bulk solution [44,45]. This mass transfer during the dissolution process is influenced by hydrodynamic as well as thermodynamic effects. For poorly soluble substances the mass transfer is mainly controlled by diffusion and / or convection [44]. Several factors influence the dissolution process, like the exposed surface and their structure, the wettability of the substance particles, the temperature, the stirring speed and the surrounding concentration of already dissolved substance in the medium [46]. From the more pharmaceutical point of view “dissolution is an important factor of drug bioavailability” [46]. Therefore, dissolution testing is an important tool of quality control for dosage forms, because differences in dissolving properties could result in large blood level differences [44,46].

### **2.2.3. State of the art: Dissolution techniques for powders for inhalation**

Unless now no pharmacopeia in vitro dissolution test for powders for inhalation exists. Nevertheless, in literature dissolution methods for powders for inhalation are described and already two reviews are published [1,20] but actually no technique has been adopted [17]. In the following the current state of the art will be described.

In 2000, McConville et al. described a modified twin stage impinger for testing their controlled release formulations for inhalation. Below stage 1 a 300 ml water reservoir was added. At the connection area between the reservoir and stage 1 the glass bottom was removed and a brass mesh inserted. On the mesh the deposited particles (6.4 - 10  $\mu\text{m}$ ) formed a gel layer and dissolution could take place. The dissolved particles diffused through the mesh in the acceptor medium. In a closed loop set up the dissolution medium was pumped through the reservoir into a spectrophotofluorometer for concentration measurements [18].

A different approach was from Davies and Feddah, who tested several inhaled corticosteroids (ICS) with an adapted flow through cell. With the flow through cell they wanted to differentiate between different formulations and provide information about the rate of release in quality control and development. For this purpose, first the substance powder was deagglomerated on a fiber glass membrane using an Andersen cascade impactor (ACI). The glass fiber membrane was covered with a cellulose acetate membrane filter with a pore size of 0.45  $\mu\text{m}$ . The membrane sandwich was then placed into a stainless steel filter holder with a small inlet and outlet tubing [19]. In literature this flow through cell set up is also described with the use of the next generation impactor (NGI) as dose collection method [47].

An approach between Franz cell and flow through cell is the horizontal diffusion cell. Thereby a nylon membrane with substance particles on top was clamped between two acrylic sheets. In the acceptor compartment a magnetic flea stirred the dissolution medium [48].

Further approaches used the paddle apparatus (USP apparatus 2) [3,49] or the USP apparatus 1 (basket apparatus) and weighed the powder directly into the vessel or basket, without deagglomeration step [50,51]. In a further test, the powder was filled into gelatin capsules. Afterwards the capsule was placed with a sinker on the vessels bottom and dissolution test was started [52].

Salama et al. compared dissolution of controlled release particles with USP apparatus 2 (paddle), adapted apparatus 4 (flow through cell), and Franz cell. The substance was directly weighed into the vessel or on a nitrocellulose membrane (0.45  $\mu\text{m}$ ), without any aerodynamic classification. The comparison of the dissolution profiles was performed with similarity and difference factor. Further the release kinetics were determined. It was found, that Weibull function best describes the release profiles. Regarding the Franz Cell Higuchi release kinetic was well fitting, suggesting a wetting and diffusion mechanism [3]. However, the usage of Higuchi model beside ointments is critically [53].

A different approach was described by Son et al.. They use the paddle apparatus and a special membrane holder. First the particles were aerodynamically classified on a polycarbonate membrane (pore size 0.05  $\mu\text{m}$  and 1  $\mu\text{m}$ ) with a NGI. The particles on the membrane were covered with a second pre soaked membrane and placed into a modified histology cassette [54]. In a second publication the whole set up was more sophisticated. In the NGI a remova-

ble dissolution cup was inserted. After dose collection the dissolution cup was removed, covered with a membrane, clamped into a cassette and placed into the paddle apparatus [55]. Due to the commercial availability of the NGI dissolution cup and to its apparently simple practicality this approach is also used in different other publications [17,56,57].

Mees et al. also used the combination of NGI and paddle apparatus for their dissolution test of powders for inhalation. In contrast to the study of Son et al., a stainless steel filter was placed directly above the nozzles in the NGI [58].

The above described techniques used all large amounts of dissolution medium, from 150 ml [54] up to 300 ml [17,18,55-57,59] or even 1000 ml [3]. The 1000 ml approach is orientated on dissolution tests for solid and semi solid dosage forms [60], 150 ml and 300 ml are chosen more or less randomly, for example Son et al. used a mini dissolution apparatus [54] or because it was described in a pioneering publication [59].

A quite different approach with a very low amount of dissolution medium was first described by Arora et al.. Instead of the "classical" dissolution techniques like paddle apparatus, flow through cell, or Franz cell, in their publication the usage of a Transwell® system for determining dissolution properties of different inhaled corticosteroids was described. The particles were collected on polyvinylidene fluoride filters on the impaction plates of the ACI. After dose collection the filters were placed face down on the polyester Transwell® membrane [61]. More sophisticated approaches are the usage of a stirred acceptor medium [62] and dose collection directly on the Transwell® membrane [63,64]. Furthermore, the combination of a Transwell® insert with the larger acceptor compartment of the Franz Cell is described [64].

Commonly, concentration measurements for determining the dissolution profiles were performed by HPLC analysis of sampled fractions or online UV / Vis detection. By using a membrane the remaining particles were rinsed after the dissolution test for determining the 100% amount [20] of applied particles.

As described above several different membrane materials (e.g. polycarbonate, cellulose acetate) with a pore size from 0.05 µm up to 1 µm were used. The most common pore sizes were 0.4 µm and 0.45 µm, respectively [20].

The used dissolution media vary strongly and are used with or without the addition of surfactants. For overcoming the problem of non sink conditions [57], due to low solubility of substances and a limited amount of dissolution media, in a couple of publications surfactants above the critical micelle concentrations were used. Beside the artificial polysorbate (Tween®) 80 [52,55] and sodium dodecyl sulfate (SDS) [57,58,62] also dipalmytoylphosphatidylcholine (DPPC) [19,47,55,59] was used. As dissolution medium with low or even no buffering capacity water [18,19] or simulated lung fluid [17,19,47,55,59] were used. A higher buffer capacity have phosphate buffers [3,55,56,61] or physiological buffered solution as described in the European Pharmacopoeia 7.2 [57]. The pH of dissolution media ranged be-

tween 6.8 - 7.4 [20] and thus is in the physiological range as described above. The described dissolution experiments were performed at 37°C, to mimic human body temperature [20]. Mechanistically the techniques are based on dissolution – diffusion processes when a membrane is used or only dissolution in set ups where API formulation or powder is directly placed into the dissolution medium.

In literature most publications in the field of inhalation dissolution required sink conditions, as it is claimed for solid and semi – solid dosage forms [1], for the testing of powders for inhalation without further explanation. Sink conditions ensure no “significant modifying effect” of the already dissolved substance on the dissolution rate of the remaining API [10]. In literature several definitions of sink conditions could be found. For dissolution testing of solid and semi – solid dosage forms the United States Pharmacopeia (USP) defines a three fold greater amount of dissolution medium as it is required to form a saturated solution of the substance [65]. In the European Pharmacopeia sink conditions “normally occur in a volume of dissolution medium that is at least 3 - 10 times the saturation volume” [10]. In a further definition the API concentration in the dissolution medium should not exceed 20% of the saturation solubility [61]. In the strictest definition found in literature the border of API concentration in the medium is 10% of saturation solubility [31] for having sink conditions. In the thesis poorly soluble but not extreme poorly water soluble substances were used, hence the strictest sink condition limit is useable.

In conclusion for the development of a suitable dissolution technique for powders for inhalation first the powder has to be classified aerodynamically for example on a membrane. Without a deagglomeration step the micronized powder is agglomerated and the particle diameter is larger than the inhalable fraction ( $< 5 \mu\text{m}$ ). The membranes pore size should be small enough that substance particles could not leave the membrane without dissolving, but large enough that solved molecules could pass the membrane. Additionally, the membrane should not hinder diffusion, because dissolution of substance is under investigation. Furthermore, the dissolution medium should have a sufficient buffer capacity, temperature should be set to 37°C and the pH should be in the physiological range. In addition, amount of substance or amount of dissolution medium should be chosen in the way, that sink conditions are provided. In this thesis the strictest definition of sink conditions (10% of saturation solubility) is utilized. Moreover, the use of surfactants in dissolution medium could be useful. Because several different dissolution techniques are described an overall comparison might be meaningful.

### 2.3. Aim of the thesis

The main motivation of this thesis was the fact that there is still no standard dissolution technique for dissolution testing of powders for inhalation. Whereas other research groups in this field focus either on comparison of different dissolution techniques without aerodynamic classified powders or uses aerodynamic classified substances but only one dissolution test set up, it was decided to combine the two different approaches. To date, no study has been performed to investigate this topic for powders for inhalation. Therefore, the major aims of this thesis were:

- 1) To evaluate the most suitable dissolution techniques for powders for inhalation using model substances.
- 2) To identify important impact factors on the dissolution process, for example membrane material, dose collection method and use of surfactants in the dissolution medium.
- 3) To evaluate a theoretical model to predict dissolution profiles of powders for inhalation and compare the model with experimental data.
- 4) To compare the used experimental techniques to each other.

Out of focus were the following aspects:

- To test or use simulated lung fluid, because of its low buffer capacity. For developing a new *in vitro* dissolution technique a higher buffer capacity of dissolution medium is much easier to handle. Usage of simulated lung fluid will be the next step.
- To perform an *in vitro in vivo* correlation. Therefore, a dissolution method needs to be established and *in vivo* data are necessary.

# Chapter 3

## Material & Methods

### 3.1. Substances and surfactants

#### 3.1.1. Budesonide

Budesonide is a glucocorticoid steroid which is used in the rhinology or for local treatment (inhalative) of asthma [66]. Like cortisol or other cortisol derivatives Budesonide is a strong anti-inflammatory medicine and reduces the inflammatory changes of the mucous membranes. Furthermore, Budesonide reduces the mucus production and the corrosion of epithelial cells, increases the mucociliary clearance, stabilizes the mast cells and shows an enforced effect of beta sympathomimetics, due to an enlarged expression of beta receptors. Due to the small absorption of swallowed Budesonide and a large first pass effect, only small systemic adverse effects are possible if Budesonide is used inhalative [67,68]. In the asthma treatment guidelines Budesonide among others is the treatment of choice for long term control [69].

Budesonide was chosen as model substance because of its low water solubility. The literature solubility in an aqueous medium is 23 µg/ml [19]. The substance used for experiments in the PhD thesis was purchased from Cipla, India and micronized via jet milling.

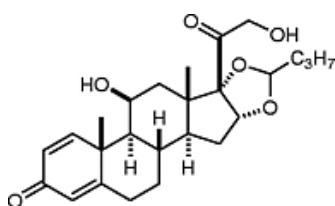


Figure 3.1: Chemical structure of Budesonide [70]

#### 3.1.2. Substances A

Substances A, current active pharmaceutical ingredients (API) in the research pipeline, were obtained from Boehringer Ingelheim (Ingelheim, Germany). Substance A dibromide and crystalline base were micronized via jet milling. For producing the amorphous base, the free base of Substance A was spray dried. The substances were chosen due to different modifications of the same substance with supposed different solubility.

#### 3.1.3. Fenoterol HBr

Fenoterol Hydrobromide (Fenoterol) is a short acting beta sympathomimetic agent for inhalation. In asthma treatment the bronchodilator is used as quick relief medication [69]. As a result of the fast onset of action, Fenoterol HBr is inhaled in case of an acute asthma attack. Due to stimulation of beta 2 receptor, the concentration of cAMP in the respiratory muscle cells is increased [66], resulting in a decreasing  $Ca^{2+}$  concentration in the airways' smooth musculature and a relaxing of the airways [67,68]. Furthermore, the mucociliary clearance is increased because of increased beating frequency of the cilia.

Fenoterol HBr has a high aqueous solubility [66] and was chosen as counterpart for the substances with low solubility and as a positive control. The substance was obtained from Boehringer Ingelheim and micronized via jet milling.

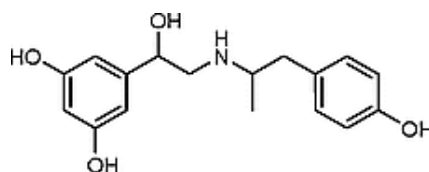


Figure 3.2: Chemical structure of Fenoterol [70]

Table 3.1: Physicochemical characteristics of substances

	Budesonide	Fenoterol HBr	Substance A free base	Substance A dibromide
chemical formula	C <sub>25</sub> H <sub>34</sub> O <sub>6</sub>	C <sub>17</sub> H <sub>21</sub> NO <sub>4</sub> HBr	-	-
molecular weight [g/mol]	430.53	384.3	683.8	-
log D	3.2 [71]	-0.9 [72]	2.4	-
soluble in	ACN	buffer	ACN	buffer

#### 3.1.4. Alveofact®

Alveofact® (dry powder ampoule) consists of 50.76 - 60.00 mg of a phospholipid (66 µmol) fraction from bovine lungs. The medicine, only available by prescription, is used as preventive medicine at prematurely born children with a high risk of a respiratory distress syndrome. Alveofact® was obtained from Boehringer Ingelheim.

#### 3.1.5. Dipalmytoylphosphatidylcholine

Dipalmytoylphosphatidylcholine (DPPC) is a native phospholipid and with approximate 40% the main component of lung surfactant. Furthermore, DPPC is able to reduce the surface tension near zero [73]. The substance was purchased from Lipoid (Ludwigshafen, Germany).

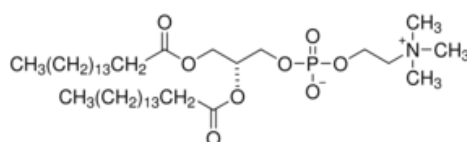


Figure 3.3: Chemical structure of DPPC [74]

#### 3.1.6. Tween®

Tween® is the trade name of mixtures of esters from polyoxyethylen sorbitan and higher fatty acids (C<sub>12</sub> to C<sub>18</sub>). They belong to the class of non ionogenic o/w emulsifying agents and act for example as solubiliser for slightly aqueous soluble or non aqueous soluble substances.

For pharmaceutical usage the sum of all ethylenoxide groups is usually 20 [31]. The polyoxyethylen sorbitan esters are well tolerated, almost non irritant and non toxic [66]. They are used in food, cosmetics and pharmaceutical products [75]. In the thesis instead of polysorbate always the trade name Tween® is used.

- Tween® 20 (Acros Organics, Geel, Belgien)  
esterfied with lauric acid
- Tween® 80  
esterfied with oleic acid

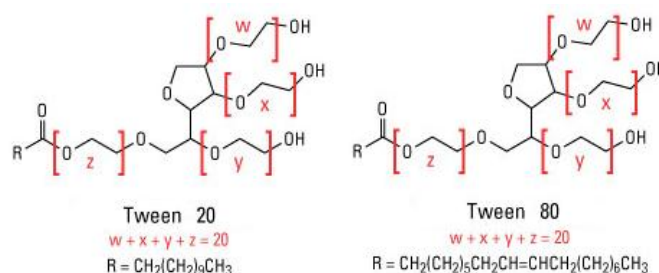


Figure 3.4: Chemical structure of Tween® 20 [74] and Tween® 80 [76]

### 3.1.7. Sodium dodecyl sulfate

Sodium dodecyl sulfate (SDS) is an anionic detergent and a very effective surfactant, which is used e.g. in ointments and cremes. It is also used for denaturing proteins and nucleic acids (SDS – Page) [66].

SDS was obtained from Karl Roth (Karlsruhe, Germany).

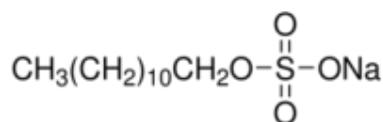


Figure 3.5: Chemical structure of SDS [74]

Table 3.2: Physicochemical characteristics of surfactants

	DPPC	Tween® 20	Tween® 80	SDS
<b>chemical formula</b>	$\text{C}_{40}\text{H}_{80}\text{NO}_8\text{P}$	$\text{C}_{58}\text{H}_{114}\text{O}_{26}$	$\text{C}_{64}\text{H}_{124}\text{O}_{26}$	$\text{C}_{12}\text{H}_{25}\text{NaO}_4\text{S}$
<b>CMC [% (w/v)]</b>	$3.3 \cdot 10^{-7}$ <sup>[77]</sup>	0.0074 <sup>[76]</sup>	0.0016 <sup>[76]</sup>	0.173-0.230 <sup>[76]</sup>
<b>molecular weight [g/mol]</b>	734	1228	1310	288

## 3.2. Methods

### 3.2.1. High performance liquid chromatography

The high performance liquid chromatography (HPLC) is a technique for separating a mixture of compounds for quantitative and qualitative analysis. HPLC depends on different chemical and physicochemical interactions of sample, column material (stationary phase) and mobile phase. The following mechanisms are often distinguished: adsorption, partition, ion exchange, size exclusion and bioaffinity.

The signal at the end of the chromatographic process can be detected e.g. by UV Vis spectroscopy and depends on the concentration of the substance. The mobile phase, e.g. a mixture of organic and non organic solvents, is pumped either isocratic or with a gradient profile through the system. The column material or stationary phase has a high surface area, normally consisting of silica particles or polymers and due to the separation mechanism defines the chromatographic system. One parameter for describing the chromatographic process is retention time (signal against time), the maximum of the substance peak on the chromatogram [31].

In this PhD thesis reversed phase (RP) chromatography for quantitative measurement of all investigated substances was performed using a LiChrospher 60 RP select B, 60x4 mm column, purchased from MZ Analysentechnik (Mainz, Germany). The column temperature was set to 40°C.

RP chromatography column material is nonpolar or chemically modified and the mobile phase is aqueous and more or less polar. Consequently, substance molecules, which are more polar, have a shorter retention time than less polar molecules. More hydrophobic molecules have a higher affinity to the stationary phase and have therefore a higher retention time [31].

The measurements were performed using Alliance system (Waters, Eschborn, Germany) with UV-VIS detector (operating at 240 nm for Budesonide, 225 nm for Substances A and 280 nm for Fenoterol). The volume of each sample injected was 10 µl. The mobile phase consisted of buffer pH 3 and Acetonitrile (ACN). The flow rate was set to 1.7 ml min<sup>-1</sup> for Budesonide and Substance A and 1 ml min<sup>-1</sup> for Fenoterol. Mobile phase degassing was performed either with helium or ultrasonic treatment for 15 minutes.

The mobile phase mixture was adapted starting from an existing HPLC method with the aim to shorten the retention time. Mobile phase composition of 60:40 (buffer/ACN) for Budesonide, 65:35 (buffer/ACN) for Substance A and 90:10 (buffer/ACN) for Fenoterol showed the best balance between retention time and peak form.

Furthermore, the limit of quantification (LoQ) of substances was determined. LoQ is the smallest amount of substance that can be reliably (suitable precision and accuracy) measured. Two different approaches based on the ICH guidelines [78] were applied: first calcula-

tion from the signal to noise ratio (10:1) and second basing on the relative standard deviation of 6 injections < 10%.

For all substances multipoint calibration with external standards was performed.

### 3.2.2. Solubility measurements

Solubility is defined as the degree, to which a substance dissolves in a solvent to make a homogenous solution [79]. The solubility of one substance is the saturation concentration in a defined solvent at a defined temperature and standard air pressure. The maximum soluble amount of a substance depends on the chemical properties of solute and solvent. The solubility of substances is influenced by particle properties like size or morphology or outer circumstances like temperature, surfactants, and pH value [31]. The European Pharmacopeia differentiates between various states of solubility. Very soluble are substances, when less than 1 ml is needed to solve one gram solute. Very slightly soluble are substances when for dissolving 1 g of substance 1000 to 10000 ml solvent is needed. If more than 10000 ml solvent is needed, substance is practically insoluble [10]. In pharmaceuticals the biopharmaceutical classification system (BCS) is well known. The BCS, based on the work of Amidon [80], classifies substances depending on their aqueous solubility and intestinal permeability into four classes. The four classes are: high solubility / high permeability (Class I), low solubility / high permeability (Class II), high solubility / low permeability (Class III), and low solubility / low permeability (Class IV). The aim of the BSC is the prediction of *in vivo* intestinal absorption due to the measurement of *in vitro* dissolution, solubility and permeability of oral dosage forms in aqueous media [81]. For improving the solubility surfactants above the critical micelle concentration (CMC) can be used [82].

Before performing solubility tests a suitable filter which does not interact with the dissolved substance has to be found. For filter determination a solution of API and dissolution medium is filtered through a Spartan 13/0.45 RC (Schleicher and Schüll, Dassel, Germany) and Millex LCR 0.45 µm membrane filter (Millipore, Molsheim, France), respectively. Of each filtered milliliter the content of substance is determined with HPLC. Aim is to reach the initial concentration with smallest amount of filtration steps. For solubility measurement the shake-flask method was used [83]. 50 fold amount of the supposed solubility of the substance is added to the solubility medium (25 - 50 ml). As solvent phosphate buffered saline (PBS) buffer pH 7.4 with or without surfactant was used. The amount of drug is sufficient to obtain a saturated solution in equilibrium with the solid phase. The flasks were stored in an overhead shaker in a climate cabinet (Espec climate cabinet, Weilburg, Germany) at 22°C and 50%r.h. for 24 h protected from light. After this time period the not solved parts are allowed to sediment. The supernatant is filtered with the previously determined filter, a Spartan filter.

### 3.2.3. Scanning Electron Microscopy (SEM)

In this PhD thesis SEM was used for visualizing substance particles and membrane material. For imaging of particles, membranes and particle distributions, large magnifications are needed. Because the resolution in light microscopy is limited due to proportionality of wavelength and resolution for these requirements scanning electron microscopy was used. In this technique at high vacuum an electron beam is emitted by thermionic emission from a wolfram cathode and accelerated due to a high voltage electric field. The electron beam is focused by condenser lenses and deflected in x and y axis by deflecting (scan) coils. This narrow - few nm thick -, focused beam of primary electrons is scanning the surface of the sample with a raster pattern.

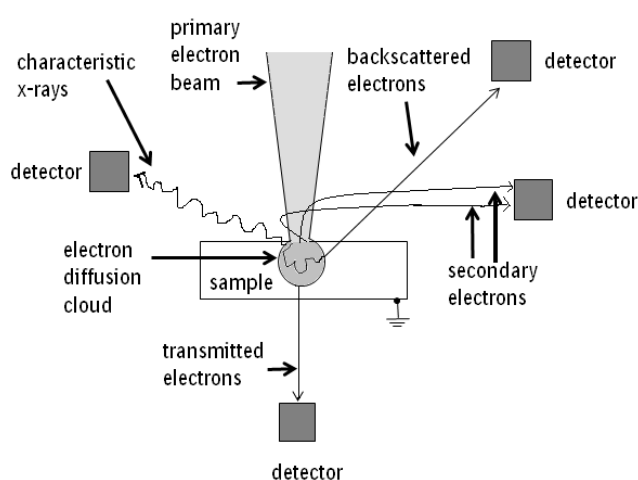


Figure 3.6: Schematic drawing of signals in the scanning electron microscopy, modified from [84,85]. Due to interaction between primary electron beam and the sample backscattered electrons, secondary electrons and characteristic x rays are detected.

The image in scanning electron microscopy is created due to the interaction between sample atoms and electron. Therefore, the detected signals contain information about sample's composition and surface topography. Depending on probe material and penetration, the signals include among others secondary electrons, backscattered electrons and characteristic X-rays. The penetration depth of the electron beam depends on the atomic number and the used acceleration voltage; the higher the acceleration voltage or the smaller the atomic number the deeper the penetration [84,85].

For non electrically conductive probes additional sample preparation is required. Without sample preparation the probe tends to charge resulting in image artifacts. For sample preparation the samples are coated with an ultrathin coating of gold or platinum by sputtering.

The Scanning Electron Microscope used in this thesis was a Supra 55 vP (Leo, Gemini, Zeiss, Oberkochen, Germany). The used acceleration voltage depends on the probe material and issue. Membranes were sputter coated with approximately 5 nm platinum with a Precision Etching Coating System ((PECS), Model 682, Gatan, München).

### 3.2.4. Dynamic light scattering

In this thesis dynamic light scattering (Zetasizer Nano Range, Malvern Instruments, Herrenberg, Germany) was used for determining the micelle size of surfactants in PBS buffer.

Dynamic light scattering or photon correlation spectroscopy (PCS) is a technique for determining particle size of small particles in suspension in a range between 3 nm to 3  $\mu\text{m}$ . With PCS particle size is not directly measured. Strictly speaking, dynamic light scattering is a method for measurement of particle velocity and flow rate above a background emission. Dynamic light scattering measures a time dependent fluctuation in the scattering intensity. Therefore, a monochromatic and coherent laser beam is focused into the suspension. The particles, depending on size, scatter the light in all directions and the signals are detected. In the medium small particles are moving faster than large particles resulting in a faster fluctuation in the scattering intensity for the small particles [31,86].

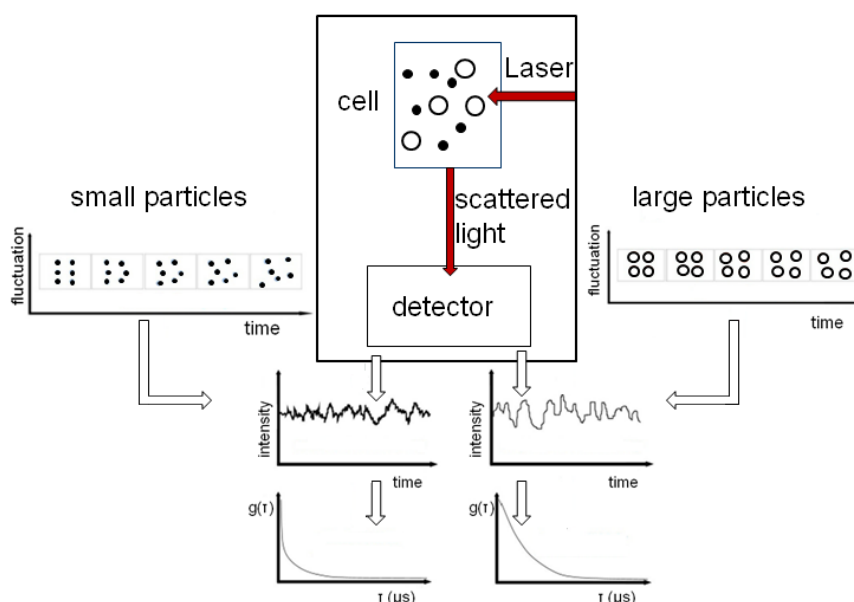


Figure 3.7: Schematic drawing of the principal of photon correlation spectroscopy modified from [86]. A laser beam is focused into the suspension, and the light is, depending on particle size, scattered in all directions. During a time interval small particles move faster than larger particles, resulting in a faster fluctuation of the scattering intensity. Software calculates from the scattering intensity at different time points the diffusion coefficient which then allows calculating particle size using Stokes - Einstein equation.

From the scattering intensity at different time points, the software calculates a correlation function ( $g(\tau)$ ). From the decrease of the slope, software calculates the diffusion coefficient and depending on the diffusion coefficient the particle size using Stokes - Einstein equation [31,86].

### 3.2.5. Laser diffraction

Geometric diameter of micronized drug powder was studied using laser diffraction (HELOS, Sympatec GmbH, Clausthal-Zellerfeld, Germany).

Laser diffraction is used for particle size analysis of particles in solid, semi-solid, liquid or aerosolized systems with a wide size range between 0.1  $\mu\text{m}$  to 9 mm. Monochromatic parallel laser light is irradiated in a measurement cell and there scattered by the particles. Dependent on particle size but independent of particle position scattered light reaches the corresponding detector. Small particles scatter the light in large angles, large particles in small angles. For spherical particles a ring structure occurs (Figure 3.8, right)

Because of several particle sizes in a probe, complex interference patterns are detected and a complex algorithm calculates the particle size “backwards” [86]. Assuming that the pattern and the intensity of all particles are identical to the sum of the individual patterns of all particles particle size distribution is calculated [87]. Mathematically the diffraction phenomena could be described by Fraunhofer or Mie theory [88]. Mie theory is used if particle size is smaller or similar to wavelength. Light is reflected or scattered in large angles. For Mie theory optical parameters of particles must be considered. A subgroup or special case of Mie theory is Fraunhofer theory. Fraunhofer theory is used if particle size is much bigger than wavelength. It describes the light scattering resulting from diffraction with small diffraction angles [89].

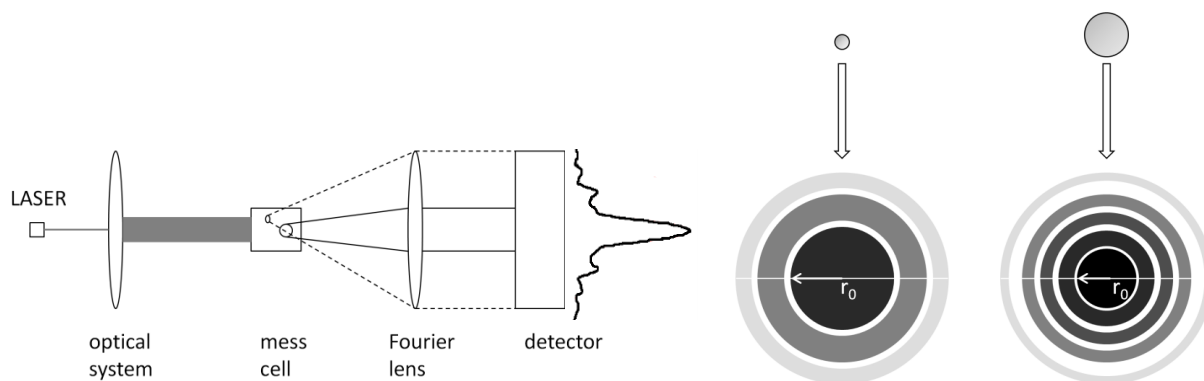


Figure 3.8: Laser diffraction

A parallel laser beam is focused into the measurement cell and light is scattered from the particles. Through a Fourier lens the light reaches the detector. The light diffraction is independent of particle position (left) [88]. One spherical particle shows a typical ring structure, depending on particle size (right) [86].

Particles were dispersed with a dry powder unit (RODOS, Sympatec GmbH, Clausthal-Zellerfeld, Germany) at a pressure of 3 bar. The powder was placed on a vibration channel and transported to the dispersion unit. As focal distance  $f = 50 \mu\text{m}$  (effective range: 0.45 - 87.5  $\mu\text{m}$ ) was chosen. Evaluation was performed using high resolution mode (Fraunhofer HRLD, Software Vision, WINDOX 5.4.0.0) under the assumption of a spherical model (shape factor = 1). For reporting median value ( $x_{50}$ ) and  $x_{10}$  and  $x_{90}$ , respectively were denoted [34]. Diameter reported for  $x_{50}$  means that 50% of particles have a smaller diameter than the de-

clared one [86]. Also interesting is Q (5.0) the percentage volume of particles with a diameter less than 5  $\mu\text{m}$ .

### 3.2.6. Budesonide-Respitose blend and determination of homogeneity

For local treatment of lung diseases with dry powder inhalers often API lactose mixtures are used. For Budesonide the blend is normally 2% API and 98% lactose. Therefore, a mixture of Budesonide and Respitose®, a fine milled lactose, was performed using a Resodyn mixer with a frequency intensity of 70% for 15 minutes or 20 minutes, respectively.

For determination the homogeneity of the mixture 5 samples were taken from different places in the powder. The samples were each dissolved in PBS buffer pH 7.4 in a 50 ml graduate flask. Concentration measurements were performed using HPLC.

## 3.3. Dose collection methods

### 3.3.1. Andersen Cascade Impactor

The respiratory tract distribution of particles inhaled depends on the aerodynamic particle sizes [33]. For classifying powders for inhalation different methods are described in the pharmacopeia [9,10]. One of the techniques for determining the *in vitro* distribution of aerodynamic fine particles is the Andersen cascade impactor (ACI). It consists of eight different stages (0-7) with decreasing nozzle size by increasing stage number. Between the stages, collection or impaction plates are placed. Depending on the decreasing nozzle size the airstream is accelerated. Particles, whose aerodynamic diameter is too large, can not follow the almost 90° deviation of the airstream and impact on the collection plate [25,33].

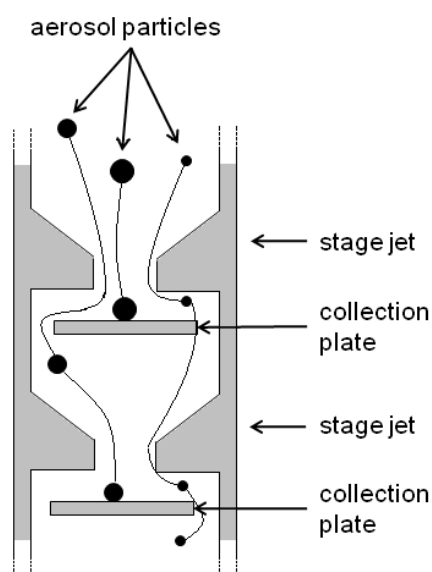


Figure 3.9: Schematic drawing for the impaction mechanism in the Andersen cascade impactor, the air stream is from up to down. With increasing stage number, the airstream speed increases and particles are impacted on the collection plates, modified from [9].

On stage 0 a pre-separator, high top and a sample induction port (SIP) are placed.

As device for dose collection a HandiHaler® (HH) (2.6, Boehringer Ingelheim, Germany) with polyethylene capsules is used. The micronized or spray dried powders are directly manually weighed into the capsules (analytical balance (AX205, Mettler Toledo, Gießen, Germany), micro balance (XP6U, Mettler Toledo, Gießen, Germany)). The amount of powder depends on ACI set up and the substances used.

The collection plates and the pre-separator are coated with a coating reagent (3% Brij 35, 14% Ethanol, 83% Glycerol) for ensuring effective impaction of the particles and avoiding bounce off effects. The USP requires for aerodynamic size distribution measurements of aerosols a 4kPa pressure drop over the inhaler and a duration that ensures “ a withdrawal of 4l air from the mouthpiece of the inhaler” [9]. Every inhaler has a device depending resistance, hence flow rate has to be adjusted to achieve the requirements. For the HH the flow rate needed is  $41.6 \pm 0.5$  l/min. After setting the flow rate an adapter is placed onto the SIP, the capsule is pierced and the HH is placed into the adapter. The valve opening time (5.77 sec) is calculated from the adjusted flow rate and the required volume of air. Due to the airflow the capsule vibrates and rotates along their long axis and the powder is released and is following the airstream into the ACI. During this process the powder is deagglomerated. For dose collection the filters of choice are either a regenerated cellulose (RC) membrane with a pore size of  $0.45 \mu\text{m}$  (Whatman, Dassel, Germany) or a polycarbonate membrane (IPC) with a pore size of  $0.4 \mu\text{m}$  (Isopore™, Millipore, Cork, Ireland). Both membranes are cut with a cutter to a diameter of 80 mm. The dose collection is performed in air conditioned rooms with a temperature of  $22^\circ\text{C} \pm 2^\circ\text{C}$  and a relative humidity of  $50\% \pm 10\%$ .

In the following sub sections special cases of dose collection with the ACI are described.

#### 3.3.1.1. Standard

For determination of the aerodynamic particle size distribution of the different substances “standard” ACI with eight stages (0-7) was used. As filter the regenerated cellulose membrane was used. The collection plates and the membrane were rinsed with 10 ml solvent (Table 3.1), pre-separator with 50 ml solvent, adapter, high top and SIP together with 100 ml and the opened capsule together with the HH with 50 ml.

#### 3.3.1.2. Abbreviated or short stack

Particles with an aerodynamic particle diameter  $< 5 \mu\text{m}$  (fine particle dose (FPD)) are supposed to reach the lungs [33]. Nichols demonstrated that the theoretical cut off points using the ACI depend on flow rate [90]. Based on the pharmacopeia method for the assessment of fine particles the flow rate is set to  $41.6$  l/min as described above. At this flow rate the cut off diameter ( $< 5 \mu\text{m}$ ) of inhalable fraction is at stage 1 [90]. Due to the interest in the whole FPD for dissolution tests, the stages 2-7 are removed and the whole FPD is collected on the

membrane on the filter stage. The fine particle fraction (FPF) in percent is calculated from the amount of substance weighed into the capsule and the FPD on the membrane.

In the following the abbreviated ACI set up is labeled as aACI.

For flow through cell dissolution testing a special pattern on the filter stage was used, for further details see chapter 3.5.2.2.

### 3.3.1.3. ACI with stage extension

To favor and allow sedimentation instead of impaction of fine particles on the collecting membrane, a stage extension (SE) between collection plate 1 (stage 1) and the filter stage is inserted in the aACI set up. The height of the stage extension was calculated depending on the volume of the abbreviated ACI. For achieving the same volume as the aACI the cylindrical stage extension has a height of 5.8 cm. For allowing sedimentation of the particles on the membrane the vacuum pump airflow profile was adapted in the way that the main aerosol reaches approximately the middle of the stage extension (pump time 0.85 s)

After the pump stop, an optimum waiting time for sedimentation was determined and the best result taken (5 minutes).

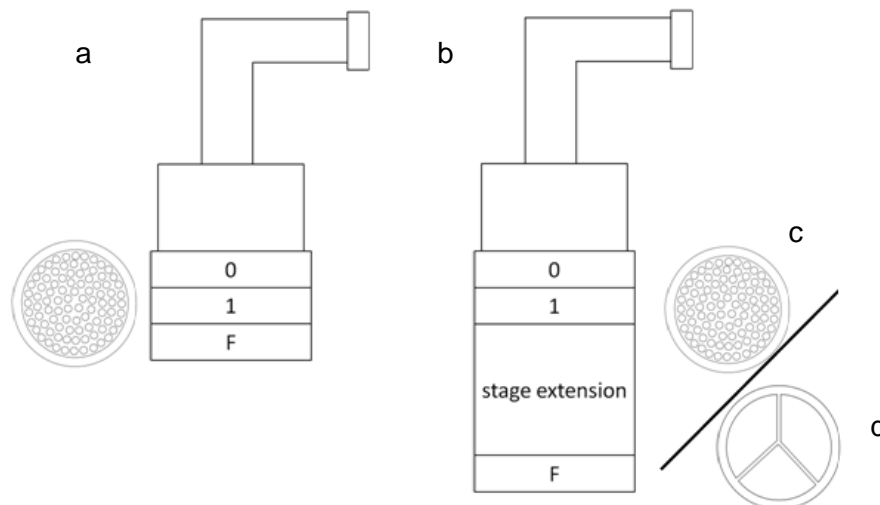


Figure 3.10: Schematic drawing of a) abbreviated ACI with normal filter stage, b) abbreviated ACI with stage extension and c) normal filter stage or d) modified filter stage, respectively.

Aim was a complete sedimentation of particles in the stage extension on the membrane. Besides the normal ACI filter stage a modified filter stage (Figure 3.10 d) was used. The modified filter stage consists of three small bars and thus changes the flow and deposition pattern. The set up with the modified filter stage is only possible using the regenerated cellulose. Due to the very thin and instable consistency of the Isopore™ polycarbonate membrane the modified filter stage is not suitable, hence the standard filter stage was used. In the following the set up with aACI, stage extension and modified filter stage is labeled mACI, the set up with aACI, stage extension and normal filter stage: aACI + SE.

### 3.3.1.4. ACI for Transwell®s

Three Transwell® inserts are placed onto the normal filter stage inside the stage extension. For avoiding drug deposition into the vacuum pump the three inserts are placed into the voids of a pattern. For avoiding drug sedimentation on the inner and outer wall of the insert a Polyetherketone (PEEK) cover is placed as cover over the Transwell® insert. This cover is very thin and does not hinder sedimentation of particles on the Transwell® insert membrane. After dose collection the PEEK cover is removed. The PEEK cover is necessary because without the cover the particles deposited on the inner and outer wall and are also rinsed after the dissolution tests, resulting in an overestimation of the amount of substance deposited on the membrane. The pump regime and waiting time are the same as described above for mACI (chapter 3.3.1.3).

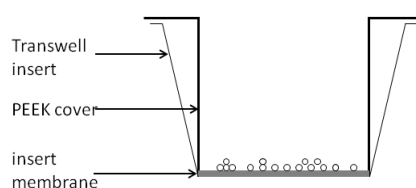


Figure 3.11: Transwell® insert with the removable PEEK cover to restrict drug deposition to the membrane.

### 3.3.2. Airbrush

A different dose collection approach is the airbrush method. Therefore, 10 mg micronized powder of the respective substances is dispersed into 25 ml antisolvent dichloromethane. The membrane is stretched onto a collection plate and the whole experiment is performed into a fume hood. Afterwards 5 ml antisolvent - substance suspension is sprayed with an airbrush onto the membrane. Finally the membrane is shortly dried.

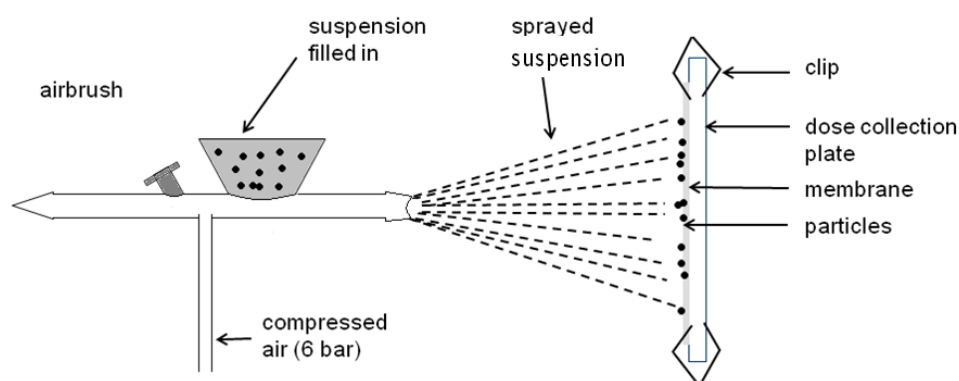


Figure 3.12: Schematic drawing of the airbrush dose collection method.

The suspension is sprayed with the airbrush onto a membrane which is fixated onto an ACI dose collection plate.

### 3.3.3. Aerosol generator

Another dose collection method is the aerosol generator, a current Boehringer Ingelheim development. Aim is a higher deagglomeration of the particles than by the use of the HH.

The substance powder is filled into a cavity and aerosolized into an aerosolisation chamber with compressed air. From there the fine dispersed powder is sucked into the mACI for dose collection as described in 3.3.1.3.

### 3.3.4. Important pretests -Fine particle dose on membrane

Important for comparison of dissolution tests is a similar mass of particles on the membrane. Therefore, before starting dissolution tests, the optimum capsule sample fill weight has to be determined for every substance and dose collection method (3.3.1.2, 3.3.1.3 and 3.3.1.4).

In addition, for the stage extension method (3.3.1.3) the optimum waiting time was determined. Therefore, the same amount of Budesonide was weighed into the capsule and waiting time was varied.

Additionally, for the flow through cell the impact of the position of the membrane in the dose collection pattern during dose collection was determined (3.3.1.2)

After dose collection the membranes were rinsed in a defined amount of solvent (Table 3.1) and concentration was measured with HPLC analysis.

## 3.4. Membrane classification

In Table 3.3 the membranes used in this PhD thesis are summarized.

Table 3.3: Membrane material

membrane	pore size [ $\mu\text{m}$ ]	pores / area [pores / $\text{cm}^2$ ]	manufacturer	techniques mem- branes used
regenerated cellulose (RC)	0.45	-	Whatmann, Dassel Germany	Flow through cell Franz cell Paddle apparatus Transwell®
Isopore™ polycarbonate (IPC)	0.4	$1.5 \times 10^8$	Millipore, Cork, Ireland	Franz cell Paddle apparatus Transwell®
polycarbonate (PC)	0.4	$1 \times 10^8$	Corning Costar, Corning, USA	Transwell®
polyester (PE)	0.4	$4 \times 10^6$	Corning Costar, Corning, USA	Transwell®

### 3.4.1. Contact angle measurement

Wetting, a phenomenon especially at the three phase boundary layer between solid, liquid, and vapor phase [91] is the possibility of substances to spread over the surface of the solid surface. The wetting and spreading phenomena are based on the cohesive and adhesive

forces. If the cohesive forces of the liquid are smaller than the adhesive forces between liquid and solid the contact angle is  $0^\circ$  and the surface is fully wettable by the liquid [92]. In particular, for dissolving of pharmaceutical active ingredients wetting of the particles is important [31]. The easiest way of measuring the wettability of surfaces is measurement of the contact angle  $\Theta$  of a droplet on a solid surface. Depending on interaction between the liquid and the solid phase, different droplet forms occur. If the contact angle is  $0^\circ$  the surface is fully wettable with the liquid, for a contact angle smaller than  $90^\circ$  the wettability is good, in the case of water as liquid this means the solid is hydrophilic. For contact angles larger than  $90^\circ$  the solid has a poor wettability; in the case of water, the solid is hydrophobic. If the solid is not wettable the contact angle is  $180^\circ$  [91]. Theoretically, contact angle measurement has to be performed on homogenous surfaces [93]. In practical contact angle measurement problems such as microscopic roughness, chemical heterogeneity and contamination of the surface [92,94], heterogeneous drop size, molecular orientation and deformation of the surface and liquid molecular transport [92] take place. All these effects lead to contact angle hysteresis which is the difference between the advancing and the retreating / receding contact angle [92,93,95]. Therefore, measurement of a static sessile drop for contact angle measurement is defective, with an accuracy of no better than  $\pm 2^\circ$  [95].

In Young's equation (Equation 3.1) [96] the equilibrium of the tangential forces of the interfaces of the three phases in the interception point is shown [91,95]. Where  $\gamma_{SL}$  is the surface tension between liquid and solid,  $\sigma_{LG}$  is the liquid vapor interfacial energy,  $\sigma_{SG}$  is the solid vapor interfacial energy and  $\Theta$  the contact angle.

$$\sigma_{SG} = \gamma_{SL} + \sigma_{LG} * \cos\theta$$

Equation 3.1: Young equation [96]

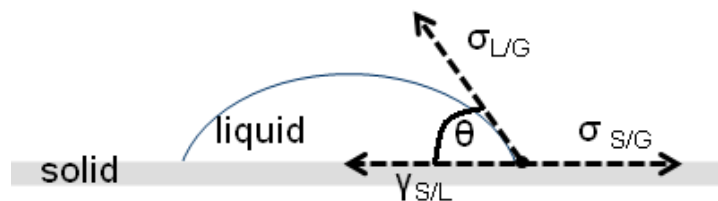


Figure 3.13: Schematic of liquid drop showing the quantities in Young's equation, where G is the vapor phase, L the liquid phase and S the solid phase, modified from [31].

For determination of the membranes' surface polarity contact angle measurement was used. The measurement was performed with water with / without 0.02% DPPC in the advancing sessile drop method at a Drop Shape Analysis (System DSA 10 MK 2, Krüss, Germany). Therefore, a drop of 8  $\mu\text{l}$  volume with a flow rate of 16  $\mu\text{l}/\text{min}$  was observed. During droplet advancing software calculated every second for 15 seconds the advancing contact angle.

The illuminated droplet is live pictured to the software by a camera vertically arranged to the sample table. For each membrane material 5 drops were performed.

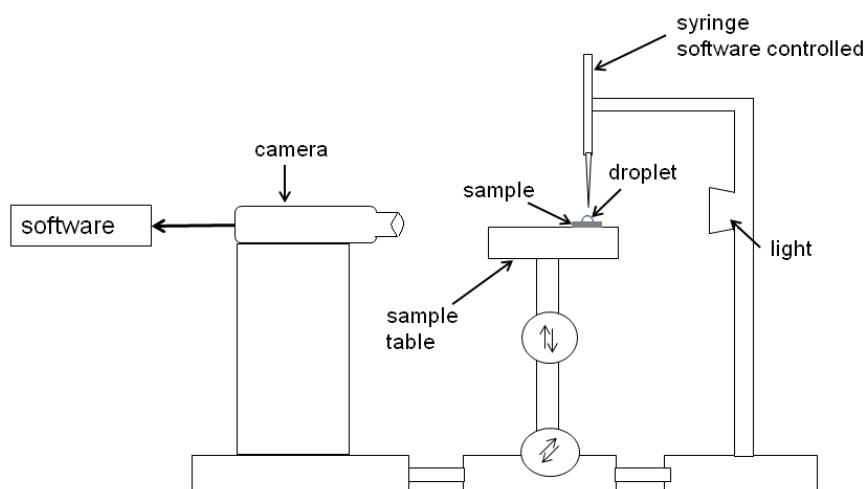


Figure 3.14: Schematic drawing of a contact angle measurement apparatus. With a syringe a droplet is placed on the sample. The sample area is illuminated. Live images are taken by a camera connected to software.

For the poorly soluble substances used in the thesis contact angle measurement was performed, too. Therefore, with a KBr press 20 mg of substance were pressed with a pressure of  $3 \cdot 10^4$  N to a small pellet. On this pellet advancing contact angle measurement with water with / without 0.02% DPPC was performed as described above for the membranes.

### 3.4.2. Membrane permeation test

For characterizing the permeability of the membranes for the test substances diluted in PBS buffer a membrane permeation test was performed. Low diffusibility of a substance dissolved in a buffer solution might influence the dissolution tests results. The tests were performed in a small glass Franz cell filled with 7.25 ml PBS buffer. Above the lower cylinder a second smaller one is placed. Between the two cylinders the membrane is clamped. The two cylinders are compressed with an external spring. Onto the membrane (permeation area approximately  $0.785 \text{ mm}^2$ ) 100  $\mu\text{l}$  of substance-buffer solution with a concentration 10  $\mu\text{g/ml}$  is placed. Stirring speed for maintaining a homogeneous mixture is set to 140 rpm. The measurements were done in a climate cabinet (Espec climate cabinet, Weilburg, Germany) at 37°C and 100% r.h.. For sampling 200  $\mu\text{l}$  of analyte containing solution is manually removed with a syringe (100 Sterican® (Braun, Melsungen, Germany) and 1 ml disposable syringe (Wicom, Heppenheim, Germany)) through the small side arm and filled into HPLC vials with micro inserts according to a defined time schedule (waiting times: 5, 10, 3 x 15, 3 x 60 minutes). The removed 200  $\mu\text{l}$  are refilled with fresh pre warmed PBS buffer. At the end of the diffusion test, the membrane is rinsed with 25 ml of solvent (Table 3.1). The concentra-

tion of substance was determined by HPLC analysis. Each experiment was performed in triplicate.

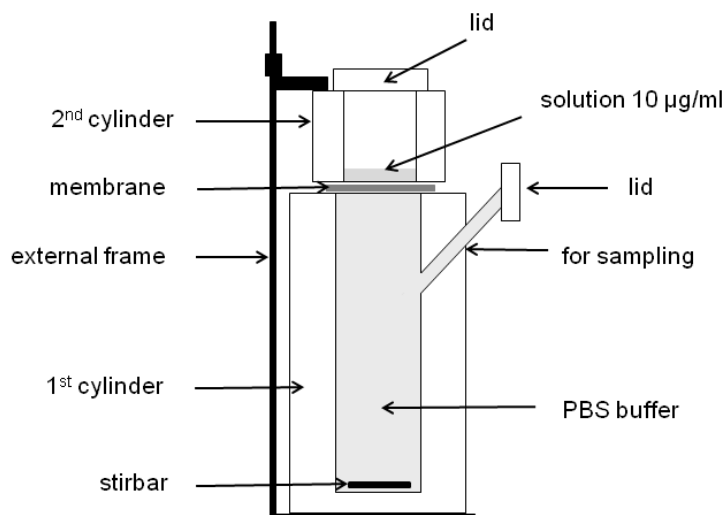


Figure 3.15: Schematic drawing of the Franz cell used for membrane permeation test.

## 3.5. Dissolution techniques

### 3.5.1. μDiss Profiler™

Fiber optic based systems for *in situ* dissolution concentration monitoring of tablets, for intrinsic dissolution rate determination or solubility measurement are well-described in literature [81,97-103]. The *in situ* measurement has several advantages i) real time measurement [98] ii) smaller time intervals of data sampling points resulting in a more detailed dissolution profile and hence the possibility of a higher discrimination ability [98,102], iii) a simplification of dissolution analysis as HPLC analysis is not necessary and the sample solute is directly analyzed by UV absorption spectroscopy [99,100,102] and iv) increased precision as improper sampling or sampling timing errors can be avoided [100-102]. Besides those advantages, several issues especially concerning the excipients and the strict dissolution testing regulatory in the pharmacopeia, especially concerning to the used apparatus, are described in literature [100,102,103]. One special case of fiber optic dissolution measurements are those with a small volume of dissolution medium. These dissolution tests are also useful in early stage of development, when only small amounts of API are available,

Currently, fiber optic systems for dissolution tests for aerodynamic classified powders for inhalation are not described in literature.

In this PhD thesis a small volume dissolution tester (μDiss Profiler™, pION, Billerica, MA, USA) with a maximum volume of 20 ml dissolution medium was used. Important difference to the other in this thesis investigated dissolution techniques is the online *in situ* UV detection of API.

The μDiss (Figure 3.16) consists of several parts, which can be divided in three main components: diode array UV-spectrometer, fiber optics and probe vessels.

The vessels are placed in a water bath heated metal block, with a small magnetic stirrer under each vessel. The fiber optics (Figure 3.17) are directly placed into the medium with API. For the simultaneous online measurement of six different samples UV light is transferred through fiber optics directly into the probe. At the end of each fiber optic a capping piece consisting of a lens, a gap (which determines the path length) and a mirror are positioned. In the lens the light is focused and sent through the liquid, reflected at the mirror again transiting the probe. In the lens transmitted light is focused and transferred to the diode array spectrometer [100]. For the μDiss profiler between different gap sizes could be selected, the more cloudy the suspension the smaller the path length should be. For low concentrations a larger path length should be used. In the following experiments no excipients were present so a gap with 5 mm was chosen

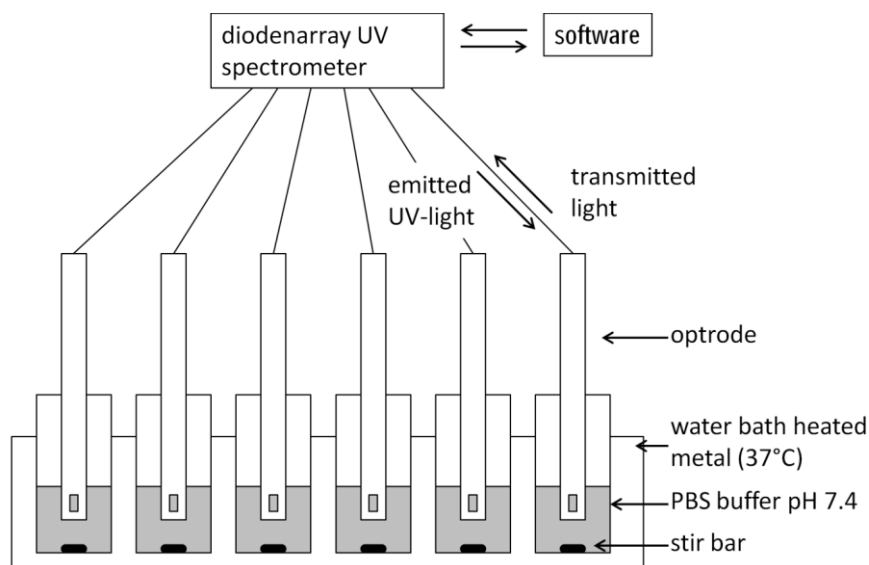


Figure 3.16: Schematic drawing of μDiss profiler™ [104]

Software controlled and according to a defined time schedule a diode array UV spectrometer emitted UV light via an optrode into a sample. The sample with stir bar is placed into a water bath heated metal block, for temperature control. The sample solution flows through a gap. Due to sample concentration a reduced amount of light is reflected at the mirror at the end of the gap, and transmitted light is measured with UV diode array spectrometer. Simultaneously measurement of six different samples is possible

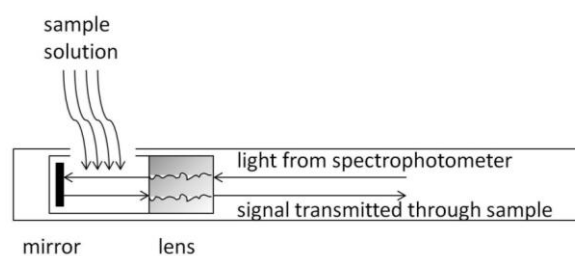


Figure 3.17: Schematic drawing of a fiber optic probe, modified from [100]

The light from the spectrophotometer is focused due to a lens into the gap, where sample solution flows through. At the end of the gap at a mirror the light is reflected, again transiting the probe, focused in the lens and then the transmitted light is transferred to the detector.

The diode array spectrometer measures the concentration of drug substance as a function of time for each channel recording the whole spectrum with each measurement. According to a defined time schedule (Table 3.4) the shutter is opened and UV light could reach the sample for measurement. Before the measurement, a calibration has to be recorded allowing determination of the concentration of the used substance according to Lambert-Beer's law. First 100% transmission and "dark spectra" of media are measured for baseline determination, followed by the measurement of the calibration curve with suitable concentrations of API in suitable media. Before the samples are measured 100% transmission, and dark spectra of the dissolution medium have to be measured again. In contrast to 100 % transmission, the "dark spectrum" is an internal calibration with closed shutter – no light should reach the diode array spectrometer. According to the calibration curve, blanks have to be created, where the

calibration curve could be inserted due to different media for calibration and dissolution tests, followed by the dissolution measurement.

### 3.5.1.1. Dose collection and dissolution method

The collection of aerosol particles less than 6.4 μm was performed using the twin stage impinger instead of the ACI. As described in the European Pharmacopoeia 7.0 7 ml and 30 ml [10] of PBS buffer were introduced in the upper and lower impingement chambers. The air-flow through the apparatus was adjusted to 60 l/min [10]. For detailed schematic see Figure 3.18. Micronized powder was weighed into polyethylene capsules and dispersed using the HH. The suspension with particles less than 6.4 μm was aliquoted (3 ml) and transferred immediately into the vessels of the μDiss. Stir bar speed was set to 700 rpm. For analysis of the μDiss spectra the exact content of API in the sample has to be known. Consequently, one extra aliquot was diluted with solvent to 50.0 ml and concentration determined using HPLC.

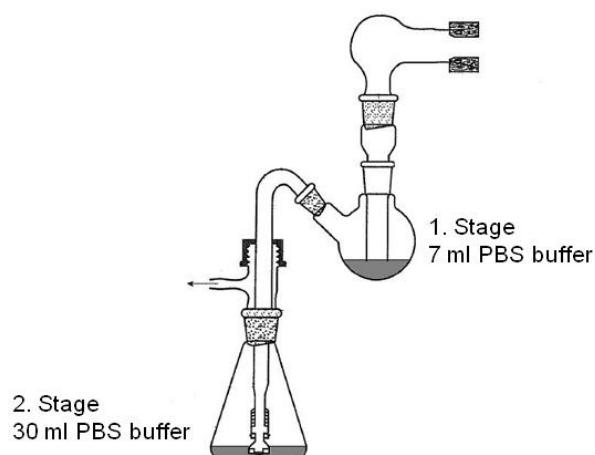


Figure 3.18: Modified schematic of twin stage impinger, modified from [10]

The twin stage impinger consists of two stages. In the upper chamber (1. stage) 7 ml medium is placed in the large chamber (2. stage) 30 ml is placed. Due to an air stream from up to down, particles are placed inside the medium.

Table 3.4: Time schedule for μDiss online UV measurement

number of measured spectra	1	40	30	30	15
interval between measurements [s]	5	15	30	120	120

### 3.5.2. Flow through cell

The history of flow through cell dissolution testing started in the late fifties (1957); in 1995 it was implemented as apparatus 4 in the USP [60,105] and in 2007 in the Ph.Eur. [10,46]. For oral solid dosage forms the pharmacopoeias describe two cells with a diameter of 12 mm and 22.6 mm, respectively [10,60]. For further dosage forms like suppositories, powders, implants and drug eluting stents different cell types are available [60]. For the standard flow through cell the pharmacopoeias usually claim the usage of glass beads in the bottom cone for avoiding drug material flowing into the inlet tubing [10,60].

The dissolution medium is pumped through the cell, from bottom to top, either in an open or closed set up [106]. In the closed set up a smaller, but well defined, amount of dissolution medium is required and is continuously pumped through the cell. This set up for example is used to overcome LoQ of the API [106], due to concentration of dissolved substance. Furthermore, in the closed as well as in the open set up an online UV detection is possible without sampling [82]. The open set up offers advantage of infinite amount of dissolution medium, which is suitable for substances with low solubility [10,82,105-108] and provides sink conditions [82,105,106,108]. Sink conditions should imitate the physiological conditions, where the dissolved drug is absorbed and the local drug concentration is low [31]. Further advantages are continuous sampling [82], a flow rate change [108] and possible easy dissolution medium change during the run [82,108]. Beside the advantages there are also some influencing parameters, which should be controlled, e.g. the size of the glass beads, the temperature in the cell, the flow rate and the level of deaeration [82,109].

The usage of flow through cell for powders is suitable due to the limit of volume and the reduced spreading of drug particles to undefined sites of the apparatus [110] compared for example to the paddle apparatus. Bhattachar et al. tested several mixing and layer set ups for powder and glass beads to achieve maximum dissolution and reproducibility. The best results could be shown for a homogenous mixture of powder and beads. But for micronized powders, especially for those with a poor solubility and wettability, the substances are floated and adsorbed at the filter, resulting in incomplete dissolution [105,110].

In this PhD thesis not only poor soluble micronized powders were used. The focus lies on the fine particle dose, so the classical flow through cell set up as described above, has to be adapted. Davies et al. used an custom made flow through cell where a membrane with FPD could be used in [19]. In this set up the dissolution medium enters the cell and thus the membrane on one place only without further distribution. Consequently, it is questionable if the membrane is wetted completely, or if the dissolution medium goes straight through. Boehringer Ingelheim developed a new flow through cell (build by Zentrale Mechaniker Werkstatt, Boehringer Ingelheim, Ingelheim, Germany) (Figure 3.19) [104], which was used

in this PhD thesis. This new cell should ensure a homogenous wetting of the whole membrane simultaneously.

This cell consists of several parts. The two outer holders are connected either to the HPLC pump (AXP, Dionex, Idstein, Germany) or to the sampling unit. The pump provides a constant flow rate and reduces the in literature described difficulty of adjusting the flow rate [82]. Between the holders on the upper and the bottom side two parts remembering on quench heads (Figure 3.20) are placed. The two quench heads are the important improvement compared to the flow through cell of Davies and Feddah [19]. Between the two “quench heads” on the bottom side a metal sieve, the membrane with powder and a covering membrane are clamped. As membrane material regenerated cellulose (RC) with a diameter of 24 mm was used exclusively. The whole cell is closed and bolted together avoiding leakage. The upper “quench head” ensures a uniform dissolution medium distribution on and wetting of the membrane. Without the fluid distribution, the dissolution medium jet goes straight through the membrane resulting in an uneven wetting. The metal sieve avoids rupturing and sliding of the membrane into the lower “quench head”, which concentrates the medium with analyt to one fluid jet. The pump pumps the dissolution medium with a constant flow rate of 1 ml/min through the apparatus in an open method set up. As dissolution medium PBS buffer pH 7.4 was used. The probe sampling procedure depends on method set up. It was either performed as “all in one” sampling over a defined time period or according to on a defined time schedule (sampling type “all” or “partial”) automated by a Gilson sample injector (Gilson, Middleton, United Kingdom) into HPLC vials.

The whole flow through cell with pump and sampling unit is placed into a climate chamber and the temperature is set to 37°C. The climate cabinet allows to control the temperature, which is often seen as problem [82].

At the end of each experiment the membrane and the remaining cell parts together are rinsed each with 50 ml of solvent (Table 3.1). Concentration measurement is performed with HPLC.

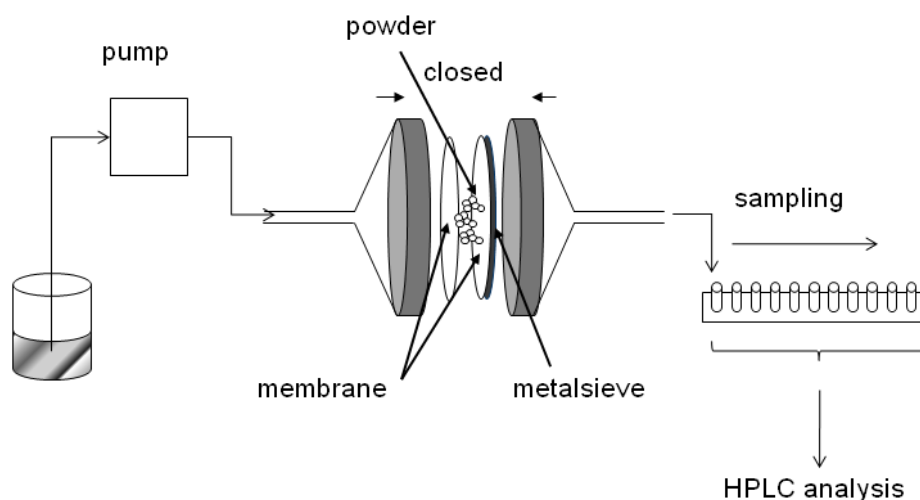


Figure 3.19: Schematic drawing of the flow through cell [104]

A HPLC pump pumps the dissolution medium through the flow through cell. The powder is entrapped between two membranes. On the sampling side an additional metal sieve is inserted. With a “quench head” the dissolution medium is uniformly distributed on the membrane, after passing membrane and metal sieve, the dissolution medium with substances is recollected with a second “quench head” and according to set up sampled.

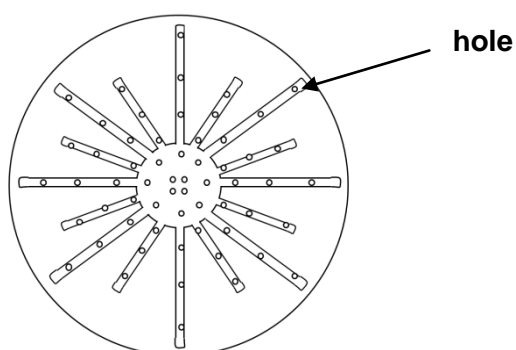


Figure 3.20: Schematic drawing of one “quench head”

The “quench heads” ensure uniform dissolution medium distribution on the membrane.

### 3.5.2.1. Diffusion pre-tests

The pre-tests were performed with Budesonide in triplicate.

For measuring the diffusion capability through the flow through cell, the following set up was used. Therefore, 0.5 mg of Budesonide is solved in PBS buffer in a 250 ml graduated flask. The substance – buffer - solution is directly pumped through the assembled cell with the two membranes and is collected in a 50 ml graduated flask. For determining the influence of pump and tube (background noise) between each probe, 5 ml substance – buffer - solution is directly collected behind the pump without use of the cell. As described above the cell is rinsed after each experiment.

For determining the validity of the flow through cell each 100 µg of Budesonide are directly weighed onto the membrane and two different sampling methods (sampling type “all” or “all in one”) are preformed.

### 3.5.2.2. Dose collection and dissolution testing

As dose collection method aACI (Chapter 3.3.1.2) with a special PEEK pattern (diameter 80 mm) with four voids inserted on the filter stage was used (Figure 3.21). Use of the pattern was required due to the small flow through cell size and therefore small membrane size (ø 24 mm) and for avoiding substance load into the vacuum pump. The use of an additional larger filter beneath the small membrane instead of the pattern is not possible because of an influence on the air flow in the aACI. Into the pattern voids simultaneously four membranes are allocated. Three of the membranes are used for dissolution experiments with the flow through cell, the fourth is used as reference membrane and rinsed with 50 ml of solvent (Table 3.1).

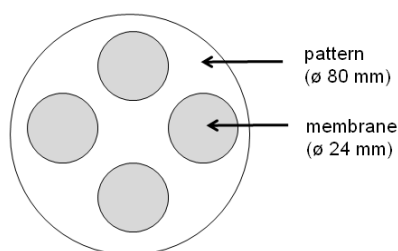


Figure 3.21: Schematic drawing of pattern with membranes for dose collection

- After dose collection the influence of the sampling was determined for Budesonide. Sampling until “4 minutes” in the first two minutes every 0.25 minutes and from 2 to 4 minutes every 0.5 minutes was performed. After sample “4 minutes” on the one side every minute one milliliter was collected (label: “all”), on the other side to defined time points one milliliter was collected and the rest was abolished (label: “partial”).
- In addition, for Budesonide different flow rates (0.5 ml/min, 1 ml/min and 5 ml/min) in the “all” sample set up were tested
- Furthermore, with a flow rate of 1 ml/min and the sampling type “partial” for the different modifications of Substance A and Fenoterol HBr the influence of different fine particle doses on membrane was determined. Furthermore, the aim was to compare a FPD of 20 µg, 60 µg and 100 µg, respectively.

Table 3.5: Time schedule for sampling

interval [min]		0.25	0.5	1	5	15
samples	partial			1	5	2
	all	8	4	57	-	-

With the “partial” sample type data treatment is more complex, because discarded amount has to be calculated. The data treatment is described on the example of sample 15, the time interval between sample 14 and sample 15 is 5 minutes. As often used in flow through cell set ups the mass is accumulated.

Therefore, the accumulated mass of sample 15 is the sum of the mass of the concentration of sample 14 calculated of 5 ml, the mass of the mean of concentration of sample 14 and 15 calculated of 5 ml and the accumulated mass of sample 14.

$$M_{acc15} = c_{14} [\mu\text{g/ml}] * 5 [\text{ml}] + \text{Mean} (c_{14}, c_{15} [\mu\text{g/ml}]) * 5 [\text{ml}] + M_{acc14} [\mu\text{g}]$$

Equation 3.2: Calculation of accumulated amount of dissolved substance

### 3.5.3. Franz Cell

The Franz diffusion cell is named after its first descriptor T.J. Franz, who described in 1975 the use of a diffusion cell for absorption studies of organic compounds in human skin [111]. Although the Franz diffusion cell is still not a pharmacopeia method, the FDA recommends the use of a diffusion cell for in vitro release testing of topical dosage forms in the SUPAC – SS guideline [112]. Up to now, the Franz Cell has become the “gold standard” for transdermal drug delivery studies [113-115]. In the classic set up real skin, or a synthetic or artificial membrane [114], is clamped between an acceptor chamber and a glass top. The dissolution medium in the acceptor chamber can be heated, due to temperature jacket. The sampling over a side arm or sampling port is performed with a syringe [111]. One major problem described in literature are air bubbles at the membrane liquid interface and the difficulty or even failure of removing them [114,116]. Due to air bubbles the precision of data can be lower and outliers are possible. Hence, the problem of air bubbles is also taken into account in the SUPAC - SS guideline [112].

In dissolution testing for inhalation powders the Franz diffusion cell, as described above, is used by the working group of Paul Young [3,64,117,118]. More details are already described in chapter 2.2.3.

For the dissolution studies in this PhD thesis Franz diffusion cell was chosen to mimic the air liquid interface of the lung. The traditional set up [111] as used for example for the membrane permeation test (3.4.2) and the manual modified Franz cell described in the NanoInhale project [119] was modified by Boehringer Ingelheim (built by Zentrale Elektronik Werkstatt and Glasbläserei, Boehringer Ingelheim, Ingelheim). The dissolution medium reservoir is enlarged from a few milliliters in the traditional set up to 1 l to allow sink conditions for poorly soluble substances. The dissolution medium (PBS buffer pH 7.4) temperature is set to 37°C and stirred with a magnetic stir bar at 100 rpm to maintain a homogenous solution. A higher stirring speed is due to the formation of a vortex not recommended, because the vortex hinders homogenous wetting of the membrane. For temperature control during dissolution testing a thermometer is placed inside the acceptor chamber.

After dose collection the membrane is placed into the membrane holder with particles faced up and clamped. During the dissolution test the holder is heated from above to avoid condensation and thus droplets. The condensed droplets can fall on the membrane and influence the dissolution process. For the used modified Franz Cell the sampling procedure is automated with a Gilson Liquid Handler 215 (Gilson, Middleton, United Kingdom). According to a defined time schedule (Table 3.8) a needle immerses through a septum into the acceptor chamber and samples 1 ml which is transferred into an HPLC vial.

Table 3.6: Time schedule for sampling

<b>interval [min]</b>	3	5	15	60
<b>samples</b>	21	11	10	18
<b>interval [min]</b>				
<b>for Fenoterol</b>	1.5	5	15	60

After sampling the needle is cleaned automatically and the removed solvent is refilled with fresh pre-warmed PBS buffer (37°C) to maintain a constant dissolution medium volume. After stopping the dissolution test, the membrane is removed and rinsed with 50 ml solvent for dissolving the remaining particles (Table 3.1). Concentration measurement is performed with HPLC. All tests were performed in triplicate.

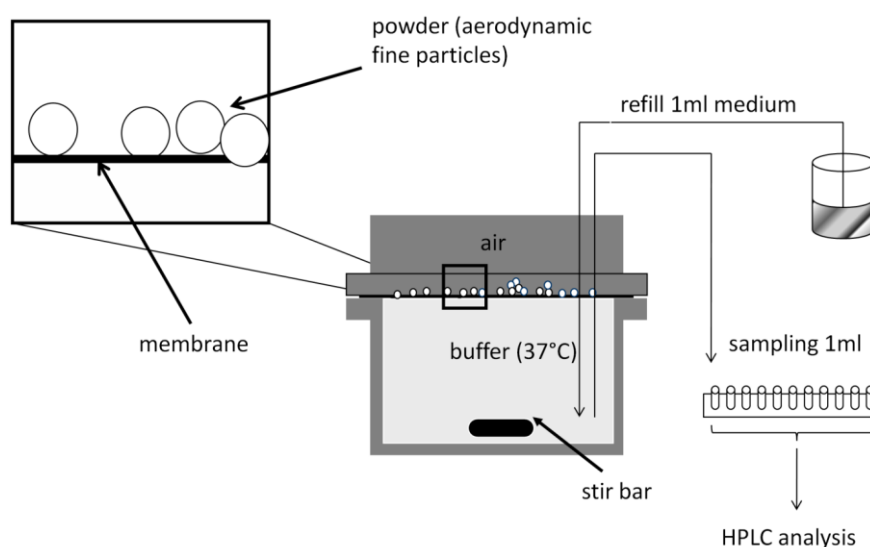


Figure 3.22: Schematic drawing of modified Franz Cell adapted from [104]

Franz cell with fine particles collected on a membrane. According to a defined time schedule sampling of one ml is automated with a Gilson robot. The sampled milliliter is refilled with fresh pre warmed PBS buffer. Typically for the Franz Cell is an air liquid interface.

### 3.5.3.1. Diffusion test

In addition to the general membrane permeation test, described in chapter 3.4.2 with the traditional Franz cell for the modified Franz cell set up a diffusion test was performed. This test allows a direct comparison between diffused and dissolved (dissolution + diffusion) amount of substance whereas the general test provides information if a membrane is suitable or not. The diffusion tests in the modified Franz Cell were performed with the regenerated cellulose and the Isopore™ polycarbonate membrane. Therefore, 10 ml of substance - buffer solution with a concentration between 10 µg/ml to 21 mg/ml and 40 mg/ml for Fenoterol, respectively were placed onto the membrane. Sampling was performed as described above.

### 3.5.3.2. Dose collection and dissolution testing

As dose collection method aACI with an additional “delrin” ring on the membrane (outer diameter: 80 mm, inner diameter 60 mm) was used (Figure 3.23). The ring is needed for guaranteeing a substance free outer area, where the membrane is clamped onto the membrane holder. For dose collection substances were weighed into polyethylene capsules (Table 3.7). The particles were collected either on a regenerated cellulose membrane (RC) or an Iso-pore™ polycarbonate (IPC) membrane.

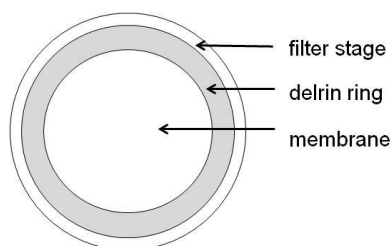


Figure 3.23: Schematic drawing of filter stage (ACI) with membrane and delrin ring for Franz Cell

Table 3.7: Substances-weights into polyethylene capsule for dose collection

<b>substance</b>	<b>weight [mg]</b>
Budesonide	1
	10
Fenoterol	1
	10
Substance A amorphous base	1
Substance A crystalline base	1
Substance A bromide	1

### 3.5.4. Transwell® Dissolution System

The Transwell® permeable supports are a commonly used device for cell culture issues. In 2010 the static Transwell® system was introduced as new approach for dissolution testing of powders for inhalation [61]. In a more sophisticated approach the acceptor medium was stirred [62].

The modified Transwell® (Corning Costar, Corning, USA) as well as the Franz Cell [111] has an air liquid interface at the membrane but with the small amount of dissolution medium it mimics more the limited capacity of lung fluid *in vivo* [61,63].

In this PhD thesis the release profiles of aerodynamically classified particles of Substance A in its different forms and Budesonide were investigated using an adapted Transwell®. For the commercially available Transwell® with 6 wells (insert membrane diameter 24 mm) a spacer plate (2 mm) was constructed, leaving the inserts open lifting the inserts and hence, adding space to use stir bars in the receptor chamber. Stirring speed was set to 140 rpm. For sampling small holes for each well were drilled into the lid.

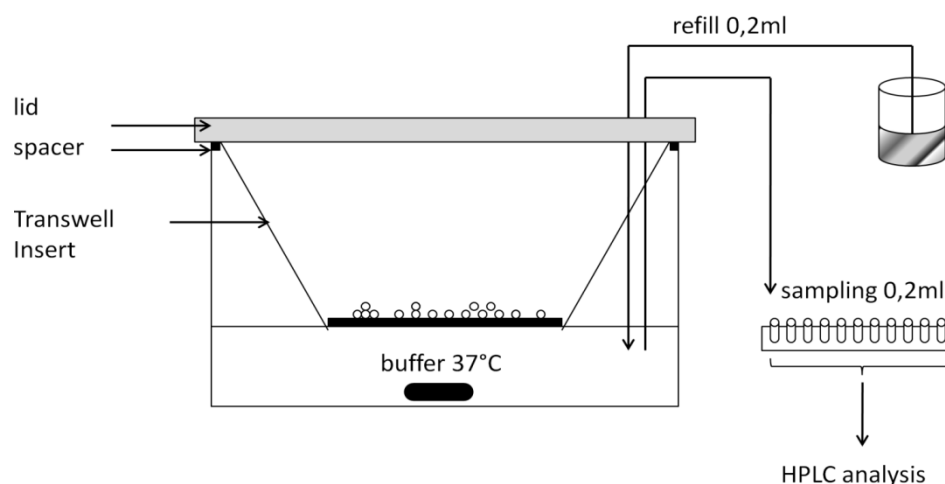


Figure 3.24: Schematic drawing of Transwell® dissolution apparatus.

The Transwells® are available with polyester (PE), polycarbonate (PC) or collagen coated polytetrafluoroethylene membranes with different pore sizes. For dissolution testing so far polyester membranes were used [61]. As for the other dissolution techniques regenerated cellulose (RC) and Isopore™ polycarbonate (IPC) membranes were used, hence these membranes were also tested. Furthermore, the membrane permeation test showed a substance retaining effect for the PE membrane (chapter 4.1.4) and in literature for the Transwell® polycarbonate also a delayed diffusion was described [62].

For using RC and IPC membrane a commercially available Transwell® insert was modified. The membrane was cut out, and a small thermoformed plastic edge was created. On this edge a small metal sieve was placed as support for the membranes. The modified inserts were reusable in contrast to the standard Transwell® insert.

Dissolution tests were performed at 37°C and 100% r.H. in a climate cabinet (Espec climate cabinet, Weilburg, Germany) using degassed PBS buffer pH 7.4 as dissolution medium. The use of a climate cabinet was necessary for avoiding evaporation of the small amount of dissolution medium. The membranes with particles facing up were touching the dissolution medium, ensuring an air liquid interface with no hydrostatic pressure on the system (Figure 3.24). Therefore, for the commercially available inserts 2.6 ml and for the adapted inserts 3.85 ml dissolution medium was placed into the acceptor compartment. According to a defined time schedule (Table 3.8) probe sampling was manually done with a syringe (needle: 100 Sterican® (Braun, Melsungen, Germany) and 1 ml disposable syringe (Wicom, Heppenheim, Germany)). The solvent removed during sampling (0.2 ml) was refilled with fresh pre-warmed PBS buffer (37°C) to maintain a constant dissolution medium volume. At the end of the experiment each insert was rinsed with 25 ml of solvent according to the used substance (Table 3.1) to determine the total recovery.

All experiments (Table 3.9) were done in triplicate and concentrations were determined with HPLC. The total amount of drug initially loaded on the membranes was measured using the maximum of the cumulatively released amounts plus the remaining quantity of particles on the membrane (determined at the end of each experiment). The amount of drug released was calculated with Equation 3.3. Percentages of drug released were calculated by dividing the amount of drug released by the drug mass which was loaded on the membrane after aerosolization and separation with the ACI.

Table 3.8: time schedule for sampling

interval [min]	5	10	15	60
samples	1	1	3	3

$$m_{t=i} = c_{t=i} * V_{\text{dissolutionmedium}} - (c_{t=i-1} * (V_{\text{Dissolutionmedium}} - V_{\text{sampling}})) + m_{t=i-1}$$

Equation 3.3: Calculation of amount of released substance  $m$ : amount of drug released,  $V$ : volume,  $c$ : concentration

#### 3.5.4.1. Dose collection

Dose collection basics are already described in Chapter 3.3.1.4, but some additional information are required. For the Transwell® insert membranes (PE and PC) set up with aACI + SE and special PEEK covers, for the RC membrane mACI and for the IPC membrane aACI + SE are used. After dose collection RC and IPC filter are cut out on the Transwell® insert size (ø 24 mm) and used with the modified insert as described above. After removing the PEEK cover the PE and PC membrane are directly usable for the experiment.

### 3.5.4.2. Addition of a dissolution layer on the membrane

Adding a dissolution layer as used by Arora [61] is thought to improve drug dissolution by providing a higher volume on the powder side and hence diffusion across the membrane.

After dose collecting the inserts were placed into the Transwell® dissolution system. Directly after placing the insert 40 µl PBS buffer were added [61] (or not) onto each membrane and the lid was closed. The tests were performed with and without this additional 40 µl, respectively. The dissolution tests were performed always with stirring.

### 3.5.4.3. Stirring

Furthermore, the influence of stirring of the dissolution medium in the acceptor chamber on the dissolution and diffusion process through the membrane was determined. Stirring should guarantee a homogeneous concentration and reduce concentration-based diffusion effects. Stirring speed was set to 140 rpm.

After dose collection the inserts were placed into the Transwell® system. The dissolution tests were performed without dissolution layer and with or without stirring, respectively.

The combination of dissolution layer and without stirring was not tested, because both setups for themselves turned out not to be beneficial.

Table 3.9: Overview of experimental procedures, experiments performed are marked with an x

	dose collection technique			influencing factors				
	aACI + cover	aACI + SE	mACI	membrane permeation	dissolution layer		stirring	
					yes	no	yes	no
Polyester	x			x		x	x	x
Polycarbonate	x			x	x	x	x	
Polycarbonate (Isopore™)		x		x		x	x	x
reg. Cellulose			x	x	x		x	x
						x	x	x

### 3.5.4.4. Comparison of the two different polycarbonate membranes

For supporting the diffusion results regarding the differences in permeation of Budesonide between the two types of polycarbonate membranes (PC & IPC), two additional tests were performed. After drug deposition on the Transwell® inserts the Transwell® polycarbonate membrane edge was perforated 32 times with a small needle (ø 0.5 mm). For the other test set up the membrane was cut out after drug deposition and placed onto the modified

Transwell® insert (as described above for RC and IPC). With the perforation a better access of dissolution medium between the upper side of membrane and acceptor medium should be possible. The test of the modified insert should show if there is a material or test set up depending difference between the two membrane types. The two tests were performed in triplicate for Budesonide with stirring and without dissolution layer.

#### 3.5.4.5. Surfactants

For the Budesonide and Substances A dissolution tests with addition of each 0.02% DPPC and 0.02% Alveofact ®, respectively in the PBS buffer were performed to simulate the lung liquid composition. As membrane material IPC membrane was used and therefore the corresponding dose collection method 3.3.1.3. The tests were performed in triplicate without dissolution layer and with stirring.

### 3.5.5. Paddle Apparatus

The paddle apparatus is a pharmacopeia dissolution testing method since 1978 (USP, apparatus 2) [46]. In addition to the rotating basket method (USP, apparatus 1), USP apparatus 2 is the most widely used technique for *in vitro* dissolution testing. The handling is simple, the methods are standardized, robust [21], and there is a large experience over more than 30 years for oral dosage forms. The scope of application is not limited to quality control of oral dosage forms but also on non - oral forms e.g., transdermal patches, implants, suppositories and so forth. The paddle apparatus is a valuable tool for formulation development, controlling of manufacturing processes and even for predicting *in vivo* performance of oral dosage forms [44] right up to bioequivalence tests in exactly defined cases [21,120]. The classic paddle apparatus consists of vessels placed into a temperate water bath, inside each vessel a paddle for stirring is immersed [60]. Dissolution testing with the paddle apparatus is sophisticated and many impact factors are known and can be controlled [10,44,60]. The dissolution medium for oral dosage forms varies from simple buffer solutions with or without surfactant up to biorelevant media, like fasted state simulated intestinal fluid or fed state simulated intestinal fluid. Some of the impact factors on dissolution are temperature, stirring speed, shaft centering and wobbling, vibrations, air bubbles, hydrodynamic conditions and last but not least evaporation. The air bubbles could slow down the dissolution [44] due to adhering at the surface of particles and acting as barrier or could hold particles on the vessel or shaft [44,65]. Therefore, the USP demands deaeration of dissolution medium for example with heat vacuum filtration [60] or other validated deaeration techniques like helium or ultrasonic treatment [44]. The hydrodynamic conditions could strongly influence the dissolution profiles and the reproducibility. Hence, the equipment used for solid dosage forms should be in accordance with the pharmacopeia to reduce irregularities and turbulences in the fluid flow [44].

The use of the paddle apparatus with a membrane holder for dissolution testing of powders for inhalation was first described in 2009 [54]. The powder is not directly placed into the apparatus but instead it is aerodynamically classified with the NGI onto a membrane. This membrane was than sandwiched with a second one and placed into a modified histology cassette, which was afterwards positioned in the paddle apparatus [54]. A more sophisticated approach used a special NGI dissolution cup which is covered with a membrane after dose collection. The cup with the membrane is fixed and then placed into the dissolution apparatus [55].

In this PhD thesis instead of the NGI, ACI as dose collection method is used. Hence, instead of the special NGI cup as described above a membrane holder (Copley Scientific, Nottingham, UK) (Figure 3.26 A, page 50) is used. This “standard” membrane holder is normally used for transdermal patches [10,121] and consists of a watch glass and a polytetrafluoroethylene mesh. The experiments were performed with two different dissolution testers. At the

beginning the experiments were performed with an apparatus consisting of one vessel with 1 l dissolution medium which was immersed in a water bath (Erweka DT70, Erweka, Heusenstamm, Germany). Sampling was automated according to a defined time schedule (Table 3.10) by a construction of the Zentrale Elektro Werkstatt, Boehringer Ingelheim (based on two Gilson Abimed syringe pumps and a Gilson Abimed 233 XL (Gilson, Middleton, United Kingdom)). The sleeves for sampling are placed in the shaft of the paddle. In the further progress of the thesis the equipment was changed to a dissolution tester with seven vessels (dissolution tester AT7 smart, piston pump CP7-35 and fraction collector C615 (Sotax, Lörrach, Germany)) with automated sampling, too (Table 3.11). For sampling a stable sleeve is remaining in the vessel during dissolution testing, 40 mm next to the shaft and 20 mm next to the vessel wall.

Dissolution tests were performed at 37°C with degassed PBS buffer pH 7.4 as dissolution medium. The solvent removed during sampling is refilled with fresh pre-warmed PBS buffer to maintain the volume of the dissolution medium at a constant level.

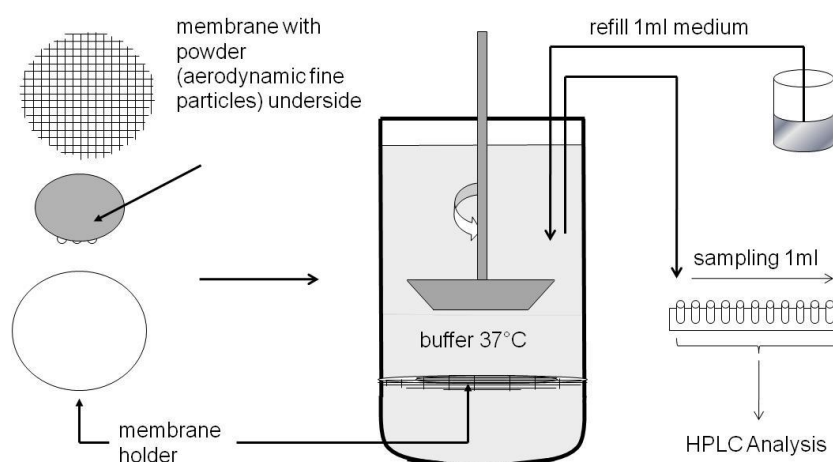


Figure 3.25: The membrane is placed with the particles faced towards the watch glass. Afterwards the membrane holder is placed into the paddle apparatus. A sampling and refill unit is adapted to the dissolution tester.

After dose collection the membrane with particles towards the watch glass is placed into the membrane holder. The membrane holder is then placed into temperature controlled paddle apparatus (37°C), release surface (membrane + mesh) sided up. The distance between bottom edge of the paddle and surface of the membrane holder is  $25 \text{ mm} \pm 2 \text{ mm}$  due to hydrodynamic effects [60].

After dissolution testing residual amounts of drug in and on the membrane and on the watch glass are determined by rinsing both parts with each 50 ml solvent (Table 3.1). The total amount of drug initially loaded on the membrane is determined using the maximum of the cumulatively released amounts plus the remaining quantity of particles on the membrane (determined at the end of each trial). The percentages of released drug over time were calcu-

lated by dividing the amount of drug released by the initial drug mass loaded on the membrane. All experiments were performed in triplicate.

Table 3.10: Erweka apparatus, time schedule for sampling

<b>interval [min]</b>	3	5	15	60
<b>samples</b>	20	11	17	7
<b>interval [min]</b>	1	5	15	60
<b>for Fenoterol</b>				

Table 3.11: Sotax apparatus, time schedule for sampling

<b>interval [min]</b>	4	6	60	120
<b>samples</b>	1	9	7	2

#### 3.5.5.1. Dose collection and dissolution testing – Erweka tester

As dose collection method aACI (chapter 3.3.1.2) was used. For dose collection 1 mg of Budesonide, modifications of Substance A, and Fenoterol HBr, and 10 mg Budesonide and Fenoterol HBr, respectively were filled into polyethylene capsules. The particles were collected either on the regenerated cellulose (RC) or the Isopore™ polycarbonate (IPC) membrane.

At the beginning of the experiments stirring speeds of 50 rpm, 100 rpm and 140 rpm were compared. For the following experiments the stirring speed with fastest dissolution and smallest standard deviation was chosen (140 rpm). Furthermore, as dose collection method an airbrush system was used (chapter 3.3.2).

#### 3.5.5.2. Dose collection and dissolution testing – Sotax tester

In the Sotax paddle apparatus the membrane holder showed irregular movement in the vessel for a stirring speed of 140 rpm, hence stirring speed had to be reduced to 100 rpm. After changing the dissolution tester equipment, comparison between the two apparatus was performed. As dose collection method aACI (chapter 3.3.1.2) was used.

The following experiments were performed to evaluate the:

##### a) best dose collection method

First three different dose collection methods were compared (aACI ((chapter 3.3.1.2), aACI + SE, mACI (chapter 3.3.1.3), respectively). Second, experiments determining the effect of different mass on the dissolution profile were evaluated. These experiments were performed for Budesonide only.

## b) different membrane holder types

As dose collection method the best method from a) was used. For dissolution of Budesonide the following three membrane holders were tested:

- commercially available membrane holder from Copley (Figure 3.26 A)
- blocked membrane holder (Figure 3.26 B)

The blocked membrane holder should avoid diffusion along the edge of the membrane. Onto the watch glass of the commercial available membrane holder the membrane is placed and locked at the rim with a stainless steel ring utilizing an o-ring.

- a membrane sandwich holder (Figure 3.26 C)

This membrane holder consists of two stainless steel rings and a mesh. After dose collection the membrane is covered with a second empty membrane and placed on the mesh. The mesh and the membranes are clamped in-between the two stainless steel rings.

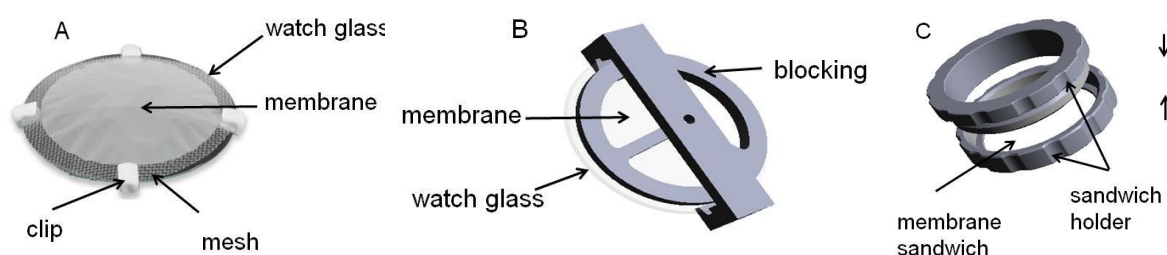


Figure 3.26. A) standard membrane holder adapted from [122], B) blocked membrane holder, and C) membrane sandwich holder adapted from [123]

## c) influence of temperature

As dose collection method the best method from a) was used. The experiments at 22°C and 37°C were performed for Budesonide only.

## d) influence of lactose

As dose collection method aACI + SE was used. The experiments were performed with Budesonide – Lactose mixture 2 (Table 4.4)

## e) dissolution medium with surfactant

Experiments were performed with the best method from a) as dose collection method and standard membrane holder.

- For Budesonide with PBS buffer containing 0.02% DPPC, 0.2% SDS, 0.2% Tween® 20, and 0.2% Tween® 80, respectively.
- For Substances A with PBS buffer with or without 0.02% DPPC, respectively.
- In addition, for Substances A and Budesonide the membrane holder set up with blocking of the membrane and PBS buffer containing 0.02% DPPC was used.

### 3.5.6. Dissolution model

From the very first the effects of experimental dissolution testing were tried to be explained theoretically [46]. There are several models especially for the dissolution of oral dosage forms described in literature. These models try to explain an existing profile or predict a dissolution profile, e.g. Nernst - Brunner, Noyes - Whitney, Hixon - Crowell, Niebergall or Higuchi [45,124-129]. In addition, these models are based on the hypothesis that the dissolution process is divided into two steps [130]. First the solution of the solid to form a stagnant film or a diffusion layer and second the diffusion of the solute from this film to the bulk liquid [45,46]. Different mathematical expressions for describing this dissolution process are the laws of Noyes-Whitney, Brunner-Tolloczko, Nernst-Brunner and Hixson-Crowell.

Yet for powders for inhalation authors used these models to fit their release profiles and draw conclusions from the correlation coefficient criterion  $R^2$  [3,54,104,131], but currently no publication determined influencing factors on or of the model.

Here an equation based on a diffusion layer concept was chosen. The so-called Nernst - Brunner equation, a modification of the Noyes - Whitney equation, combines the diffusion layer concept with Fick's 2<sup>nd</sup> law [46].

For describing dissolution kinetics of monodisperse powders with the Nernst - Brunner equation several assumptions were made, e.g.: the surface area of particles changes during dissolution, the dissolution of all particles contributes to the total concentration of the solution, and the thickness of the diffusion layer depends on the particle size [125]. For the model in the thesis the following form of the Nernst - Brunner equation (Equation 3.4) was used.

$$\frac{dm}{dt} = \frac{DS}{h} (c_s - c_t)$$

Equation 3.4: Nernst - Brunner equation

Where  $m$  is the mass of solid material at time  $t$ ,  $S$  is the surface area of the particles,  $D$  the diffusion coefficient of the substance in the solvent,  $h$  is the diffusion layer thickness,  $c_s$  is the solubility of drug and  $c_t$  is the concentration of the drug in the solution at time  $t$

The diffusion coefficient  $D$  was calculated by applying the Hayduk - Laudie equation (Equation 3.5) [129,132]. The van-der-Waals volume  $V_M$  for each substance was theoretically determined in a two step procedure from the chemical structure of the molecule with CORINA v3.46 (Molecular Networks (<http://www.molecular-networks.com/products/corina>)) and MOE v2011.10 (CCG (<http://www.chemcomp.com/>)).

$$D = \frac{13.26 * 10^{-5}}{\eta_{water}^{1.4} * V_M^{0.589}}$$

Equation 3.5: Hayduk - Laudie equation [129,132].

Where  $D$  is the diffusion coefficient,  $\eta_{water}$  the dynamic viscosity of water at 37°C, and  $V_M$  the molecular volume

The dissolution layer thickness  $h$  during dissolution process is a well described parameter in the literature. Classically the diffusion layer is defined as unstirred liquid layer adhering to the solid surface [45]. Bisrat and Nystrom suggested that the diffusion layer might be smaller for small particles than for large particles. In their dissolution tests they could not find an influence of agitation speed on the surface specific dissolution rate for the size fraction  $< 5 \mu\text{m}$  in contrast to the fraction of  $25\text{-}35 \mu\text{m}$  [133].

However, in literature there is no clear opinion on the behavior of the diffusion layer during the dissolution process. On the one hand a time independent diffusion layer with a constant diffusion layer during particle shrinking [125] is postulated; on the other hand a time dependent diffusion layer is assumed with a shrinking diffusion layer during particle shrinking [124,134] (Figure 3.27).

In literature there is a consensus that below a certain particle size the diffusion layer is approximated by the particle radius [125,129,135]. The critical particle radius is assumed to be  $30 \mu\text{m}$  [134]. In the case of a critical particle radius for a spherical particle the diffusion layer thickness and the particle radius is given by Equation 3.6 [135].

$$h(t) = r(t)$$

Equation 3.6: Correlation of diffusion layer thickness  $h$  and particle radius  $r$ , for particles with a diameter less than  $30 \mu\text{m}$

Furthermore, the influence of hydrodynamic conditions on the diffusion layer is discussed. Sheng et al. showed, that the paddle speed primarily influences the diffusion layer of large particles while particles with a particle radius smaller than  $13 \mu\text{m}$  showed no effects on the diffusion layer [129].

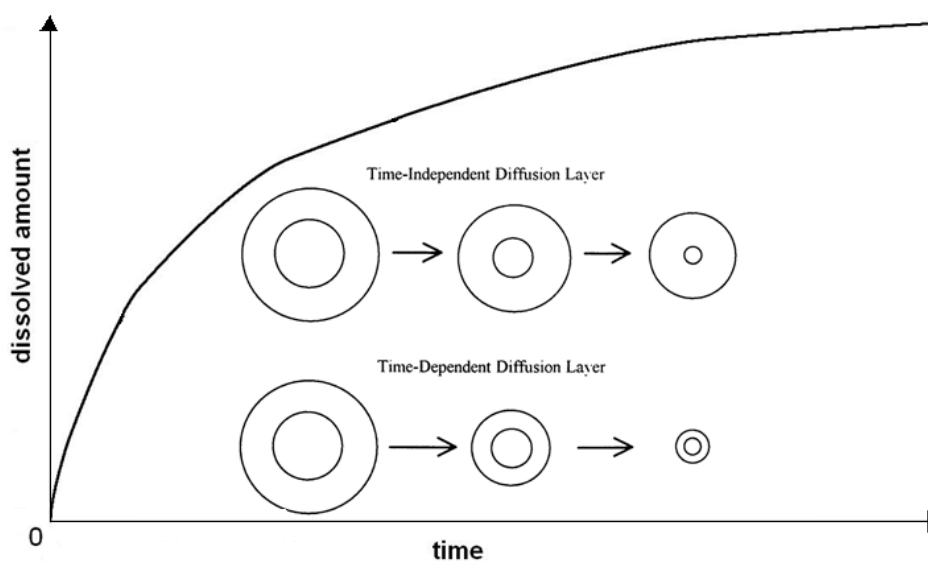


Figure 3.27: Time dependence of diffusion layer, modified from [124].

The modeling of the dissolution layer of particles in this work is based on the following assumptions: sink conditions (chapter 2.2.3) (but the concentration change is taken into account), spherical particles, well stirred medium, isotropic dissolution, concentration at the surface of the particle / interface is saturated, the diffusion coefficient is assumed to be constant along the diffusion layer and no direct influence of stirring on the dissolution process due to the membrane.

Because the fine particle fraction from an experiment is polydisperse, different fractions of the particle size distribution are taken into account by the model (Table 3.12).

In order to model the particle size distribution, the sum of monodisperse particle fractions is applied [128,134] (Equation 3.7). Each group is represented by subscript  $e$ .

$$\frac{dX_{sum}(t)}{dt} = \sum_{e=1}^n \frac{dX_e(t)}{dt} = \sum_{e=1}^n \frac{DS_e(t)}{h_e t} \left( c_s - \frac{X_d}{V} \right)$$

Equation 3.7: Sum of monodisperse particle fraction to take the assumption of polydisperse powder into consideration

$X_{sum}(t)$  is the total amount of undissolved drug at time  $t$ ,  $X_e(t)$  the amount of undissolved drug in a particle size group  $e$ ,  $S_e$  the surface area of each particle size fraction,  $h_e$  the thickness of the diffusion layer which depends on the particle radius  $r_e$ .

The number of particles in each fraction is assumed to be time independent as described by Hintz et al. [134].

The particle size fractions are based on the cut off diameter of the ACI as described by Nichols [90]. For spherical particles the surface area of a particle size group is calculated as described in the Equation 3.8- Equation 3.10 [128,134].

$$N_e = X_e(0) \left( \frac{4\pi r_e(0)^3}{3} \rho \right)^{-1}$$

Equation 3.8: Calculation of particle number  $N_e$  in a particle size fraction

$X_e(0)$  is the amount of undissolved drug in a particle size group,  $r$  the radius and the  $\rho$  the density

$$r_e(t) = \left( \frac{3X_e(t)}{4\pi\rho N_e} \right)^{1/3}$$

Equation 3.9: Calculation of radius of one particle size fraction  $r_e$  at time  $t$

$X_e$  is the amount of undissolved drug in a particle size group,  $N_e(t)$  is the particle number at any time

$$S_e(t) = N_e 4\pi r_e(t)^2$$

Equation 3.10: Calculation of surface area  $S_e(t)$  of one particle size group at time  $t$

$N_e$  is the number of particles in a particle size fraction,  $r_e$  the radius

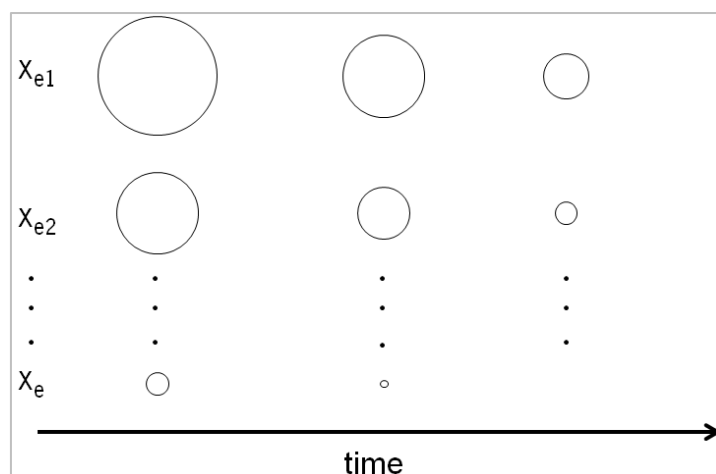


Figure 3.28: Dissolution of a polydisperse powder over time for  $e$  particle size fractions (schematic).

In Table 3.12 (page 55) the used parameters are summarized. The particle mass for calculation corresponds to the mass on the membrane from experimental data. Furthermore, the particles of the substances used in this thesis are not spherical, thus influence of shape on the dissolution process needs to be taken into account. Consequently, the aerodynamic diameters need to be converted into the geometric ones. For this calculation (Equation 3.11) shape is important and a shape factor has to be used, the shape factor for spherical particle is 1 and for cubic particles 1.08 [136]. The assumed particle density of Budesonide is  $1.27 \text{ gcm}^{-3}$  [137].

Starting particle sizes at time point  $t = 0$  are the diameters listed in Table 3.12. The whole calculation is based on a stepwise procedure with  $dt = 0.01 \text{ min}$ , till each particle fraction is dissolved.

$$d_{aero} = d_{geo} \sqrt{\frac{\rho}{k}}$$

Equation 3.11: Correlation between aerodynamic and geometric particle diameter  $\rho$  is particle density,  $k$  the shape factor

Table 3.12: Data for model calculation

	Budesonide	crystalline base	Substance A amorphous base	Dibromide
solubility [µg/ml]	17	7	211	265
van der Waals volume (A <sup>3</sup> )	419	619		701
drug diffusion coefficient [cm <sup>2</sup> /min]	6.19x10 <sup>-6</sup>	4.92x10 <sup>-6</sup>	4.92x10 <sup>-6</sup>	4.57x10 <sup>-6</sup>
Dissolution volume [ml]	1000			
Diffusion layer thickness [µm]	h(t) = r(t)			
dt [min]	0.01			
mass on membrane [µg]	200			
Particle size distribution [%] for fine particle fractions [µm]:				
5.29 µm	18.8 %	10.4 %	15.4 %	14.2 %
4.16 µm	29.7 %	25.0 %	25.7 %	22.9 %
2.49 µm	27.4 %	37.2 %	27.5 %	52.1 %
1.53 µm	18.1 %	21.8 %	21.9 %	60.8 %
0.70 µm	3.2 %	3.7 %	5.2 %	8.2 %
0.41 µm	1.3 %	1.1 %	2.5 %	3.6 %
0.21 µm	1.5 %	1.1 %	1.8 %	1.1 %

For evaluating possible influence factors for Budesonide, the fine particle fraction on the membrane, the particle shape, the solubility, the diffusion layer thickness, and the particle size distribution were varied individually. In each case the other parameters were kept constant. Selected calculated graphs are compared with each other due to the use of the “fit factor” test as described in chapter 3.6.2.2.

Model calculations were done with Excel 2007 (Microsoft Office, Windows).

## **3.6. Data Treatment**

### **3.6.1. Evaluation of Dissolution Tests**

After dissolution testing residual amounts of drug in and on the membrane and additional parts of the dissolution set up (the whole cell for the flow through cell, membrane holder at the paddle apparatus) were determined by rinsing the membrane and the parts with defined amounts of solvent (Table 3.1). Detailed information regarding the amount of solvent are mentioned in the corresponding dissolution technique chapter. The total amount of drug initially loaded on the membranes was measured using the maximum of the cumulatively released amounts plus the remaining quantity of particles on the membrane (determined at the end of each attempt). Percentages of drug released were calculated by dividing the amount of drug released by the drug mass loaded on the membrane after application with the ACI. Calculations were done with Excel 2007 (Microsoft Office, Windows).

### **3.6.2. Comparison of dissolution profiles**

Dissolution profile comparison is divided into two different methods, either model dependent or model independent approaches.

Model dependent approaches are distinguished whether they are used for modeling or comparison of dissolution profiles. In literature several approaches are described. The predominant rate of authors use existing models (e.g., zero order, first order (Noyes - Whitney), Hixson - Crowell, Weibull, Higuchi, Korsmeyer - Peppas) [45,124-129] and convert them for example into integral equations [138]. Nevertheless, in literature are also new approaches described [130]. As disadvantageous of the model dependent comparison could be seen that the chosen model does not fit over the complete dissolution curve and that the predicted asymptotic value of the concentration is not with the necessary accuracy [139,140]. Furthermore the best function is often more shape than mechanism descriptive [139]. Additionally, for similarity test between experimental and modeled curves an extra similarity test could be performed [141]. Beside dissolution profile comparison model dependent approaches could give a mechanistic point of view. Sometimes two or more models are capable in this case the information that essentially describes the dominant mechanism is chosen [139].

The model dependent approach is used for prediction of dissolution profiles and described in chapter 3.5.6. Focus in this PhD thesis for dissolution profile comparison are the model independent methods, which could be ordered into ratio test procedure (e.g. mean dissolution time) and pair wise comparison [140].

### 3.6.2.1. Mean Dissolution Time

The Mean Dissolution Time (MDT) is a strict empirical model [35]. Advantageous is the amenability to direct data treatment. Disadvantageous is the strong dependence on the upper limit of the dissolution profile [139].

In this PhD thesis comparison of profiles was not only done visually but also with calculation of the MDT. The MDT summarizes the whole profile into one number. It was calculated with Equation 3.12. Where  $\bar{t}_i$  is the midpoint of time period during which the fraction  $\Delta M_i$  has been released from the dosage form [35,139]. Calculations were performed applying program "R".

$$MDT = \frac{\sum_{i=1}^n \bar{t}_i * \Delta M_i}{\sum_{i=1}^n \Delta M_i}$$

Equation 3.12 For determining the mean dissolution time from the respective data set [35,139].

### 3.6.2.2. Difference and Similarity Test

Comparison of the different dissolution profiles was performed with the difference and similarity factor introduced by Moore and Flanner [142]. The European Medicines Agency (EMA) [120] as well as the Food and Drug Administration (FDA) [21] advice for the comparison of dissolution profiles the use of these "fit factors". The difference ( $f_1$ ) (Equation 3.13) and the similarity ( $f_2$ ) (Equation 3.14) factor are model independent approaches that directly compare the difference between percent drug released per unit time for a test and a reference product. Where  $n$  is the number of dissolution samples taken (number of samples),  $R_t$  and  $T_t$  are the mean percent drug released at each time point for reference and test product, respectively. For two curves to be considered similar  $f_1$  needs to be smaller 15 ( $f_1 < 15$ ) and  $f_2$  needs to be larger than 50 ( $f_2 > 50$ ) [21,120].

$$f_1 = \frac{\sum_{t=1}^n |R_t - T_t|}{\sum_{t=1}^n R_T}$$

Equation 3.13: Formula to derive the difference factor

$$f_2 = 50 * \log \left[ \frac{1}{\sqrt{1 + \frac{1}{n} \sum_{t=1}^n (R_t - T_t)^2}} * 100 \right]$$

Equation 3.14: Formula to derive the similarity factor

FDA and EMA require for the correct calculation of the similarity factor the following conditions I) same test conditions for test and reference product, and especially same sampling points, II) only one more value after reaching 85% dissolved drug amount [21,120], III) using the mean values, the coefficient of variation should be less than 20% for the first point and less than 10% for following points [21] and IV) twelve individual values for every time point for each formulation [21,120].

Advantageous is the reduction of complex dissolution profiles through an easy calculation into one number. Additionally, to the requirements of EMA and FDA for ensuring real similarity between profiles are the shape and the maximum dissolved amount [143]. In literature several disadvantages of the two fit factors are discussed. The drawbacks listed are I) no indication of sense of the deviation (below, above), II) no consideration of the shape of the curve, III) no information about variability inside the batch [139,143], IV) the factors are sensitive for measurements above 85% of the drug amount dissolved, V) sensitivity to the number of dissolution time points [143], VI) level of confidence for the  $f_2$  test is uncertain with low statistical power [143,144] and large difference between individual extremes are ignored due to usage of the arithmetic mean [144].

Calculations were performed applying Excel 2007 (Microsoft Office, Windows)

# Chapter 4

## Results & Discussion

## 4.1. Pre - test Results

In this chapter the results of the pre - tests are summarized. A detailed discussion of the results follows according to the dissolution techniques.

### 4.1.1. Determination of LoQ, solubility and micelle size

Table 4.1: HPLC LoQ results

	Budesonide	crystalline base	Substance A amorphous base	bromide
concentration [µg/ml]	0.052	0.099	0.044	0.046
RSD [%]	4.45	5.99	2.29	4.54
signal noise ratio	< 10	< 10	< 10	<10

Table 4.1 displays the LoQ concentrations for Budesonide and Substance A. The FPD masses on the membrane for dissolution tests should be above the LoQ of HPLC analysis but still allow sink conditions in the dissolution test set up.

Table 4.2: Solubility of substances in PBS buffer with and without surfactant (22°C, 24h)  
Budesonide, Fenoterol and Substance A in PBS buffer, n = 3, for Substance A in PBS buffer with surfactant n = 1

	Budesonide [µg/ml]	Fenoterol HBr [µg/ml]	Substance A [µg/ml]		
			cryst. base	amorp. base	bromide
PBS buffer	17	43000	7	211	265
+ 0.02% DPPC	21	-	6	116	2505
+ 0.2% SDS	406	-	847	504	2033
+ 0.2% Tween® 20	40	-	22	663	3865
+ 0.2% Tween® 80	53	-	-	-	-

The solubility of substances, expect of Substance A base using DPPC, is increased. Interestingly the solubility increases for the poor soluble Substance A crystalline base and Budesonide is for SDS highest. For the amorphous base and the dibromide the increase of solubility using Tween® 20 is higher than using SDS (Table 4.2).

The micelles of SDS, Tween® 20 and 80 can pass the pores of the used membranes with a pore diameter of 0.4 – 0.45 µm. DPPC forms large objects, which are too large for passing the membrane (Table 4.3).

Table 4.3: Micelle size of surfactants in PBS buffer (measured with dynamic light scattering)

	Peak 1 Mean [nm]	Peak 2 Mean [nm]
PBS buffer		
+ 0.02% DPPC	1106	0
+ 0.2% SDS	7	222
+ 0.2% Tween® 20	12	2473
+ 0,2% Tween® 80	11	0

## 4.1.2. Substance classification

### 4.1.2.1. Budesonide – Respirose blend

Table 4.4: Mixture homogeneities of Budesonide – Respirose blend content in % is referred to Budesonide weight

samples	mixture 1 (20 minutes)	mixture 2 (20 minutes)
1	1.5 %	1.5 %
2	1.6 %	1.6 %
3	2.0 %	1.7 %
4	1.5 %	1.4 %
5	1.9 %	3.7 %
RSD	15.0 %	47.2 %
RSD without outlier	12.4 %	8.6 %

Both mixtures show no optimum homogeneity (Table 4.4). However, without the outlier mixture 2 is more homogeneous and therefore was used for further experiments.

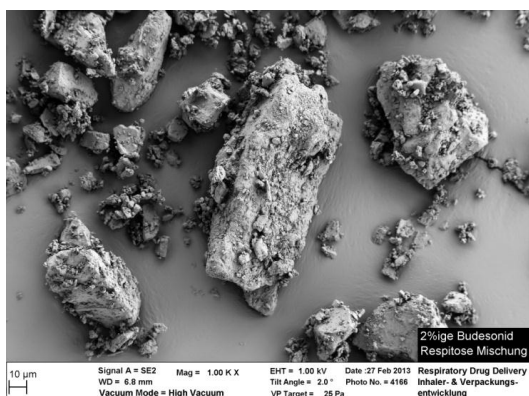


Figure 4.1: SEM picture: 2%Budesonide-Respirose blend

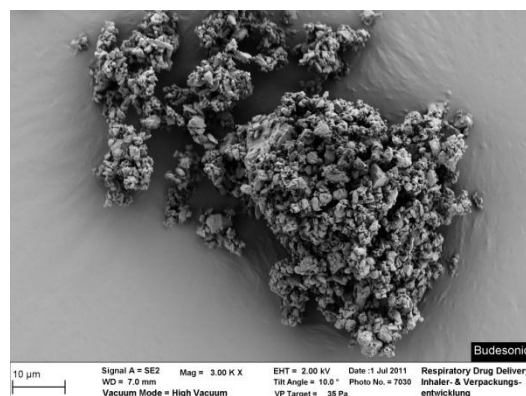


Figure 4.2: SEM picture micronized Budesonide

In Figure 4.1 the smaller particles are probably Budesonide and the larger ones Lactose. If the SEM picture is compared to the micronized Budesonide (Figure 4.2) a definite differentiation is not possible.

#### 4.1.2.2. Particle size

Table 4.5: Geometric particle size (measured with laser diffraction)  
mean  $\pm$  SD, n = 3, x10, x50, x90 = 10%, 50%, 90% of particle diameter in  $\mu\text{m}$   
Q5 = volume% of particles with a diameter  $\leq 5\mu\text{m}$

	Budesonide	Fenoterol HBr	cryst. Base	Substance A amorp. base	bromide
x10 [ $\mu\text{m}$ ]	0.54 $\pm$ 0.01	0.69 $\pm$ 0.01	0.71 $\pm$ 0.02	0.52 $\pm$ 0.02	0.62 $\pm$ 0.01
x50 [ $\mu\text{m}$ ]	1.53 $\pm$ 0.02	1.90 $\pm$ 0.01	1.64 $\pm$ 0.00	1.24 $\pm$ 0.03	1.67 $\pm$ 0.07
x90 [ $\mu\text{m}$ ]	3.69 $\pm$ 0.03	4.03 $\pm$ 0.01	3.54 $\pm$ 0.08	3.07 $\pm$ 0.10	6.65 $\pm$ 0.63
Q5 [Vol%]	96.52 $\pm$ 0.18	95.83 $\pm$ 0.07	97.68 $\pm$ 0.48	97.45 $\pm$ 0.32	84.02 $\pm$ 2.24

Size distribution of Budesonide, Fenoterol HBr and modifications of Substance A particles measured by the laser diffraction technique is shown in Table 4.5. All substances except of Substance A dibromide showed a high amount of particles less than 5  $\mu\text{m}$ .

For determining the aerodynamic particle size distribution of Substance A, Budesonide and Fenoterol HBr ACI was used. Results are shown in Table 4.6. Percentages were calculated based on the capsule load (1 mg, Fenoterol 10 mg). As shown in Table 4.6 particle size distribution of Substance A dibromide and amorphous base is not significantly different to each other except stage 5. Furthermore, the amount of smallest particles (stage 6 - filter) of Substance A is increased versus Budesonide. Table 4.6 also shows only small difference between FPF calculated of data from particle size measurement of the whole ACI and directly determination of the FPF with the abbreviated ACI.

Table 4.6: Aerodynamic particle size distribution using the ACI, mean  $\pm$  SD, n = 3

	Substance A				
	Budesonide [%]	Fenoterol HBr[%]	cryst. base [%]	amorp. base [%]	Br <sub>2</sub> [%]
HH + capsule	24.0 $\pm$ 1.8	11.2 $\pm$ 1.8	27.7 $\pm$ 3.0	10.6 $\pm$ 3.4	8.9 $\pm$ 2.6
Adapter SIP High Top	20.5 $\pm$ 7.2	20.8 $\pm$ 7.2	9.6 $\pm$ 1.1	24.9 $\pm$ 5.0	12.0 $\pm$ 7.5
Presep	25.6 $\pm$ 3.8	48.7 $\pm$ 13.2	8.1 $\pm$ 1.9	41.3 $\pm$ 4.3	46.3 $\pm$ 8.2
Stage 0	2.2 $\pm$ 0.1	1.2 $\pm$ 0.2	0.1 $\pm$ 0.2	0.4 $\pm$ 0.1	1.1 $\pm$ 0.2
Stage 1	4.0 $\pm$ 0.2	2.0 $\pm$ 0.2	2.2 $\pm$ 0.3	0.8 $\pm$ 0.1	1.2 $\pm$ 0.2
Stage 2	4.7 $\pm$ 0.3	3.3 $\pm$ 0.2	3.9 $\pm$ 0.5	1.3 $\pm$ 0.4	0.9 $\pm$ 0.1
Stage 3	7.5 $\pm$ 0.6	4.6 $\pm$ 0.5	9.3 $\pm$ 1.1	2.2 $\pm$ 0.6	1.5 $\pm$ 0.5
Stage 4	6.9 $\pm$ 0.8	3.3 $\pm$ 0.7	13.9 $\pm$ 1.9	2.3 $\pm$ 0.9	1.7 $\pm$ 0.5
Stage 5	4.6 $\pm$ 0.4	1.3 $\pm$ 0.5	8.1 $\pm$ 1.4	1.9 $\pm$ 0.7	2.0 $\pm$ 0.5
Stage 6	0.8 $\pm$ 0.1	0.2 $\pm$ 0.1	1.4 $\pm$ 0.2	0.4 $\pm$ 0.2	0.3 $\pm$ 0.2
Stage 7	0.3 $\pm$ 0.1	0.1 $\pm$ 0.0	0.4 $\pm$ 0.1	0.2 $\pm$ 0.2	0.1 $\pm$ 0.1
Filter	0.4 $\pm$ 0.1	0.1 $\pm$ 0.0	0.4 $\pm$ 0.1	0.2 $\pm$ 0.1	0.1 $\pm$ 0.0
FPF (%) ACI	25.2 $\pm$ 1.9	12.9 $\pm$ 2.4	37.4 $\pm$ 4.6	8.5 $\pm$ 2.8	6.5 $\pm$ 1.8
FPF (%) aACI	27.8 $\pm$ 2.7	17.6 $\pm$ 1.7	45.5 $\pm$ 2.7	17.8 $\pm$ 3.7	6.5 $\pm$ 4.0

#### 4.1.2.3. Wettability

Table 4.7: Advanced contact angle for the different substances

Substances were pressed to tablets, (3 drops, 15 measurements per drop). Due to small remaining amount of Substance A amorphous base the test was performed one time

		Budesonide	Substance A		
		crystalline base	amorphous base	dibromide	
water	$\Theta$ [°]	72.7 $\pm$ 4.6	64.65 $\pm$ 30.21	83.5	78.9 $\pm$ 27.5
+ 0,02% DPPC	$\Theta$ [°]	52.2 $\pm$ 11.5	direct spreading	73.5	56.1 $\pm$ 20.1

In Table 4.5 results of contact angle measurement of small substance pellets with water or water containing 0.02% is displayed. Contact angle of substances are near the 90° border, above 90° the wettability is poor and below 90° the wettability is good. Hence, the used substances have a still hydrophilic character but they are near the “border” which advises to a reduced wettability. Results for Substance A dibromide and crystalline base show a reduced reproducibility. By adding 0.02% DPPC to the water the contact angle decrease, indicating a better wettability. For Substance A crystalline base the wettability increasing is such as high, that the droplet could directly spread on the pellet surface.

### 4.1.3. Dose collection

In the following dose collection pre – tests are summarized. Without the tests it is not possible to perform reliable dissolution tests because of possible unknown effects during dose collection.

Table 4.8: ACI flow through cell pretests, FPD on membrane in membrane pattern, mean  $\pm$  SD, n = 3

Position	Budesonide	Substance A		Br <sub>2</sub>
		crystalline base	amorphous base	
0 o'clock [ $\mu$ g]	58.1	69.6	24.1	46.4
3 o'clock [ $\mu$ g]	55.0	75.2	23.6	43.2
6 o'clock [ $\mu$ g]	54.3	50.3	19.6	46.8
9 o'clock [ $\mu$ g]	54.2	72.1	22.7	50.8
Mean $\pm$ SD [ $\mu$ g]	55.4 $\pm$ 1.9	66.8 $\pm$ 11.3	22.5 $\pm$ 2.0	46.8 $\pm$ 3.1

Table 4.8 displays no influence of membrane position in the pattern on FPD on each membrane. Hence, each membrane could be used for dissolution test or as reference filter, respectively.

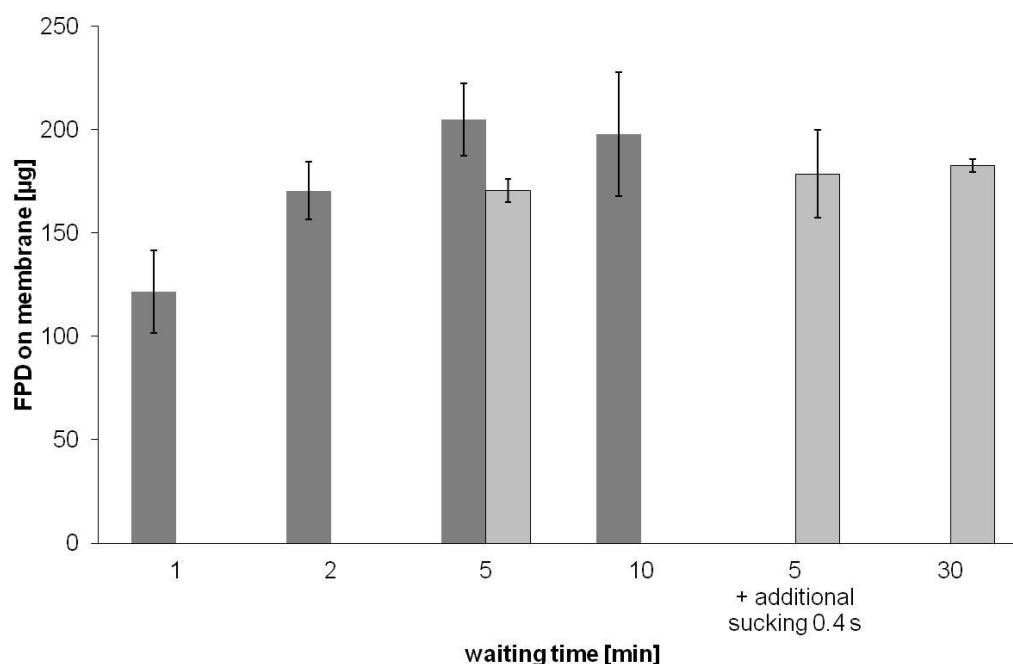


Figure 4.3: mACI pretest determination of waiting time, FPD of Budesonide on membrane, mean  $\pm$  SD, n = 3. The tests were performed on two different days, black bars on the one, grey bars on the other day

Figure 4.3 shows the impact of sedimentation or after pump stop waiting time on the FPD on membrane. Particles of the same substance have according to their size different sedimentation times. Therefore, with an increased sedimentation time up to 5 minutes the particle mass on the membrane is increased. Theoretically particles with an aerodynamic diameter of 1  $\mu$ m

need for a distance of 10 cm approximately 55 minutes [145]. An increased sedimentation time up to 10 minutes or even 30 minutes shows no significant higher amount of particles on the membrane. Furthermore, an additional pump time of 0.4 s after 5 minutes waiting was performed for impaction of the smallest particles. It is obvious that the variability compared to 5 minutes (grey bar) is highly increased and the amount of particles on the membrane was not increased.

Due to no significant higher amount of particles on the membrane for a sedimentation time larger than 5 minutes and the low amount of particles with an aerodynamic diameter of less than 1  $\mu\text{m}$  a waiting time of 5 minutes for all further experiments with the mACI set up was chosen.

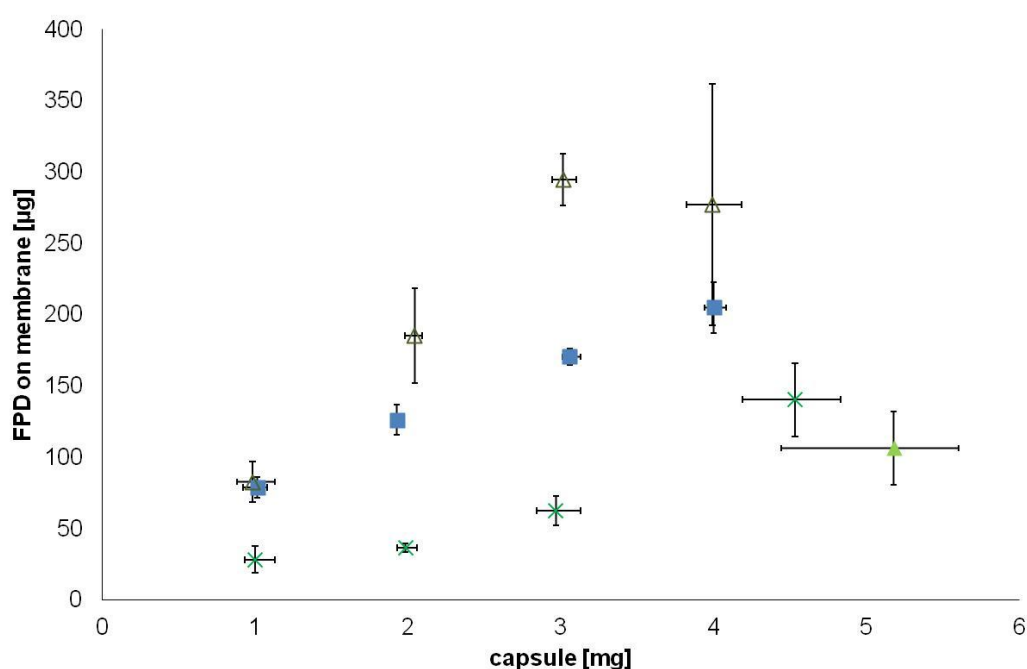


Figure 4.4: mACI determination of optimum powder weight into capsule, FPD: mean  $\pm$  SD, Budesonide (blue square), Substance A crystalline base (open dark green triangle), Substance A amorphous base (light green triangle) and Substance A Br<sub>2</sub> (green x), mean  $\pm$  SD, n = 3

In Figure 4.4 the determination of the required powder weight into capsule is shown. The FPD on the membrane is plotted against the amount of powder in the capsule before dose collection. Aim is to achieve a similar FPD on membrane for all the different substances. The limiting factors are time for emptying the capsule in the HH and LoQ of HPLC method. The pump time during dose collection and hence the time for capsule emptying is limited by the height of the used stage extension. As described in chapter 3.3.1.3 the aerosol should only reach the middle of the stage extension for allowing sedimentation of particles. Hence, the substance mass in the capsule should not be higher than 4 mg to 5 mg. The LoQs of all substances are summarized in Table 4.1. The amount of dissolution medium used in Franz cell

and paddle apparatus is 1 l, thus the minimum FPD is 99  $\mu\text{g}$  (LoQ crystalline base: 0.099  $\mu\text{g}/\text{ml}$ ). Therefore, a FPD between 100  $\mu\text{g}$  and 200  $\mu\text{g}$  was chosen.

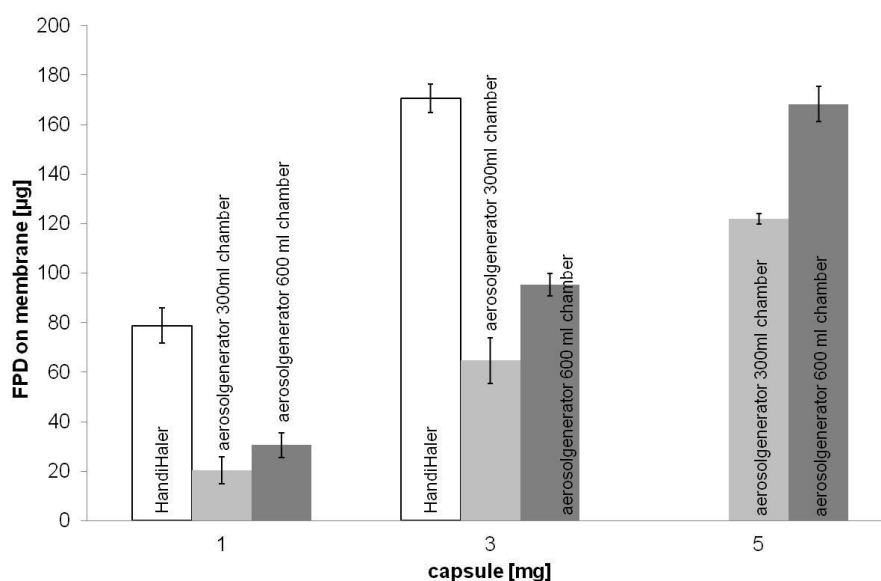


Figure 4.5 Comparison of HH and aerosol generator with mACI FPD on membrane for Budesonide, mean  $\pm$  SD, n = 3

Table 4.9: Comparison of HH and aerosol generator with mACI, FPD on membrane, n = 1

substance	capsule [mg]	FPD on membrane [ $\mu\text{g}$ ]		
		HandiHaler	aerosol generator chamber volume	
			300ml	600 ml
Substance A crystalline base	1	82.7	26.9	13.4
	3	294.5	65.3	38.0
	5	-	116.8	53.9
Substance A amorphous base	1	-	33.77	16.8
	3	-	82.75	77.6
	5	-	124.9	114.2
Substance A di-bromide	1	28.1	3.3	8.1
	3	62.3	33.1	20.4
	5	-	75.5	39.9

The results from Figure 4.5 and Table 4.9 show as expected a difference between the 300 ml and 600 ml aerosolisation chamber of the aerosol generator. Using the larger chamber the aerosol has more space for expansion without sticking at the walls and a higher amount reaches the membrane. Astonishingly, a comparison of aerosol generator and HH displays a higher amount of FPD for HH than for aerosol generator. Hence, the HH has the better de-agglomeration properties and the usage is justified.

#### 4.1.4. Membrane classification

The SEM pictures (Figure 4.6) demonstrate the different structures and pore densities of the used membrane materials. Polycarbonate (PC) and polyester (PE) membrane are both tracked-etched filters having more or less straight pores crossing the membrane. However, the regenerated cellulose membrane has more spongy structure.

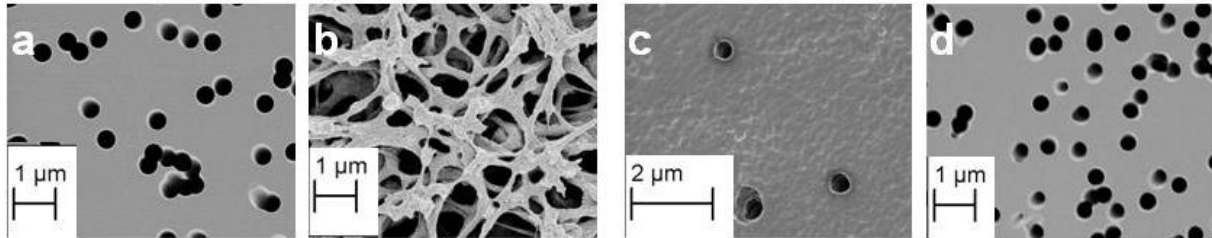


Figure 4.6: a) Isopore® Polycarbonate, b) regenerated cellulose, c) Transwell®-Polyester, d) Transwell® Polycarbonate

The Figure 4.7 - Figure 4.10 display the results of membrane permeation tests for the four used membrane materials and the substances. The figures show the diffused amount of substance through the membrane. It is obvious that there are substance depending differences but similar is a substance retaining effect of the Transwell® PE and PC membrane. For Budesonide (Figure 4.7) and Substance A dibromide (Figure 4.10) the Transwell® PE has the slowest diffusion process. For Budesonide the rank order of membrane permeability is IPC > RC > PC and PE membrane.

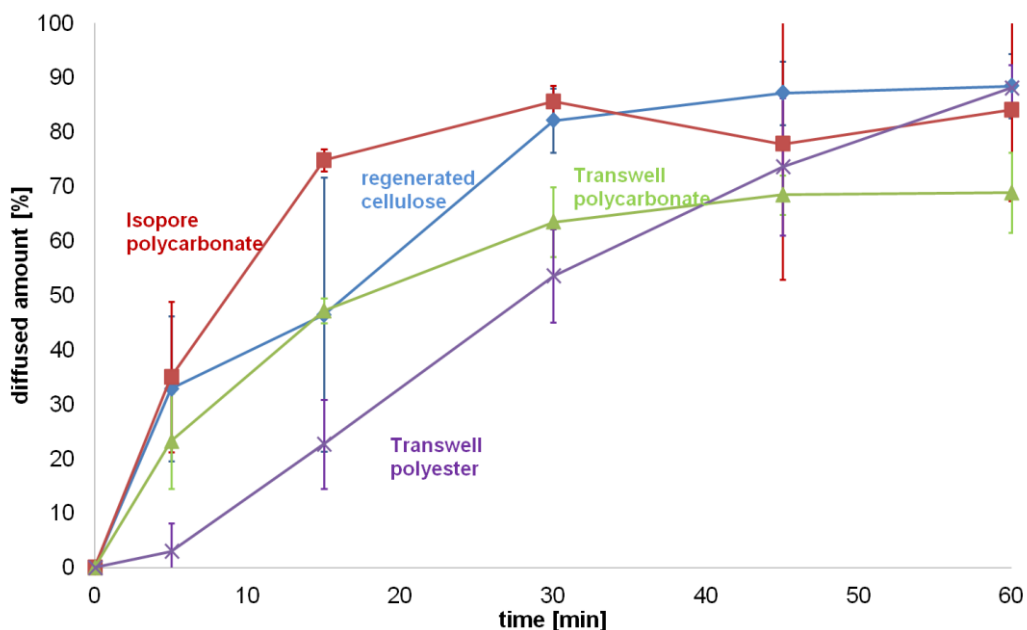


Figure 4.7: Membrane permeation test for Budesonide Isopore™ polycarbonate (red square), regenerated cellulose (blue rhomb), Transwell® polycarbonate (green triangle) and Transwell® polyester (purple x), mean ± SD, n = 3.

For Substance A base (Figure 4.8 and Figure 4.9) the rank order of the mean of membrane permeability is RC > IPC > PE > PC. However, due to the large error bars the profiles of RC and IPC appear to be similar.

The results are confirmed by the experiments of Bhagwat et al. who could demonstrate a reduced diffusion using the PC membrane [62].

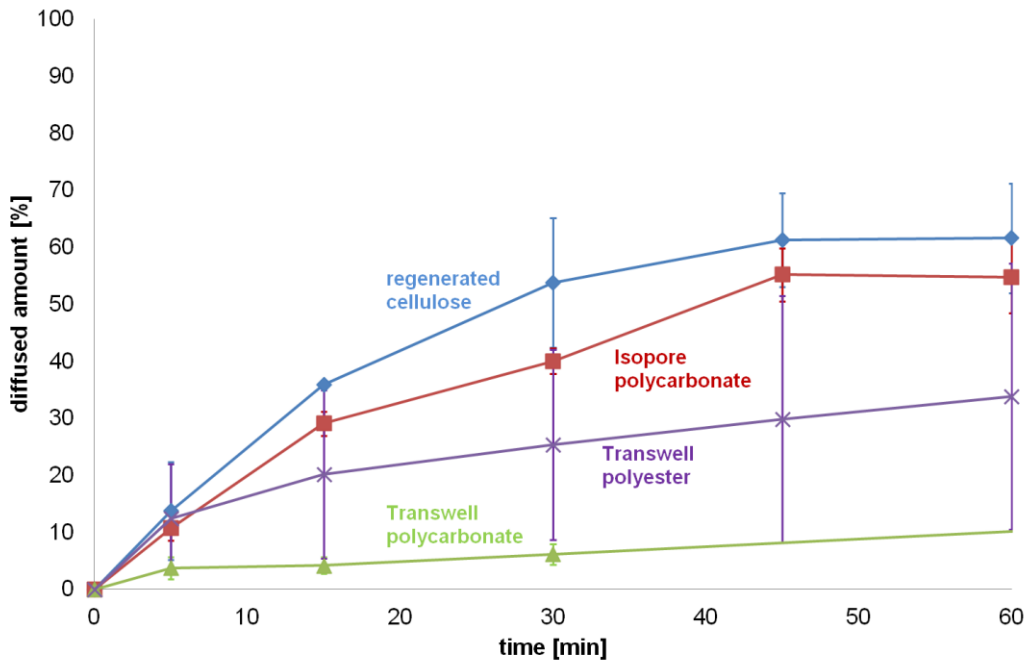


Figure 4.8: Membrane permeation test for Substance A crystalline base Isopore™ polycarbonate (red square), regenerated cellulose (blue rhomb), Transwell® polycarbonate (green triangle) and Transwell® polyester (purple x), mean  $\pm$  SD, n = 3.

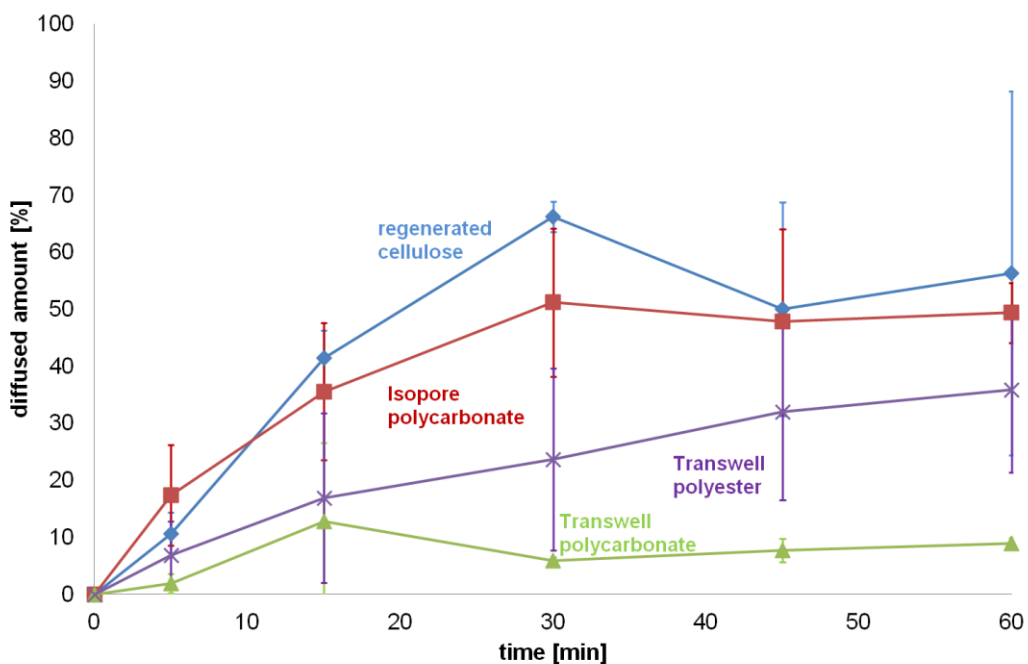


Figure 4.9: Membrane permeation test for Substance A amorphous base Isopore™ polycarbonate (red square), regenerated cellulose (blue rhomb), Transwell® polycarbonate (green triangle) and Transwell® polyester (purple x), mean  $\pm$  SD, n = 3.

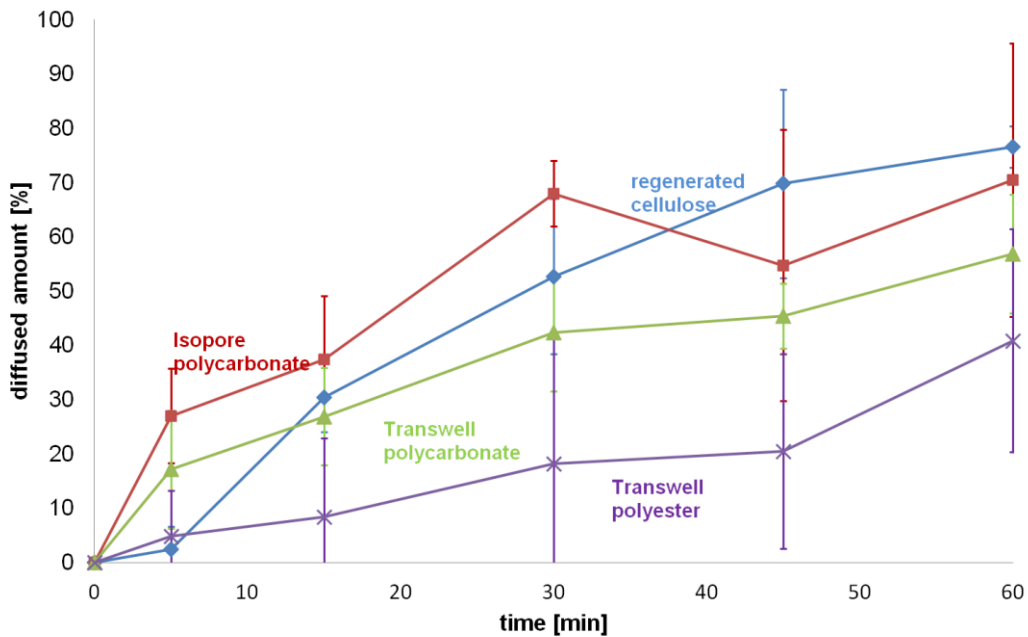


Figure 4.10: Membrane permeation test for Substance A dibromide Isopore™ polycarbonate (red square), regenerated cellulose (blue rhomb), Transwell® polycarbonate (green triangle) and Transwell® polyester (purple x), mean  $\pm$  SD, n = 3.

Table 4.10: Advanced contact angle for the different membranes (mean  $\pm$  SD, n = 4, 15 measurements per drop)

		Isopore™ poly-carbonate	Transwell® poly-carbonate	Transwell® polyester
water	$\Theta$ [°]	$57.4 \pm 1.9$	$63.7 \pm 9.3$	$43.5 \pm 4.2$
+ 0,02% DPPC	$\Theta$ [°]	$36.3 \pm 2.0$	$45.5 \pm 15$	$35.7 \pm 7.4$

Table 4.10 shows the results of contact angle measurements. For the regenerated cellulose a measurement was not possible due to spreading of the droplet because of the spongy structure and the high hydrophilicity (complete wetting). The contact angles for PC and PE membrane are less than  $90^\circ$  hence the chosen membranes have a more hydrophilic surface. Comparison of Isopore™ and Transwell® PC membrane displays a lower reproducibility for the Transwell® membrane. Hence, on the Transwell® membranes are areas with different hydrophobic or hydrophilic properties.

As expected by adding DPPC the surface tension of the droplet is reduced and thus the wettability of membrane increased.

## 4.2. μDiss Profiler™

In Figure 4.11 dissolution profiles for the tested substances are shown. The lag time from zero to one minute is the time needed for transferring the API suspension from the twin stage impinger to the μDiss vessels. It is obvious that for Substance A amorphous base and dibromide 100 % were dissolved within the lag time and thus no discrimination is possible. For Budesonide the process starts from 28% and reaches in the first 10 minutes a plateau at around 85%. As expected from the solubility data Substance A crystalline base shows the slowest dissolution process, after 60 minutes only 10% are dissolved.

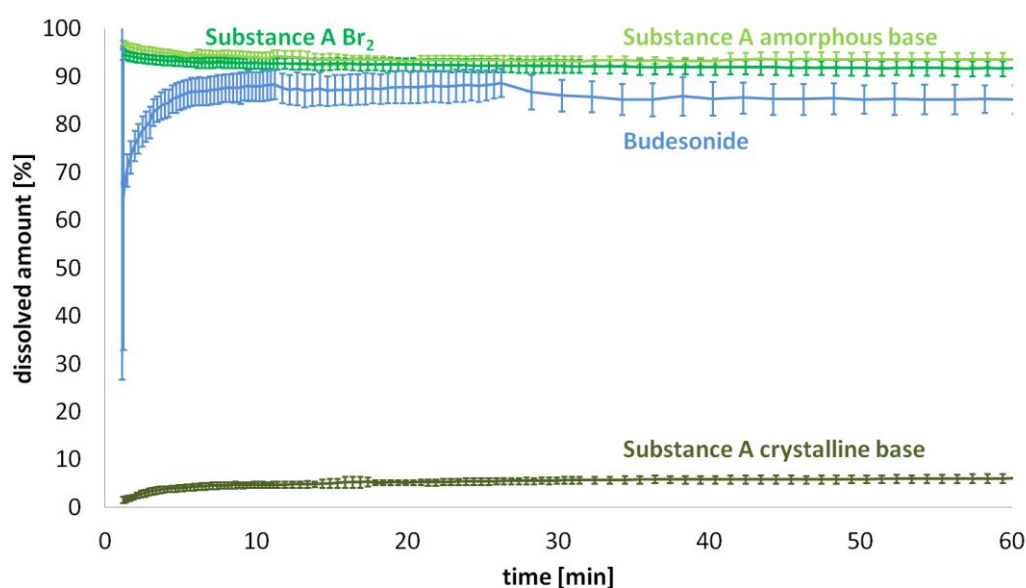


Figure 4.11: Dissolution profiles μDiss profiler after dose collection with Twin Stage Impinger, Substance A amorphous base (light green), Substance A dibromide (green), Budesonide (blue), and Substance A crystalline base (dark green), mean ± SD, n = 3.

Advantage of the μDiss is undoubtedly the real time measurement with short time intervals. Furthermore, there is the possibility to weight a small amount of the powder directly into the vessel without an aerodynamic classification and deagglomeration step. Without a deagglomeration step the possibility of increasing variability in dissolution profiles is given due to varying particle sizes or agglomerates. In addition, it is the only dissolution technique without membrane, therefore possible substance - membrane interactions are not existent.

If there is an interest in dissolution of fine particle dose, first a dose collection method is necessary. The twin stage impinger has been proved as beneficial compared to the ACI, due to the direct collection as suspension. For transferring the suspension into the dissolution vessels a lag time is required. During this lag time the dissolution processes could already be started and when sample measurement starts for some substances 100% dissolved are already reached. A further disadvantage is the unknown particle mass in the sample because

for calculating and reporting the software needs the exact amount of substance. Hence, HPLC analysis must be used additionally

Another drawback is the complicated and error - prone calibration, especially if there is a difference between solvent and dissolution media needed. This difference might be necessary, if concentration in the dissolution medium is at the solubility limit.

With a view to the used substances, Substance A amorphous base and Substance A dibromide have already reached 100% dissolved at the starting point, resulting in an impossible discrimination. Hence, the dissolution is too fast, for this technique.

Summarizing the μDiss dissolution technique is not useful for dissolution of inhalative powders, but a useful tool for determination of the solubility of substances in early stage of development.

### 4.3. Flow Through Cell

#### 4.3.1. Diffusion pre-tests

The diffusion test (Figure 4.12, left) demonstrates the applicability of the modified flow through cell. By pumping the substance – buffer - solution without the cell (background noise) directly into graduated flask 89.3 %  $\pm$  3 % of the dissolved amount are recovered. The amount is lower as expected. A value of almost 100% was expected. If the cell is used, interestingly recovery rate of diffused substance increases. Hence, the question arises were the substance is lost.

A possible interaction between substance and tube could be excluded, because PEEK tubes were used.

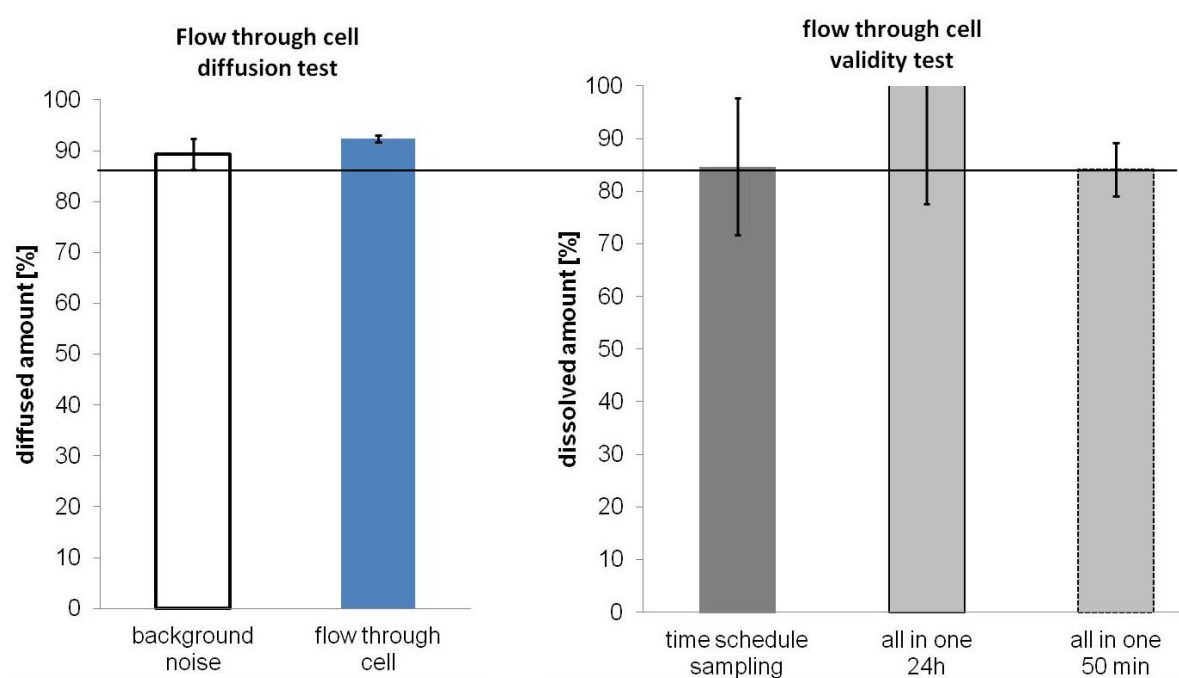


Figure 4.12. Left side: diffusion test with background noise (white) and flow through cell (blue), right side: validity test with time schedule sampling (dark grey), all in one 24 h (light grey), all in one 50 min (light grey, dashed line), mean  $\pm$  SD, n = 3

The validity test (Figure 4.12 right) for time schedule sampling over 60 minutes and the “all in one” sampling over 50 minutes shows similar results. However, for the “all in one” sampling standard deviation is smaller. The validity test for all in one sampling over 24 h shows a high variability of data. Comparison of diffusion test and validity test indicates a larger variability of data for the validity test. Additionally, the standard deviation exceeds the background noise base line. One possible reason might be that the powder is directly weighed onto the membrane, resulting in a less uniform particle distribution on membrane, due to the micronisation of Budesonide. In micronized powders, amongst others, triboelectric forces between particles might be high and the fine particles stick together [146]. Hence, the fine particles form agglomerates, which are not splitted during the weighing process. The agglomerates have a

smaller surface compared to their volume than the fine particles, resulting in a different dissolving behavior, with decreasing surface solubility rate is increased [31,146].

### 4.3.2. Dissolution testing

Due to possible influence of the sampling on the results (Figure 4.13), the two possible sampling methods –“all” vs. “partial”- are compared. Drawing inferences from the dissolution profiles about similarity or differences is due to the high variability of dissolution profile data not possible. Calculation of the discarded amount in the partial set up was double checked with a different calculation attempt. In this different calculation approach the slope between single points was calculated. Both calculation attempts gave the same result.

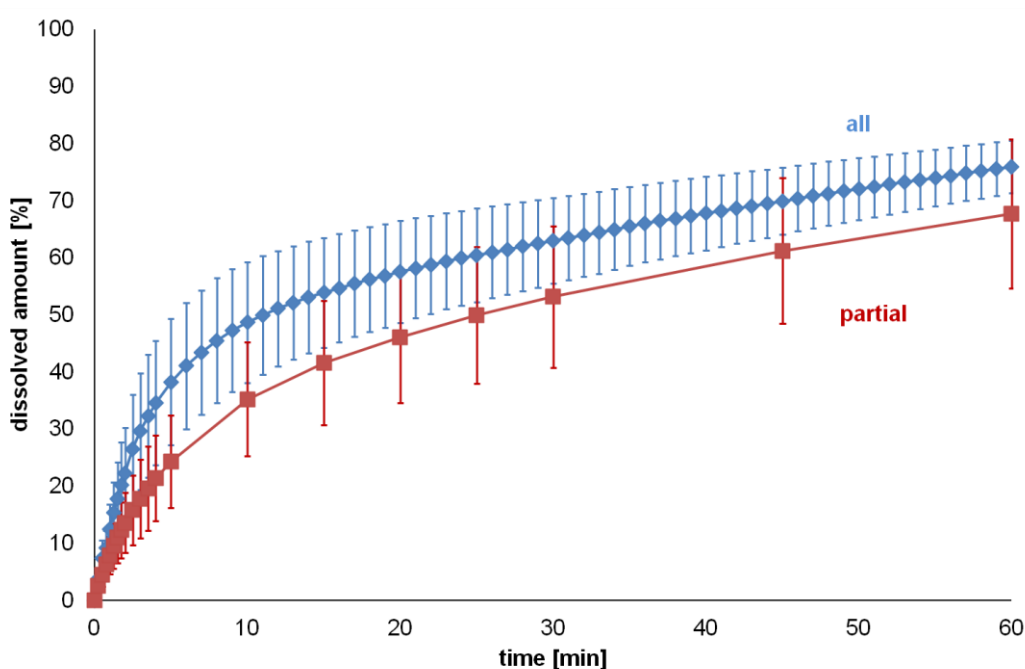


Figure 4.13: Influence of sampling type on Budesonide dissolution profile all (blue rhomb), partial (red square), mean  $\pm$  SD, n = 3

A further experiment determined the influence of flow rate (Figure 4.14) on the dissolution process and thus on the dissolution profile. The dissolution profiles show all a high variability, therefore only trends should be mentioned. Rank order expected was 0.5 ml/min as slowest and 5 ml/min as fastest dissolution profiles. With a slower dissolution rate the process in the cell should be more diffusion controlled. If the flow rate increases in addition pressure and hydrodynamic effects increases and they should be the controlling effects. This order is only in the first two minutes and the last ten minutes given: in between 1 ml/min dissolution profile is faster than the 5 ml/min. As previously described the high variability of the data reduces the interpretability. For this reason and for the more convenient handling for further experiments a flow rate of 1 ml/min was used.

A reason for high variability might be pump depending. If the dissolution medium is not pumped continuously through the cell, already dissolved substances could be flow back in the inlet tubing. For avoiding these effects a HPLC pump with internal pulse damper was used, for ensuring an almost pulsating free dissolution medium flow.

Concerning the MDT (Table 4.11) no significant difference between the profiles is shown.

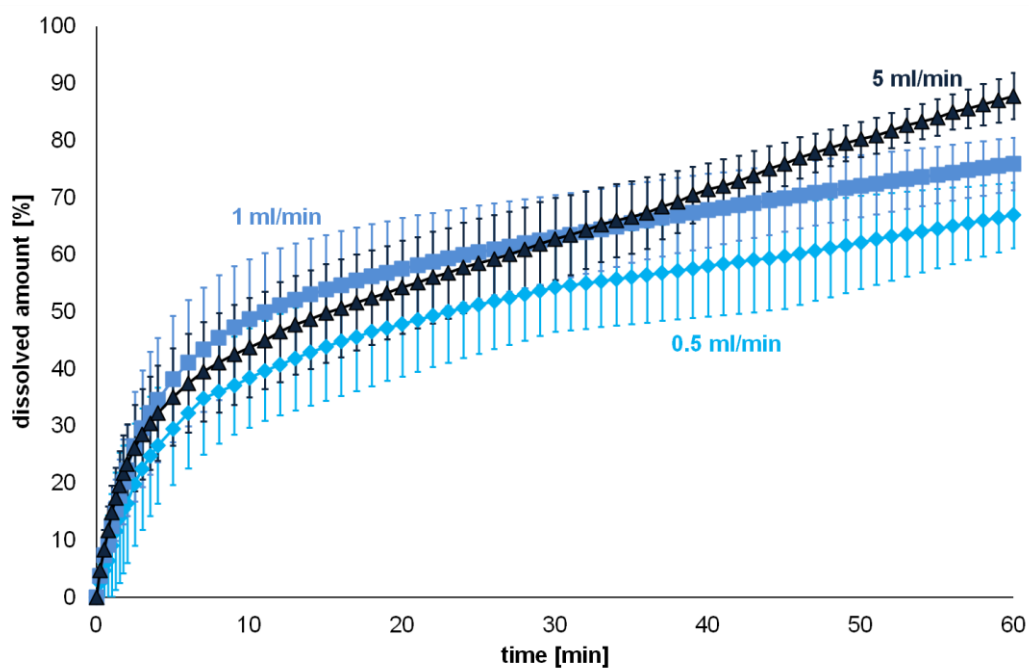


Figure 4.14: Influence of flow rate on Budesonide dissolution profile  
0.5 ml/min (turquoise rhomb), 1 ml/min (light blue square) and 5 ml/min (dark blue triangle) mean  $\pm$  SD, n = 3

Table 4.11: Summary of substance, flow rate, FPD on reference filter, recalculated FPD on filter (mean  $\pm$  SD) and MDT (mean  $\pm$  SD)

substance	Flow rate [ml min <sup>-1</sup> ] sampling type	powder weight [mg]	reference filter [ $\mu$ g]	filter flow through cell [ $\mu$ g] n = 3		MDT [min]	
				mean	$\pm$ SD	mean	$\pm$ SD
Budesonide	0.5; all 1; all 1; partial 5; all	1	25.9	12.5	$\pm$ 2.4	17.0	$\pm$ 6.9
			7.5	11.0	$\pm$ 2.8	13.5	$\pm$ 3.1
			7.4	30.3	$\pm$ 9.9	16.6	$\pm$ 2.1
			15.4	31.3	$\pm$ 15.0	18.2	$\pm$ 4.1
Fenoterol	1, partial	5	10.9	15	$\pm$ 1.8	6.3	$\pm$ 0.2
		10	11.7	10.2	$\pm$ 2.1	11.1	$\pm$ 7.2
		15	42.5	32.6	$\pm$ 5.1	1.5	$\pm$ 0.3
Substance A crystalline Base	1, partial	3	13.2	35.0	$\pm$ 5.4	44.5	$\pm$ 3.8
		10	32	44.6	$\pm$ 3.5	44.5	$\pm$ 0.3
		15	54.7	66.5	$\pm$ 18.0	41.2	$\pm$ 5.4
Substance A amorphous base	1, partial	10	10.4	21.8	$\pm$ 3.6	9.2	$\pm$ 2.9
		30	120.6	158.0	$\pm$ 13.7	9.0	$\pm$ 1.7
		50	110.3	151	$\pm$ 17.3	11.5	$\pm$ 1.9
Substance A Br <sub>2</sub>	1, partial	10	10.7	18.9	$\pm$ 4.8	12.2	$\pm$ 3.6
		25	56.1	87.1	$\pm$ 9.6	5.7	$\pm$ 0.6
		40	179.7	164.5	$\pm$ 22.5	4.9	$\pm$ 2.3

In Figure 4.15 the dissolution profiles of Substance A amorphous base and in Table 4.11 the corresponding FPDs are shown. The dissolution profile 10 mg (light green rhomb) with a FPD of 10  $\mu$ g is in the first few minutes similar to the profile 30 mg (green square) with a FPD of 120  $\mu$ g. Over time the two profiles diverge. From the beginning the dissolution profile 50 mg (dark green triangle, FPD 110  $\mu$ g) shows a slower increase. It is obvious that variability of data is high and interpretability is difficult. The expected rank order, 10 mg - fastest dissolution profile due to smallest mass on membrane and 50 mg -slowest dissolution profile, is not given. In contrast, the profile with the highest mass on the membrane shows the fastest progression. The results for the other substances are similar concerning the variability and the non linearity between mass on membrane and speed of the dissolution (Table 4.11, Figure 4.16, Figure 4.17 and Figure 4.18).

Another very remarkable result is the relationship between reference filter amount and recalculated amount on experiment filter (Table 4.11), except for Fenoterol HBr. It is noticeable that there are often large differences between the results. The direction of divergence alternate so that a systematic bias could be excluded.

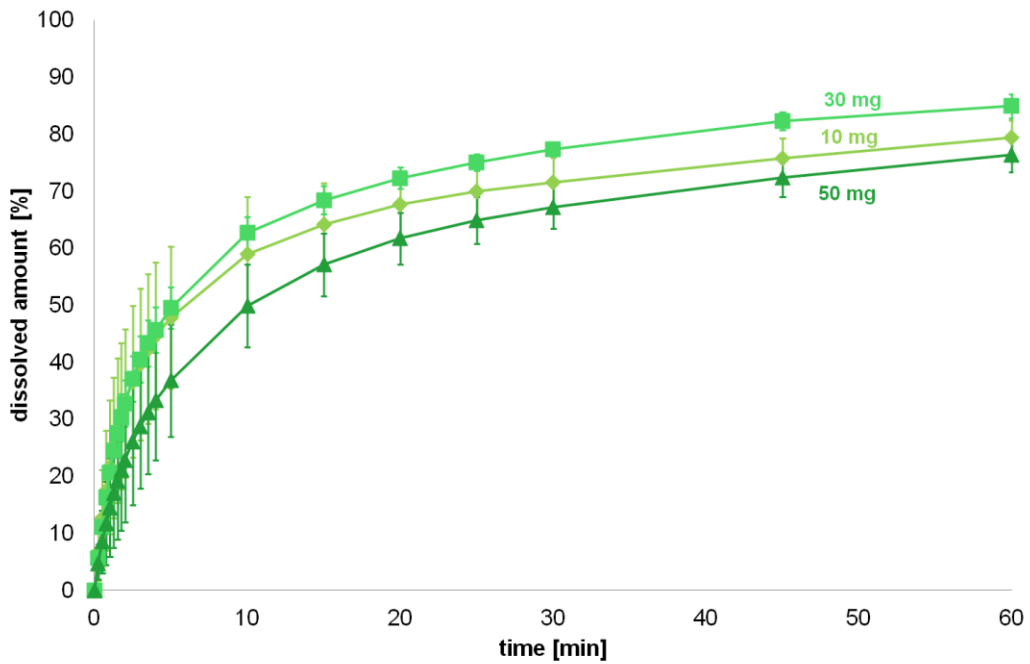


Figure 4.15: Substance A amorphous base

Influence of FPD on the membrane on dissolution profile.

10 mg (light green rhomb, FPD:  $21.8 \mu\text{g} \pm 3.6 \mu\text{g}$ ), 30 mg (green square,  $158.0 \mu\text{g} \pm 13.7 \mu\text{g}$ ) and 50 mg (dark green triangle,  $151 \mu\text{g} \pm 17.3 \mu\text{g}$ ) mean  $\pm$  SD, n = 3

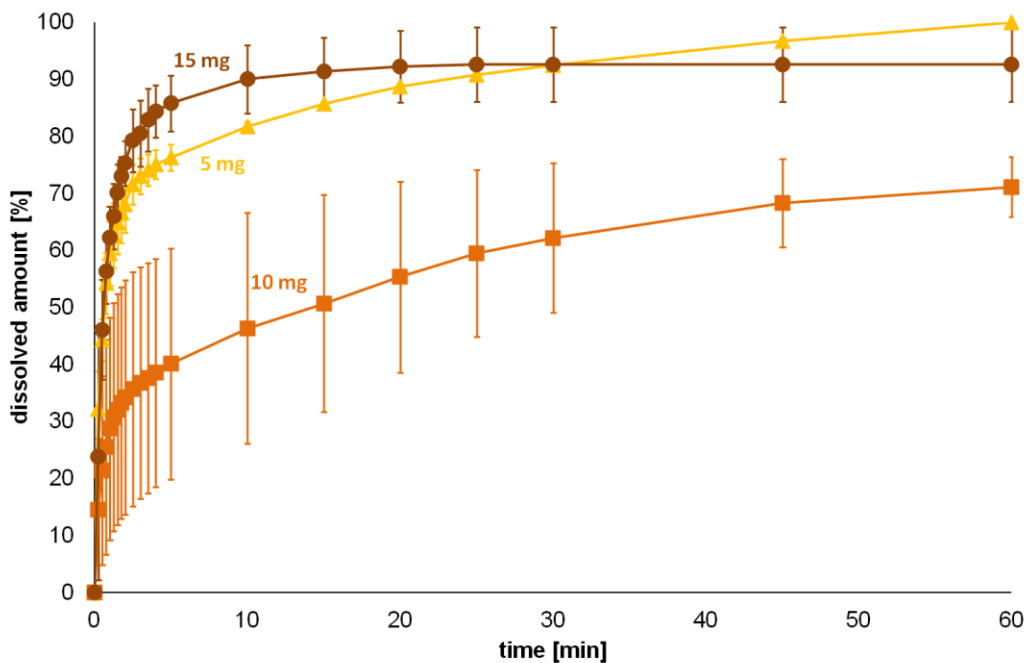


Figure 4.16: Fenoterol HBr

Influence of FPD on the membrane on dissolution profile.

5 mg (yellow triangle,  $15 \mu\text{g} \pm 1.8 \mu\text{g}$ ), 10 mg (orange square,  $10.2 \mu\text{g} \pm 2.1 \mu\text{g}$ ) and 15 mg (brown dot,  $32.6 \mu\text{g} \pm 5.1 \mu\text{g}$ ) mean  $\pm$  SD, n = 3

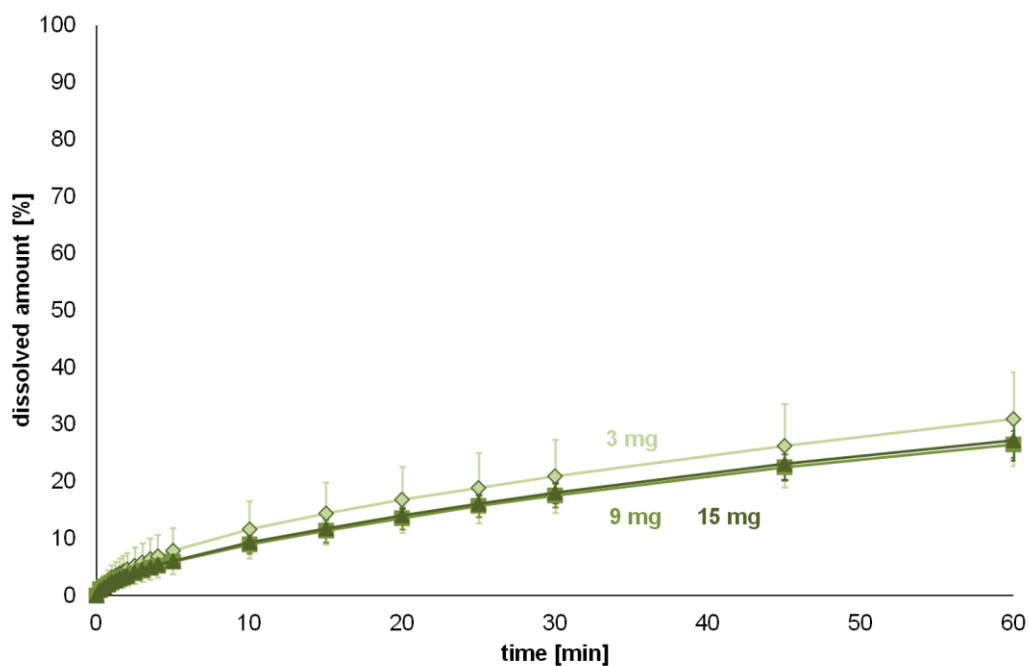


Figure 4.17: Substance A crystalline base

Influence of FPD on the membrane on dissolution profile.

3 mg (light green rhomb,  $35 \mu\text{g} \pm 5.4 \mu\text{g}$ ), 9 mg (green square,  $44.6 \mu\text{g} \pm 3.5 \mu\text{g}$ ) and 15 mg (dark green triangle,  $66.5 \mu\text{g} \pm 18 \mu\text{g}$ ) mean  $\pm$  SD, n = 3

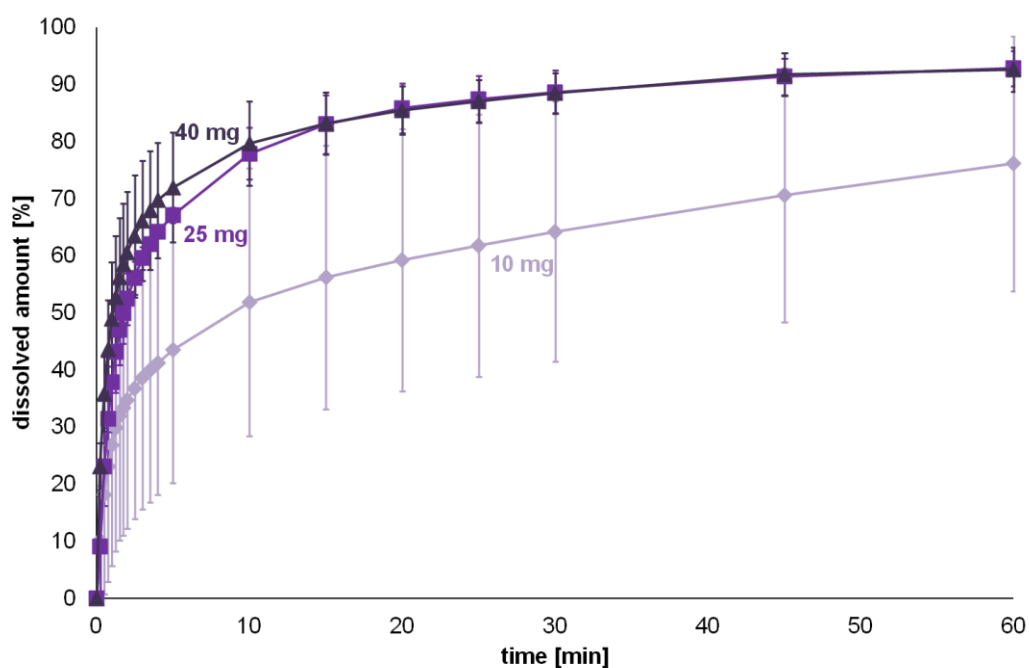


Figure 4.18: Substance A dibromide

Influence of FPD on the membrane on dissolution profile.

10 mg (light mauve rhomb,  $18.9 \mu\text{g} \pm 4.8 \mu\text{g}$ ), 25 mg (purple square,  $87.1 \mu\text{g} \pm 9.6 \mu\text{g}$ ) and 40 mg (dark purple triangle,  $164.5 \mu\text{g} \pm 22.5 \mu\text{g}$ ) mean  $\pm$  SD, n = 3

The newly developed flow through cell should combine the advantageous of standard flow through cell with usage for powders for inhalation. As described above the benefits of standard flow through cell are sink conditions due to infinite amount of dissolution medium in the open set up [82,105,106,108] and continuous sampling [82]. For testing of powders for inhalation, on detail the FPD, a particle size classification step is required. Therefore, aACI as dose collection method was used and the pre-test results (Table 4.8), concerning the homogenous mass on the four membranes, were promising. Furthermore, the diffusion pre-tests (4.3.1) prove the functionality of the flow through cell. The validity tests with a direct weighing onto the membrane without deagglomeration step, resulted in a high variability of data with a limited validity. Langebucher et al. advised that dead edges inside the flow through cell has to be avoided, because undissolved particles could deposited outside the fluid stream [105]. The new developed “quench heads” allow a homogenous fluid stream over the whole membrane area, dead edges should be eliminated. Additionally, material of flow through cell was changed to PEEK, which is predominantly inert against the used substances and the solvent (ACN) used in the rinsing step. Consequently, adsorption and interaction is reduced to a minimum. As described above there are further aspects concerning the difference between the sampling methods, flow rate, mass depending dissolution and difference between recalculated amount on membrane and reference filter.

Theoretically, the two profiles with the different time schedule based sampling methods are similar. Probably the suggested difference is not real, due to one possible outlier in each profile, resulting in a mean based bias and higher standard deviations. Hence, both sampling methods might be similar. The expected influence of flow rate on dissolution profile rank order (5 ml/min fastest, 0.5 ml/min slowest profile) was not detectable, due to the large standard deviation. One possible reason for the high variability might be the membrane material. The membrane has a small “pore” diameter for retaining undissolved particles. Hence, the small pores avoid a homogenous fluid stream in the cell and thus a homogenous wetting of the substance particles.

As shown in literature for paddle apparatus, Franz cell, and Transwell® dissolution process depends on the particle mass deposited on the membrane [55,61,131]. With increasing particle mass, dissolution profiles become slower. Under this assumption the expected rank order is not reached for the flow through cell, which is seen individually not critical, but for flow through cell no other tendency is detectable. In contrast, once the dissolution profile with the smallest FPD is fastest, once the one with the highest FPD is fastest.

The difference between recalculated FPD on experiment filter and reference filter is from dose collection point inexplicable, due to homogenous amounts on the membranes during pre-tests (Table 4.8). Conceivable might be a concentration processes or accumulation in-

side the flow through cell during dissolution experiment [105]. However, the same effect has to be discoverable for the diffusion experiment, but this is not given.

Furthermore, definition depending the open set up provides sink conditions [82,105,106,108] during the different experiments some samples showed even a higher concentration than solubility. Consequently, sink conditions weren't given over the whole dissolution process and the dissolution process is affected.

The last critical point is the data treatment. Due to the open set up, one sample represents the amount dissolved at a specific time interval. For a "traditional" dissolution profile these data has to be transformed into the cumulative form, with the consequence of mistake dragging [108]. As already described above calculation was double checked with a different approach, hence mistakes concerning the calculation are avoided.

Concerning the unexplainable problems with the new designed flow though cell for inhalation powders this technique is not advisable for dissolution testing of powders for inhalation.

## 4.4. Franz Cell

### 4.4.1. Diffusion test

As already shown in the general membrane permeation test (chapter 4.1.4) the permeability of the membrane depends on membrane material as well as on substance membrane interactions. In Figure 4.19 the results of diffusion test for the IPC membrane, in Figure 4.20 the results for the regenerated cellulose membrane are displayed

For Budesonide and Substance A amorphous base membrane permeation for IPC and RC is similar. For the crystalline base a trend is difficult to state because of large variability. For Fenoterol the diffusion through the IPC is faster and less variable compared to the regenerated cellulose membrane. The overall comparison of diffusion behavior through the IPC membrane is difficult due to large standard deviation for Substance A (Figure 4.19). Comparison between substances beside Fenoterol show quite similar diffusion through the regenerated cellulose membrane for all substances (Figure 4.20). Diffusion of Fenoterol through the membranes is much faster than for all other APIs.

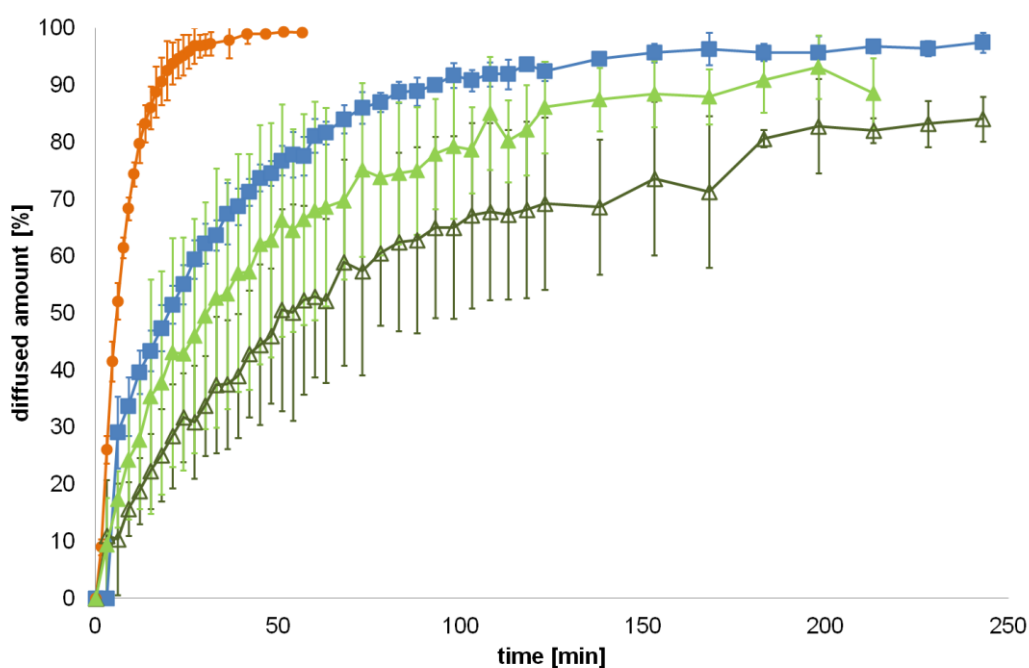


Figure 4.19: Diffusion of substances through IPC membrane  
Fenoterol HBr (orange dot), Substance A amorphous base (light green triangle), Budesonide (blue square) and Substance A crystalline base (dark open triangle), mean  $\pm$  SD,  $n = 3$ , error bars are in all cases existent but sometimes too small to be displayed

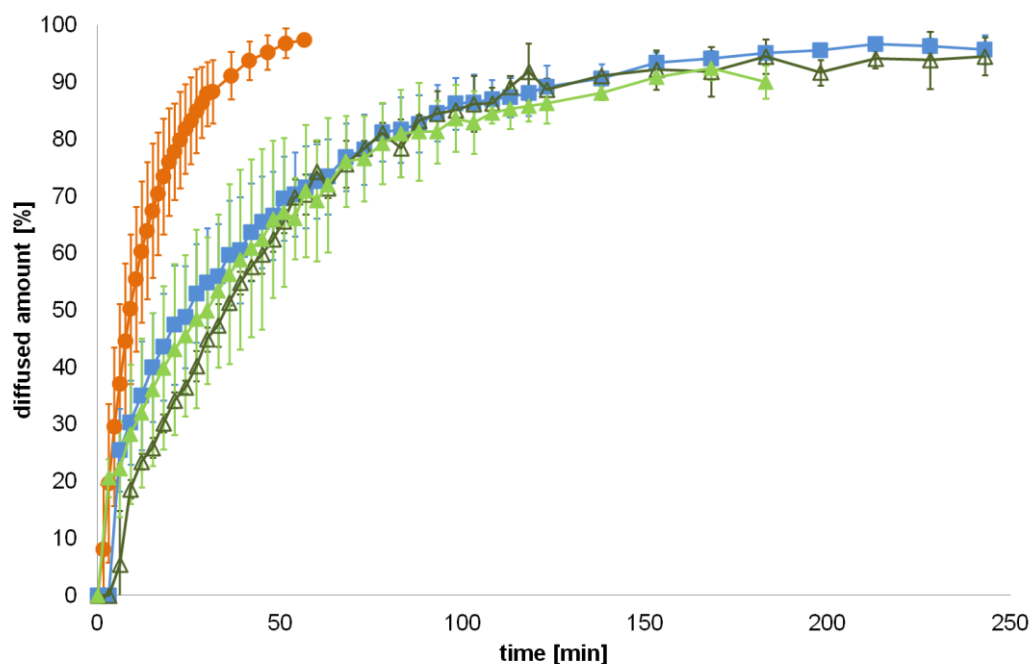


Figure 4.20: Diffusion of substances through RC membrane  
 Fenoterol HBr (orange dot), Substance A amorphous base (light green triangle), Budesonide (blue square) and Substance A crystalline base (dark open triangle), mean  $\pm$  SD,  $n = 3$ , error bars are in all cases existent but sometimes too small to be displayed

#### 4.4.2. Dose collection and dissolution testing

In Figure 4.21 the influence of fine particle mass collected on the membrane (Table 4.12) on the dissolution profiles for Fenoterol and Budesonide is displayed. Fenoterol shows a faster dissolution process than Budesonide due to its higher solubility (43 mg/ml, Budesonide 17  $\mu$ g/ml) (Table 4.2). Furthermore, the dissolution profiles of Fenoterol for FPD of 131.7  $\mu$ g  $\pm$  16.6  $\mu$ g and 1201.9  $\mu$ g  $\pm$  260.2  $\mu$ g on the membrane are not significantly different. For Budesonide a FPD on membrane dependency of the dissolution profile could be shown. The dissolution process with 189.7  $\mu$ g  $\pm$  15.5  $\mu$ g membrane loading is much faster than the profile with a FPD of 1151.3  $\mu$ g  $\pm$  7.8  $\mu$ g. It is obvious that for Budesonide “1 mg” only a few particles are widespread on the membrane, whereas for Budesonide “10 mg” the surface is completely covered, and the particles are agglomerated. The influence of the agglomerates and therefore a reduced surface area is larger for Budesonide than for Fenoterol. Reason could be found in the high solubility of Fenoterol. Due to the high wettability and solubility of Fenoterol the dissolution rate is almost independent of available surface area in this context. In contrast, for Budesonide the wettability and solubility are poor and the dissolution rate depends strongly on the available surface.

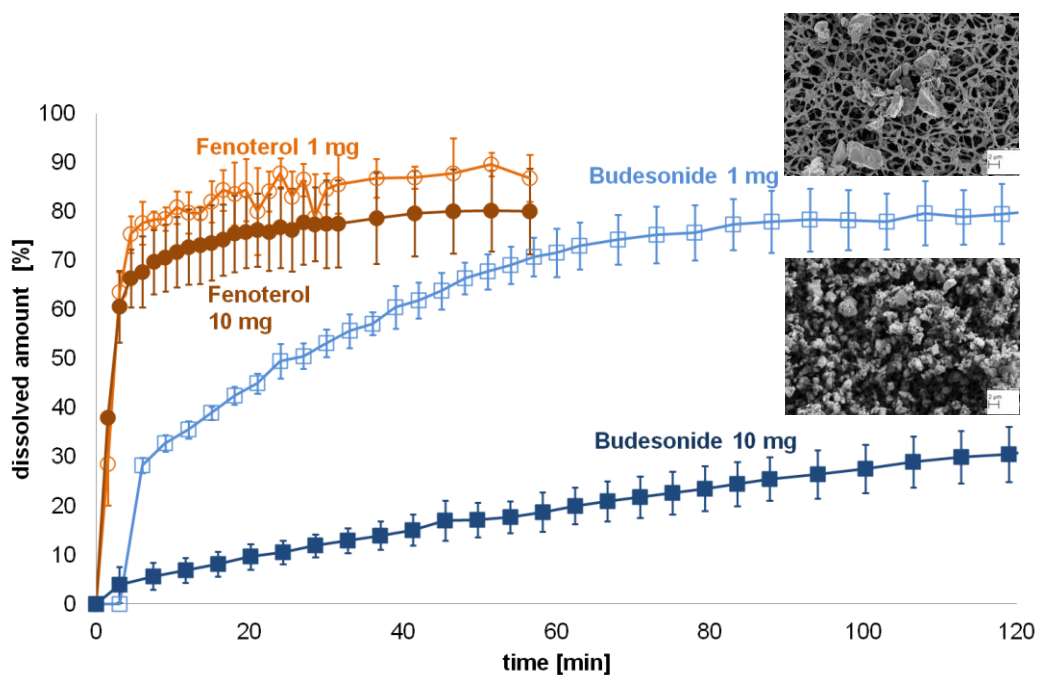


Figure 4.21: Influence of FPD on membrane on the dissolution of Budesonide and Fenoterol HBr RC membrane, Fenoterol HBr 1 mg (open orange dot), Fenoterol HBr 10 mg (dark orange dot), Budesonide 1 mg (open blue square) and Budesonide 10 mg (dark blue square), mean  $\pm$  SD,  $n = 3$ , error bars are in all cases existent but sometimes too small to be displayed, SEM picture for Budesonide 1 mg and Budesonide 10mg

Table 4.12: Summary of substance, membrane material, powder weight into capsule, recalculated FPD on filter (mean  $\pm$  SD) and MDT (mean  $\pm$  SD). The amount on membrane is recalculated from the maximum dissolved amount and the remaining particles on the membrane as described in chapter 3.6.1

substance	membrane material	powder weight [mg]	recalculated FPD on filter [ $\mu$ g]		MDT [min]	
			n = 3 mean	$\pm$ SD	mean	$\pm$ SD
Budesonide	IPC	1	195.3	$\pm 29.2$	78.3	$\pm 24.7$
		10	1151.3	$\pm 7.8$	248.9	$\pm 40.1$
	RC	1	189.7	$\pm 15.5$	80.7	$\pm 19.5$
Fenoterol	IPC	10	1286.4	$\pm 70.4$	1.7	$\pm 0.3$
		1	131.7	$\pm 16.6$	2.6	$\pm 0.1$
	RC	10	1201.9	$\pm 260.2$	4.5	$\pm 1.0$
Substance A crystalline Base	IPC	1	281.2	$\pm 63.6$	488.0	$\pm 9.7$
	RC	1	100.2	$\pm 15.5$	467.6	$\pm 73.1$
Substance A amorphous base	IPC	1	106.3	$\pm 16.8$	67.9	$\pm 32.3$
	RC	1	97.8	$\pm 9.5$	42.8	$\pm 14.4$
Substance A Br <sub>2</sub>	IPC	1	102.3	$\pm 49.8$	48.7	$\pm 32.4$
	RC	1	80.8	$\pm 30.2$	10.7	$\pm 3.1$

In Figure 4.22 and Figure 4.23 the dissolution profiles and in Table 4.12 the MDT for the different substances using RC and IPC membrane are shown. The rank order of dissolution

profiles for both membrane types is identical: Fenoterol – Substance A dibromide and Substance A amorphous base - Budesonide – Substance A crystalline base. This rank order, except Substance A dibromide and Substance A amorphous base depends on the solubility (Table 4.2). Assuming same particle density, spherical shape and similar aerodynamic and geometric diameter the reason for similar dissolution profile despite different solubility for Substance A dibromide and Substance A amorphous base could be found in particle size distribution (Table 4.6). The aerodynamic particle size distribution for Substance A amorphous base shows a higher rate of fine particles than for Substance A dibromide. The solubility rate of the substance beside others depends also on particle size. With decreasing particle diameter the surface increases dramatically, resulting in a faster dissolution for small particles.

Comparison between IPC and RC membrane type shows for Budesonide and Fenoterol for IPC a faster dissolution and for Substance A vice versa. The membrane permeation tests show a higher permeability for Fenoterol and Budesonide through the IPC than the through RC membrane (Figure 4.7, Figure 4.19, and Figure 4.20) due to smaller membrane-substance interactions. For Substance A diffusion test through the IPC membrane (Figure 4.19) displays a high standard deviation, because of larger interactions with the membrane material.

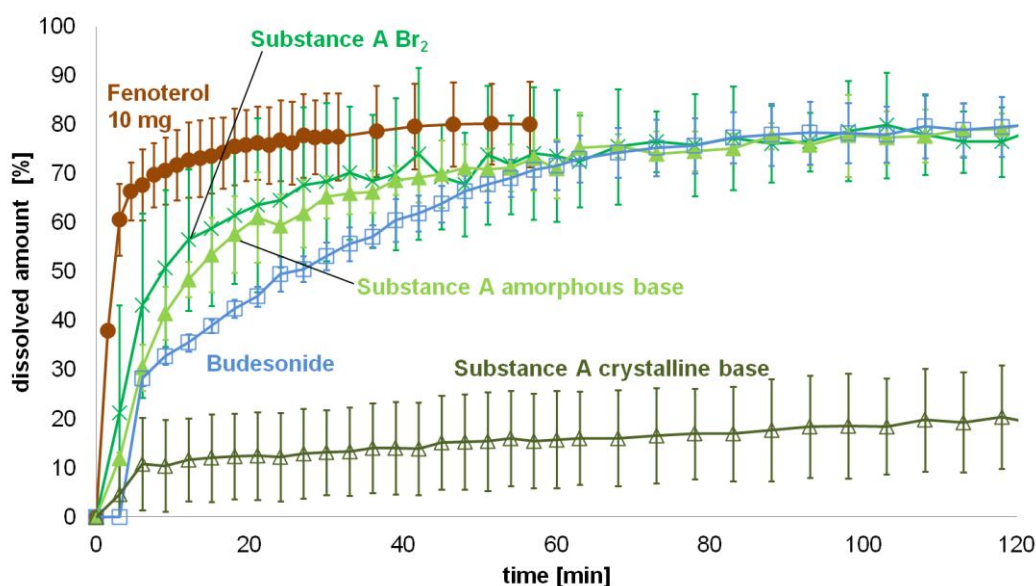


Figure 4.22: Dissolution profiles using RC membrane  
 Fenoterol HBr 10 mg (dark orange dot), Substance A Br<sub>2</sub> (green x), Substance A amorphous base (light green triangle), Budesonide 1 mg (open blue square) and Substance A crystalline base (dark open triangle), mean ± SD, n = 3, error bars are in all cases existent but sometimes too small to be displayed

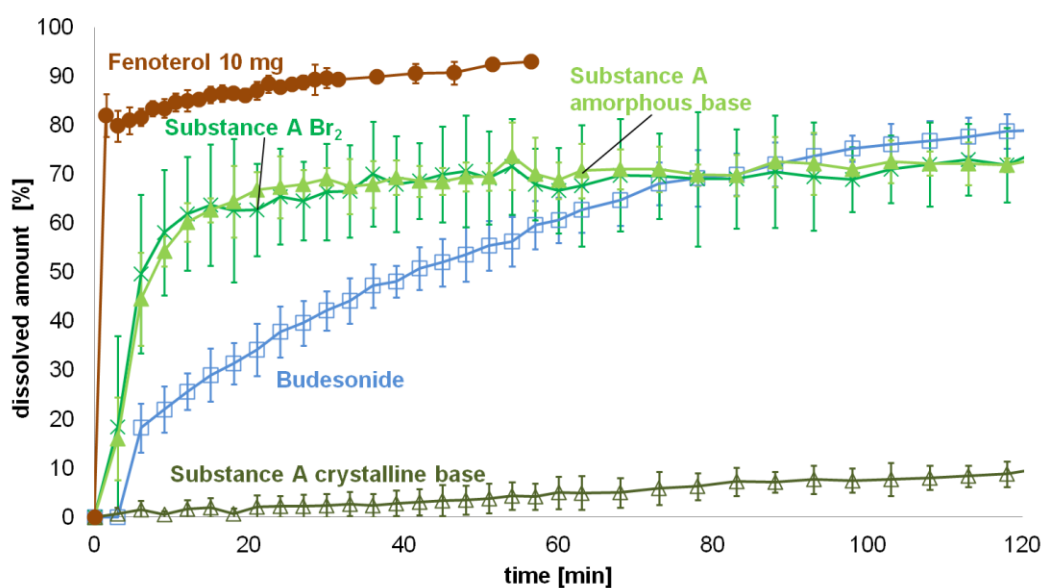


Figure 4.23: Dissolution profiles using IPC membrane  
 Fenoterol HBr 10 mg (dark orange dot), Substance A Br<sub>2</sub> (green x), Substance A amorphous base (light green triangle), Budesonide 1 mg (open blue square) and Substance A crystalline base (dark open triangle), mean  $\pm$  SD, n = 3, error bars are in all cases existent but sometimes too small to be displayed

A further step in data interpretation is the comparison of diffusion and dissolution profiles. First there are membranes depending differences.

Regarding the IPC membrane (Figure 4.19 and Figure 4.23), as expected the diffusion profile of Budesonide and Substance A base is much faster than the dissolution profile, but for Fenoterol it is inverted. For the RC membrane (Figure 4.20 and Figure 4.22) as expected for Substance A crystalline base the diffusion process is faster than the dissolution plus diffusion through the membrane. For Budesonide both profiles are quite similar. As already described for the IPC membrane for Fenoterol and also for Substance A amorphous base the dissolution process is faster than the diffusion.

This phenomenon could be explained with Fick's First law [45]. For Fenoterol and Substance A, respectively the diffusion gradient across the membrane of solid particles is higher than the gradient of the substance-solution. Therefore, the dissolution profile is faster than the diffusion profile.

It is noticeable that using the RC membrane the dissolved amount never exceeds 90 %. Furthermore, the reproducibility is reduced using the RC membrane. In Figure 4.24 the mean relative standard deviations (RSD) of the two membrane types are plotted against each other. For the IPC a higher reproducibility could be found. Likely is the swelling of the regenerated cellulose membrane and therefore a wave or wrinkle formation of the membrane, due to the clamping in the membrane holder.

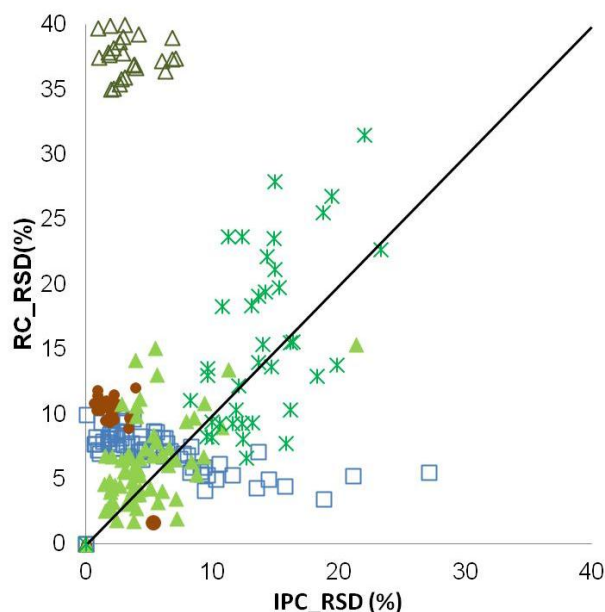


Figure 4.24: Comparison of reproducibility using IPC or RC membrane in Franz cell Budesonide 1 mg (open blue square), substance A crystalline base (open green triangle), substance A amorphous base (light green triangle), substance A Br<sub>2</sub> (green x) Fenoterol (dark orange dot), relative standard deviation (RSD) [%], n = 3, less symbols in the respective part above or below the bisecting line means less variability and higher reproducibility. Therefore, the IPC is more suitable for dissolution testing in Franz Cell than the RC membrane.

Particles on top of the wrinkles are less or even not wetted and hence have a reduced dissolution rate or do not dissolve compared to particles being wetted and being in contact with the dissolution medium.

For visualization of the wetting problems methylene blue was placed onto the membrane. Also the substance is not homogenous distributed on the membrane Figure 4.25 demonstrates the inhomogeneous wetting of methylene blue due to swelling of the regenerated cellulose membrane. In areas with direct contact to the dissolution medium methylene blue is fast dissolved whereas on the peaks only low dissolution takes place.

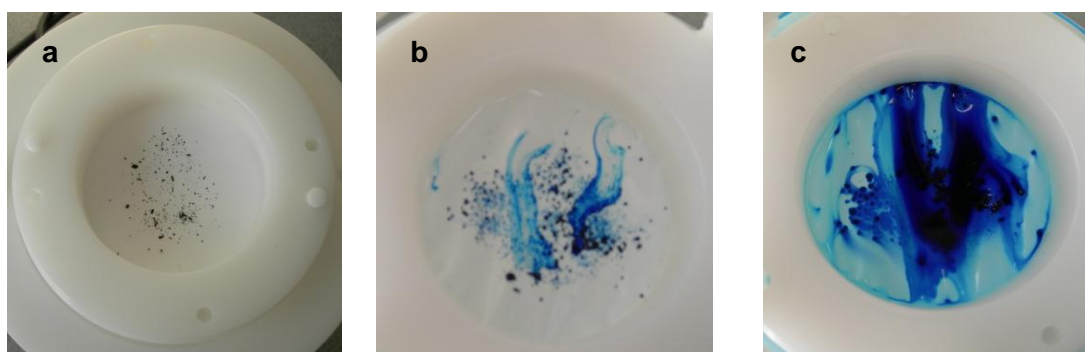


Figure 4.25: regenerated cellulose membrane in adapted Franz Cell membrane holder with methylene blue

- methylene blue powder on the clamped membrane, without dissolution medium contact
- after a few seconds dissolution medium contact
- after a few minutes dissolution medium contact

Nevertheless, for Substance A dibromide and amorphous base using the IPC membrane the standard deviations are also quite large. One reason could be found in air bubbles beneath the membrane, which is described in literature as typically Franz Cell problem [112,114,116]. Due to the air bubbles no consistent wetting is possible.

The use of MDT as reporting method is difficult. The trends displayed for MDT compared to the dissolution profiles are not in all cases consistent. For example the profiles of Substance A amorphous base and dibromide using the RC membrane are similar but the MDT suggests a difference. A detailed discussion on the MDT “problematic” is following in the chapter 5.1.1. Concerning the dissolution profiles Franz cell could discriminate between good and poor soluble substances. For substances with low solubility the deposited mass on the membrane has a larger effect than for good soluble substances. A higher mass loading leads to almost complete coverage of the membrane with particles, forming heaps and agglomerates. These agglomerates compared to a single particle, have a smaller surface resulting in a slower solubility rate. Furthermore, a wetting of the inner particles in agglomerates is more difficult than the wetting of a single particle, resulting in a more decreasing of the solubility rate.

The Franz cell for dissolution testing of inhalation powders has a limited applicability, due to complicated handling and the risk of air bubbles beneath the membrane.

Therefore, further experiments especially concerning the mass on membrane were performed with the paddle apparatus.

## 4.5. Transwell® Dissolution System

### 4.5.1. Addition of a dissolution layer on the membrane

The use of the additional diffusion layer was expected to be beneficial relating to the reproducibility and acceleration of dissolution. A closed view on the profiles of the different substances shows substance depending differences.

Using a regenerated cellulose membrane for Budesonide in the first 20 minutes the profiles show no difference (MDT Table 4.13). During further progress of dissolution the profile without additional dissolution medium reaches almost 100 % with small error bars. In contrast the profile with additional dissolution medium reaches in middle 70 % with large error bars. The observed effect is not mass depending, because the FPDs on the membranes are quite similar (Table 4.13, page 89). The expected benefit of the additional dissolution layer is only visible for Substance A crystalline base at the beginning of the dissolution process (Figure 4.26). In the further progress of dissolution the two profiles converge. The expected acceleration of the dissolution process by adding an additional layer is not given. The plateau phase for Substance A crystalline base was not reached after 240 min, hence calculation of MDT is not meaningful.

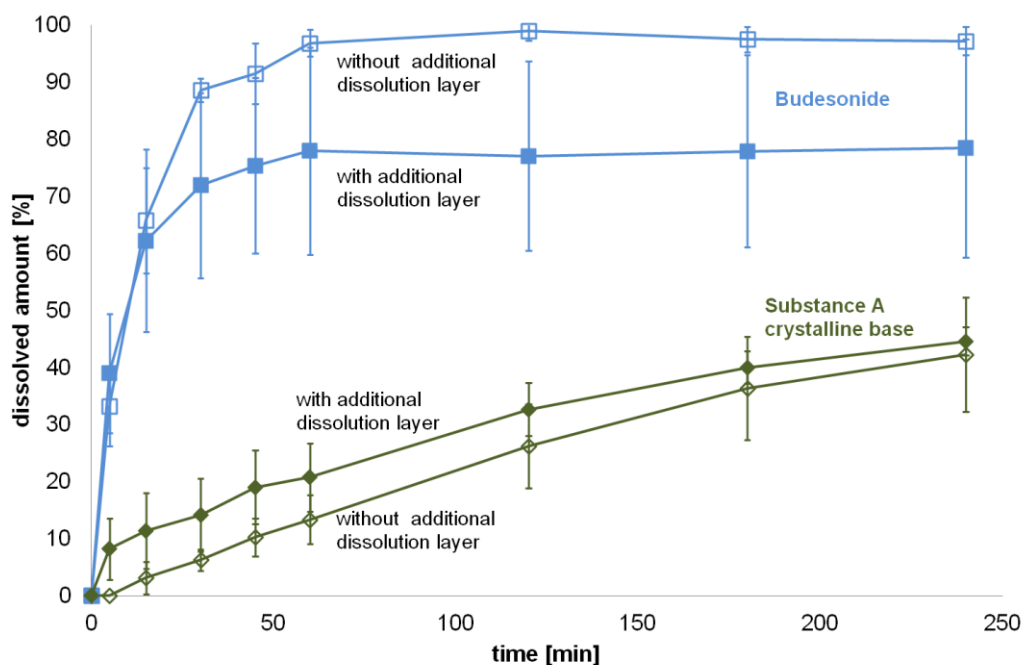


Figure 4.26: Influence of dissolution layer on the dissolution process using the RC membrane. Additional diffusion layer (full symbols), without additional diffusion layer (open symbols), Budesonide (blue squares), Substance A crystalline base (dark green rhombs), mean  $\pm$  SD, n = 3

For Substance A amorphous base and the dibromide dissolution profiles with and without dissolution layer appear to be similar. The results of MDT calculation (Table 4.13, page 89)

and the dissolution profiles for Substance A dibromide (Figure 4.27) show not the same results. Whereas the profiles show a similarity ( $f_1 = 9.9$ ,  $f_2 = 61.7$ ) the MDT does not. For the amorphous base MDT with dissolution layer is shorter than without layer.

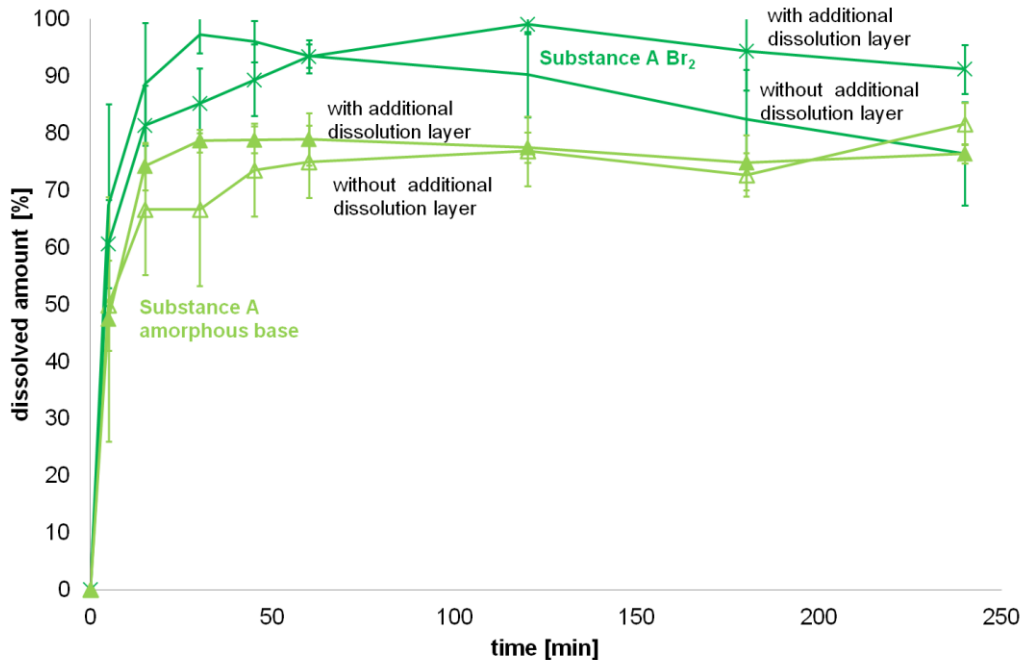


Figure 4.27: Influence of dissolution layer on the dissolution process using the RC membrane. Additional diffusion layer (full symbols), without additional diffusion layer (open symbols), Substance A amorphous base (light green triangles), Substance A Br<sub>2</sub> (green X), mean  $\pm$  SD,  $n = 3$

In Figure 4.28 the data variability indicates that dissolution profiles with dissolution layer show a similar to even smaller reproducibility than without dissolution layer, with the exception of the amorphous base.

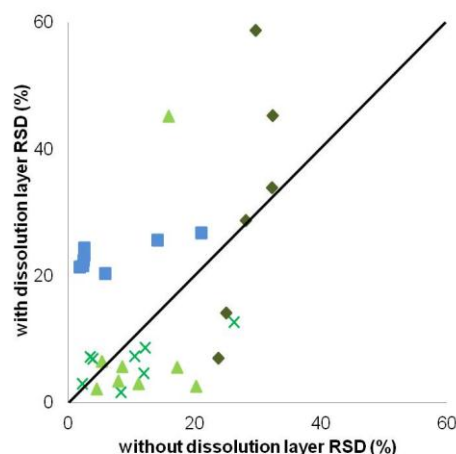


Figure 4.28: Comparison of reproducibility with and without dissolution layer using the RC membrane Budesonide (blue square), Substance A amorphous base (light green triangle), Substance A crystal-line base (dark green rhomb) and Substance A Br<sub>2</sub> (green X). Relative standard deviation (RSD) [%],  $n = 3$ , symbols in the respective part above or below the bisecting line mean less variability and higher reproducibility. Therefore, performance without dissolution layer is more suitable for dissolution testing in Transwell® system than with dissolution layer.

Table 4.13: Summary of used substances and membrane material with corresponding dissolution set up, recalculated FPD on filter (mean  $\pm$  SD) and MDT (mean  $\pm$  SD), dl = dissolution layer, + = with, - = without, rpm = stirring, n.p. = calculation not possible, because profile "plateau" was too low

substance	mem-brane material	additional information	recalculated FPD on filter [ $\mu$ g] n = 3		MDT [min]	
			mean	$\pm$ SD	mean	$\pm$ SD
Budesonide	PC	+ dl, + rpm	5.5	$\pm$ 0.7	n.p.	
		- dl, + rpm	5.9	$\pm$ 1.5		
	RC	+ dl, + rpm	3.9	$\pm$ 1.5	12.8	$\pm$ 2.6
		- dl, + rpm	4.2	$\pm$ 0.2	16.6	$\pm$ 0.7
		- dl, - rpm	5.2	$\pm$ 0.6	40.6	$\pm$ 13.3
	PE	- dl, + rpm	4.4	$\pm$ 0.5	21.6	$\pm$ 8.9
		- dl, - rpm	4.4	$\pm$ 0.5	40.5	$\pm$ 15.8
IPC	- dl, + rpm	15.2	$\pm$ 1.0	40.4	$\pm$ 6.3	
	- dl, - rpm	17.7	$\pm$ 0.5	94.6	$\pm$ 4.6	
	-dl, + rpm, 0.02%DPPC	16.5	$\pm$ 0.8	54.5	$\pm$ 1.7	
	-dl, + rpm, 0.02%Alveof	18.8	$\pm$ 1.9	41.9	$\pm$ 2.6	
Substance A crystalline base	PC	+ dl, + rpm	5.6	$\pm$ 1.7	n.p.	
		- dl, + rpm	6.7	$\pm$ 5.0		
	RC	+ dl, + rpm	3.8	$\pm$ 0.5	n.p.	
		- dl, + rpm	3.8	$\pm$ 0.6		
		- dl, - rpm	2.3	$\pm$ 0.1	112.4	$\pm$ 3.8
	PE	- dl, + rpm	5.2	$\pm$ 0.5	n.p.	
		- dl, - rpm	3.5	$\pm$ 0.7		
IPC	- dl, + rpm	15.8	$\pm$ 1.3	n.p.		
	- dl, - rpm	16.9	$\pm$ 1.5			
	-dl, + rpm, 0.02%DPPC	17.9	$\pm$ 1.2	112.4	$\pm$ 0.7	
	-dl, + rpm, 0.02%Alveof	15.4	$\pm$ 1.4	109.7	$\pm$ 1.4	
Substance A amorphous base	PC	+ dl, + rpm	26.2	$\pm$ 5.4	n.p.	
		- dl, + rpm	37.8	$\pm$ 5.6		
	RC	+ dl, + rpm	9.0	$\pm$ 0.5	6.9	$\pm$ 1.5
		- dl, + rpm	8.6	$\pm$ 0.9	13.6	$\pm$ 10.1
		- dl, - rpm	1.8	$\pm$ 0.1	29.7	$\pm$ 6.9
	PE	- dl, + rpm	6.5	$\pm$ 1.0	n.p.	
		- dl, - rpm	10.4	$\pm$ 3.3		
IPC	- dl, + rpm	17.6	$\pm$ 4.3	16.9	$\pm$ 3.9	
	- dl, - rpm	33.1	$\pm$ 7.6	27.9	$\pm$ 4.7	
	-dl, +rpm, 0.02%DPPC	27.3	$\pm$ 3.7	18.4	$\pm$ 1.4	
	-dl, +rpm, 0.02%Alveof	28.8	$\pm$ 6.9	15.9	$\pm$ 1.8	
Substance A Br <sub>2</sub>	PC	+ dl, + rpm	7.1	$\pm$ 1.5	n.p.	
		- dl, + rpm	12.0	$\pm$ 1.2		
	RC	+ dl, + rpm	2.2	$\pm$ 0.2	14.6	$\pm$ 3.0
		- dl, + rpm	3.2	$\pm$ 0.5	6.5	$\pm$ 2.8
		- dl, - rpm	1.6	$\pm$ 1.0	36.4	$\pm$ 9.7
	PE	- dl, + rpm	3.5	$\pm$ 1.6	n.p.	
		- dl, - rpm	1.6	$\pm$ 0.5		
IPC	- dl, + rpm	19.6	$\pm$ 2.5	4.4	$\pm$ 0.5	
	- dl, - rpm	4.9	$\pm$ 0.3	24.7	$\pm$ 7.0	
	-dl, +rpm, 0.02%DPPC	25.3	$\pm$ 2.1	10.1	$\pm$ 4.9	
	-dl, +rpm, 0.02%Alveof	17.1	$\pm$ 0.4	15.3	$\pm$ 3.6	

Furthermore, the impact of the dissolution layer was tested for the PC membrane (Figure 4.29). The membrane permeation tests (Chapter 4.1.4) provide only for Substance A base a low diffusibility. It appears that for Substance A base the additional dissolution layer increases the dissolution process in the first 50 minutes, later the profiles converge. For Budesonide and Substance A dibromide data variability is too high, so a conclusion is not possible

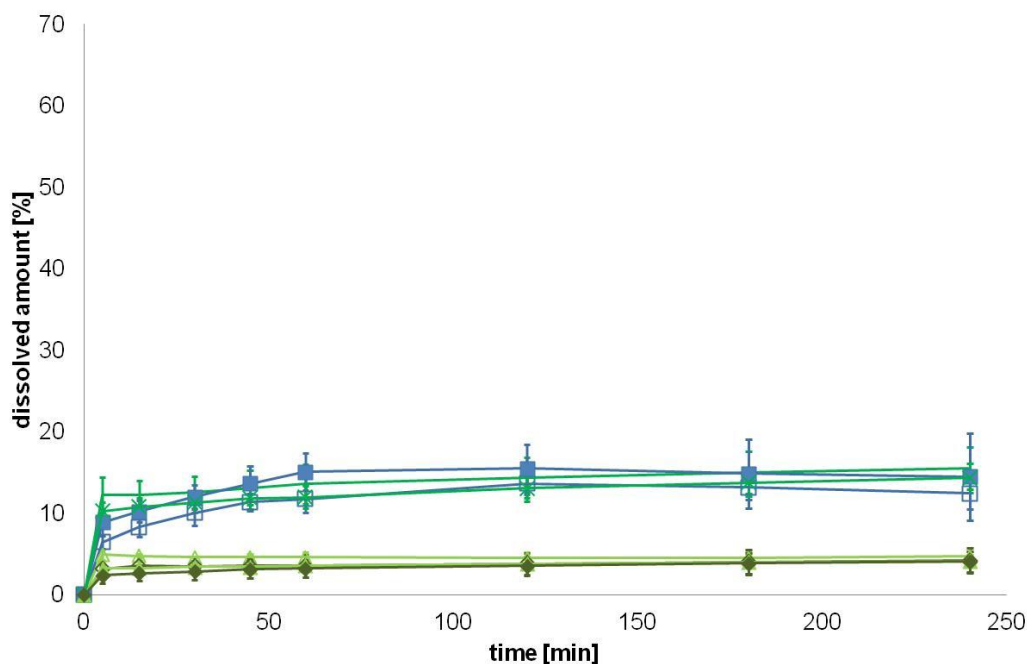


Figure 4.29: Influence of dissolution layer on the dissolution process using the PC membrane. Additional diffusion layer (full symbols), without additional diffusion layer (open symbols), Budesonide (blue square) Substance A amorphous base (light green triangles), Substance A Br<sub>2</sub> (green X) and Substance A crystalline base (dark green rhomb) mean  $\pm$  SD, n =3

The impact of the dissolution layer is substance dependent but in most cases leads to higher variability of the dissolution profiles and is consequently not advantageous. Under the assumption that the 40  $\mu$ l are uniformly distributed on the membrane, PBS buffer has a height of 88  $\mu$ m; so particles with diameters of less than 5  $\mu$ m are covered. As already described the contact angle measurement provides a hydrophilic character of the membranes (RC contact angle  $< 20^\circ$ ) (Table 4.10). Hence, the buffer spreads over the membrane and a uniform layer could be assumed. This uniform layer was confirmed by an optical inspection during the test. Nevertheless, the substance particles on the membrane showed still a poor dissolution rate.

#### 4.5.2. Stirring

Due to the poor solubility for Substance A crystalline base ( $c_s = 7 \mu\text{g/ml}$ ) stirring has the smallest effect (RC, Figure 4.32) or even no effect (IPC Figure 4.30 and PE Figure 4.34). The profiles for the crystalline base are similar as well as for the PE and IPC membrane. As

expected due to a better homogenization of the dissolution medium, using the IPC and the RC membranes stirring leads to faster dissolution and higher dissolved amounts for all other tested substances (Figure 4.30 - Figure 4.35).

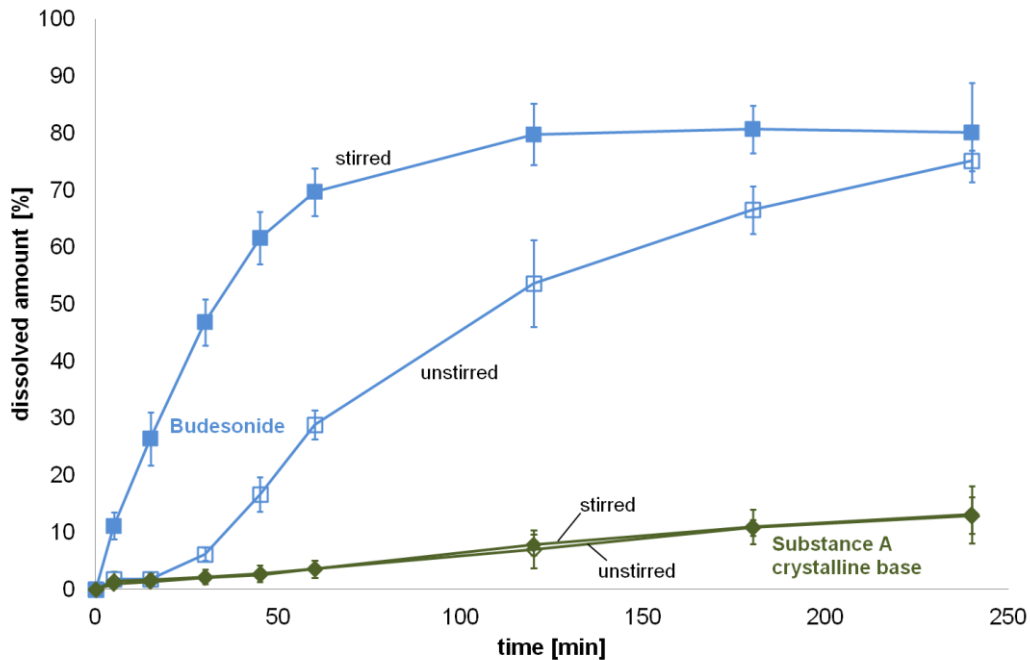


Figure 4.30: Dissolution profiles by the use of IPC membrane with (full symbols) and without (open symbols) stirring

Budesonide (blue squares), Substance A crystalline base (dark green rhombs), mean  $\pm$  SD, n = 3, error bars are in all cases existent but too small to be displayed

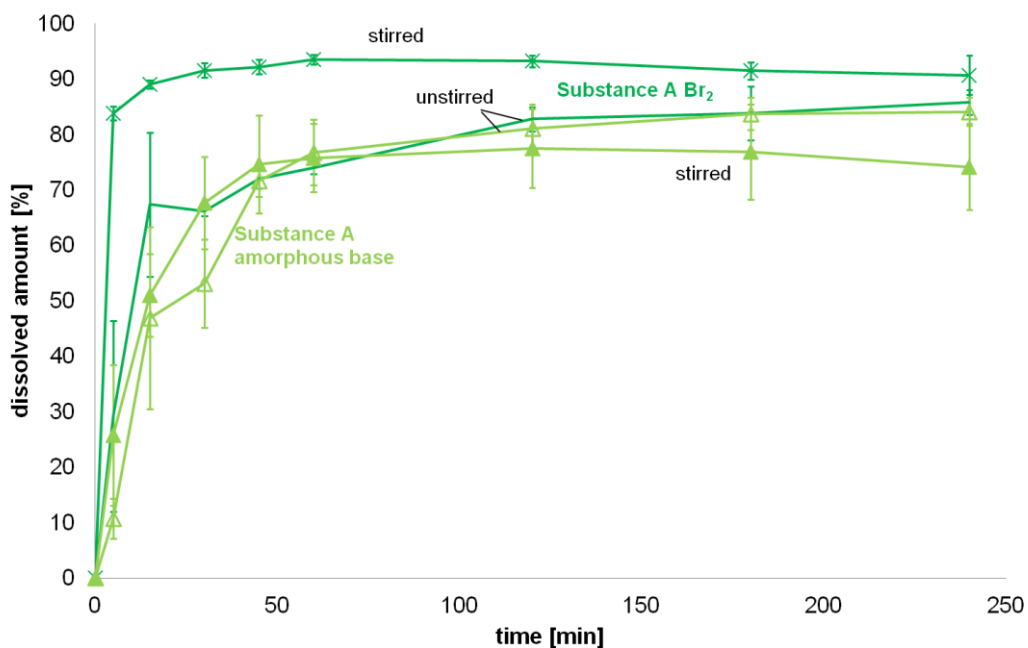


Figure 4.31: Dissolution profiles by the use of IPC membrane with (full symbols) and without (empty symbols) stirring

Substance A amorphous base (light green triangle), Substance A Br<sub>2</sub> (green X), mean  $\pm$  SD, n = 3, error bars are in all cases existent but sometimes too small to be displayed

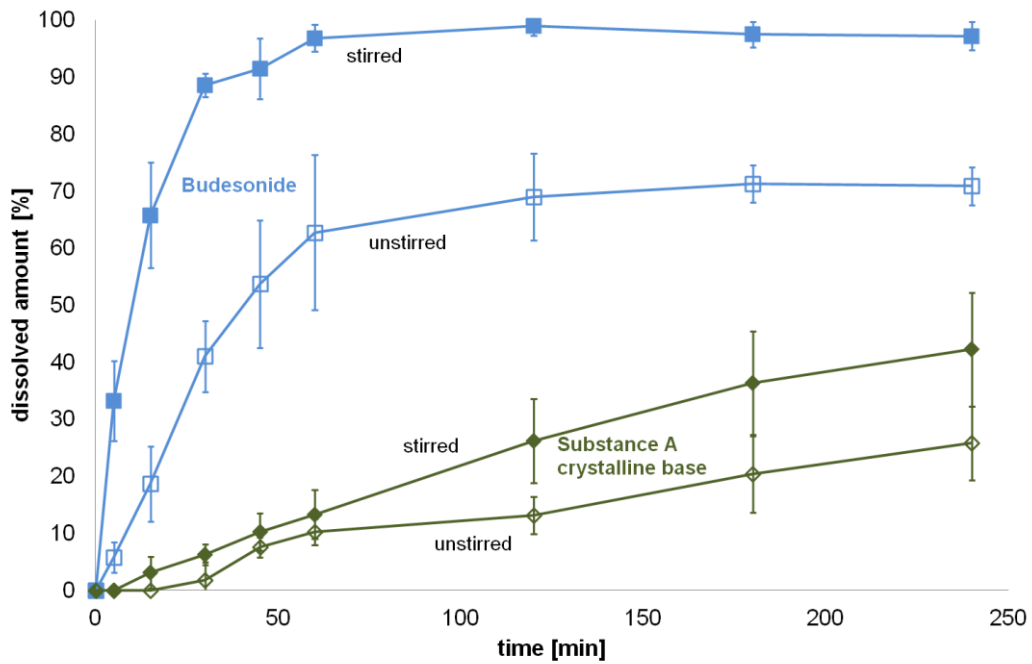


Figure 4.32: Dissolution profiles by the use of RC membrane with (full symbols) and without (open symbols) stirring  
 Budesonide (blue squares), Substance A crystalline base (dark green rhombs), mean  $\pm$  SD,  $n = 3$ , error bars are in all cases existent but sometimes too small to be displayed

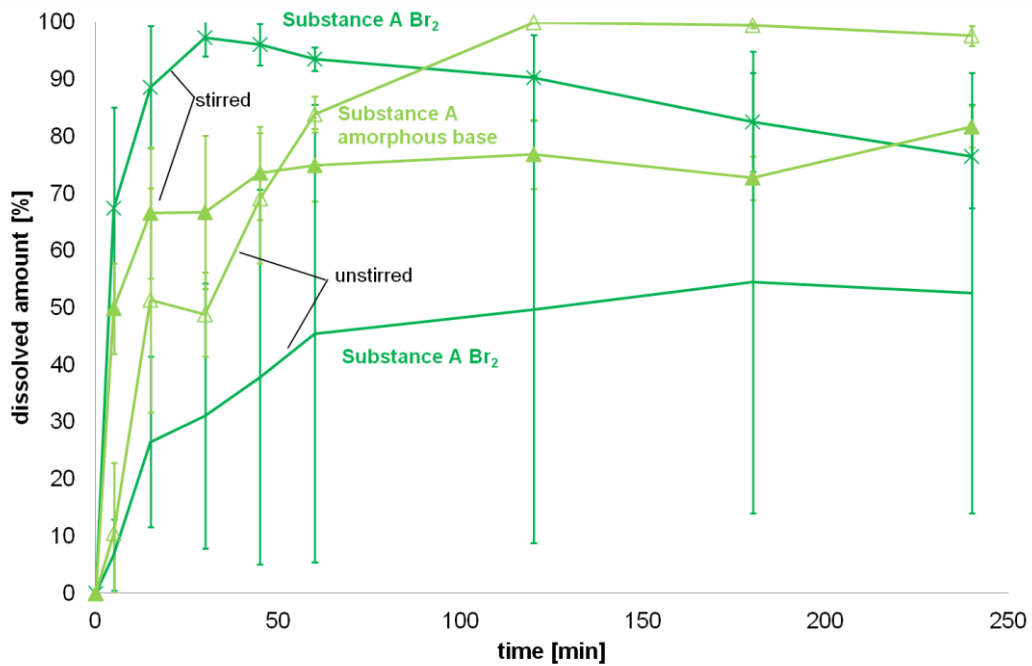


Figure 4.33: Dissolution profiles by the use of RC membrane with (full symbols) and without (open symbols) stirring  
 Substance A amorphous base (light green triangle), Substance A Br<sub>2</sub> (green X), mean  $\pm$  SD,  $n = 3$ , error bars are in all cases existent but sometimes too small to be displayed

As expected from the membrane permeation test chapter 4.1.4 the dissolution profile plateaus using the PE membrane (Figure 4.34 and Figure 4.35) are on a low level (< 40% dissolved amount). Due to the hindered diffusion process using the PE membrane, the dissolution process is probably also slowed down. For Budesonide the dissolution profile plateau in the unstirred set up for the PE membrane reaches in contrast to the other membrane types a higher plateau (30%), than the stirred one (<20%) (Figure 4.34).

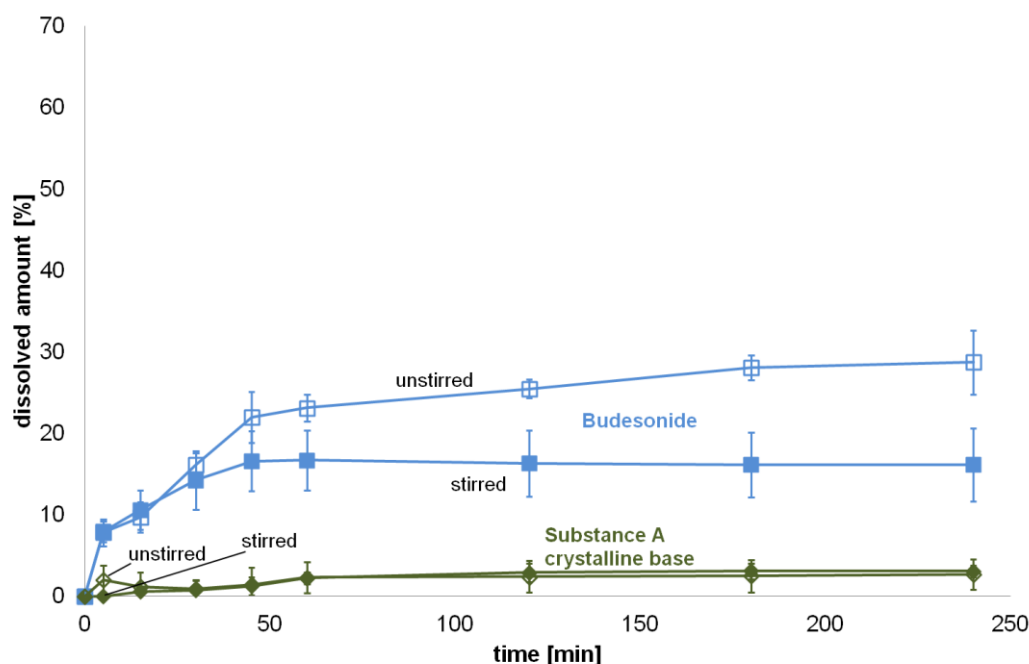


Figure 4.34: Dissolution profiles by the use of PE membrane with (full symbols) and without (open symbols) stirring  
Budesonide (blue squares), Substance A crystalline base (dark green rhombs), mean  $\pm$  SD, n = 3, error bars are in all cases existent but sometimes too small to be displayed

The corresponding MDT and FPD are summarized in Table 4.13 (page 89). As already described above again MDT is not in all cases consistent with the corresponding dissolution profiles. For Substance A amorphous base (IPC, with and without stirring) the dissolution profiles are similar whereas the MDT is different.

For comparison of dissolution profiles it is mandatory that particle size distribution and drug loading are almost identical [55,61,131]. In Table 4.13 (page 89) FPD of the different substances on the membrane for dissolution tests are summarized. The membrane loading is found to be very similar for PE and PC membrane. Hence, differences in the dissolution profiles are not mass effects but caused by the method used. A FPD-based comparison of IPC and RC for stirred / non stirred has to be done carefully, due to significant different masses on the membrane. For RC although at the non stirred experiments a lower mass is on the membrane, the dissolution process for the stirred experiments is faster. For experiments including the IPC membrane on the substances has to be looked individually. For Substance A

crystalline base the absence of any effect of stirring is most likely based on the poor solubility. This is supported by the equal mass and homogeneous mass distribution on the membrane thus not influencing the dissolution profile. For Budesonide the large difference between the dissolution profiles could be definitely explained by the positive effect of stirring, as the particle mass on the membrane is similar and hence has no effect.

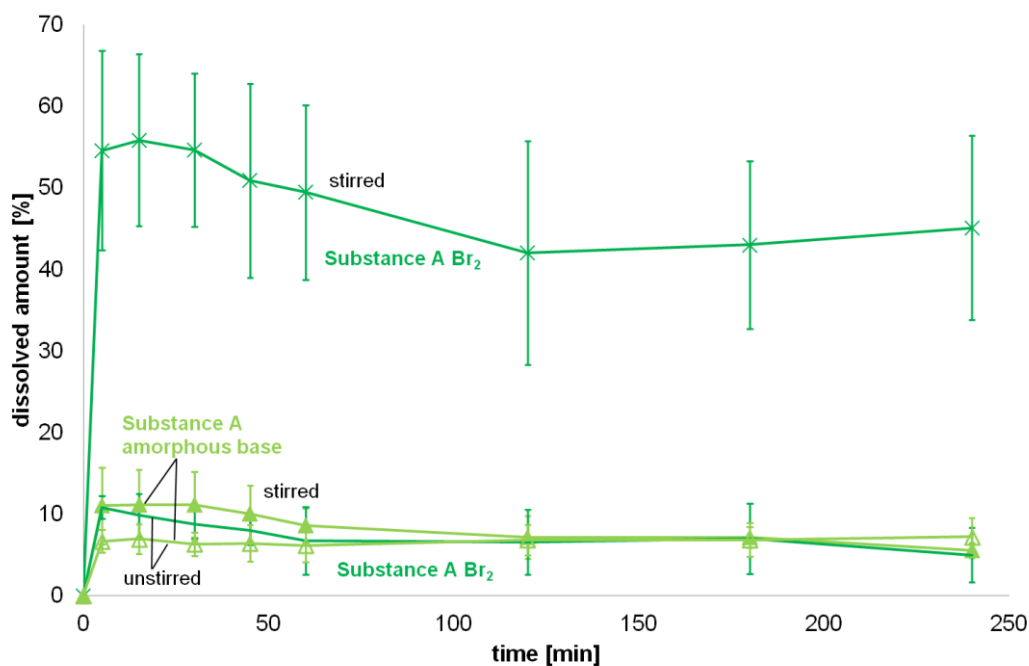


Figure 4.35: Dissolution profiles by the use of PE membrane with (full symbols) and without (open symbols) stirring  
 Substance A amorphous base (light green triangle), Substance A Br<sub>2</sub> (green X), mean  $\pm$  SD, n = 3, error bars are in all cases existent but sometimes too small to be displayed

In Figure 4.36 RSD of substances for the different membrane types and substances are compared. The use of stirring during dissolution test is beneficial due to faster distribution of the dissolved substance in the acceptor chamber [114] and hence an increased reproducibility. These positive aspects of stirring in the Transwell® dissolution system were underlined by the results of Bhagwat et al. [62]. Mechanistically the advantageous effect of stirring is based on acceleration of diffusion phenomena [147]. Directly under the membrane in acceptor medium the concentration of API is highest, without stirring the dissolution is limited because of the high surrounding concentration. Hence, diffusion of API to areas with lower concentration in the acceptor medium is the rate determining step. With stirring a concentration gradient through the membrane is established and the rate determining step is the dissolution of the particles.

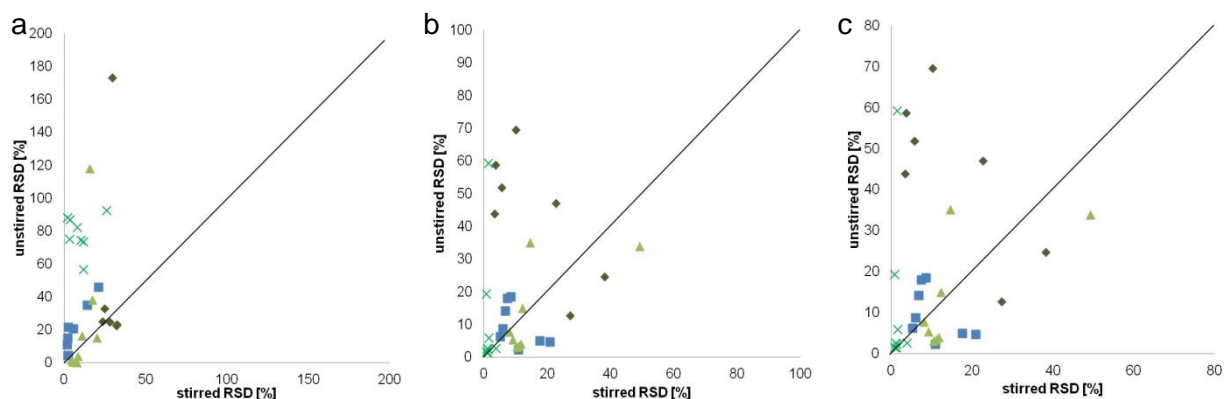


Figure 4.36: Comparison of reproducibility with and without stirring for different membrane types  
a) RC, b) IPC and c) PE membrane

Budesonide (blue square), Substance A amorphous base (light green triangle), Substance A crystalline base (dark green rhomb) and Substance A Br<sub>2</sub> (green X)  
Relative standard deviation (RSD) [%], n = 3, less symbols in one triangle divided through the bisecting line means less variability and higher reproducibility. Therefore, stirring is more suitable for dissolution testing in Transwell® system than without.

#### 4.5.3. Comparison of the two different polycarbonate membranes

As already mentioned above, from the membrane permeation tests the low dissolved / diffused amounts of Budesonide and Substance A dibromide using the PC membrane was unexpected. The dissolution profiles of all substances never reach more than 20% of drug in the receptor compartment (Figure 4.37 and Figure 4.38).

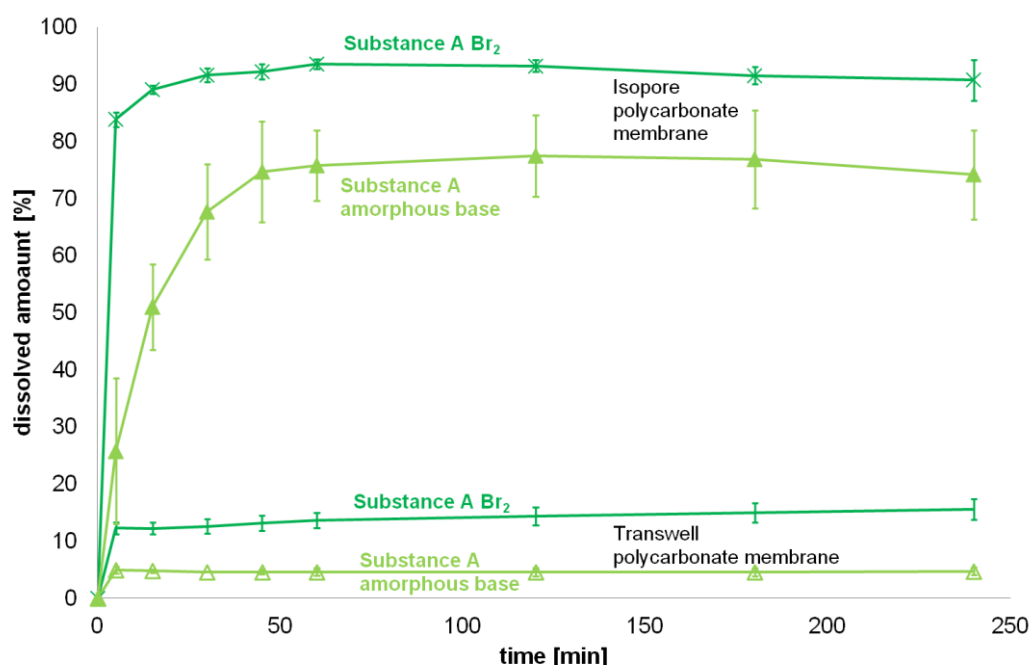


Figure 4.37: Dissolution profiles with the use of PC (open symbols) and IPC (full symbols) membrane, respectively. Set up was with stirring of the dissolution medium and without dissolution layer, Substance A amorphous base (light green triangles), Substance A Br<sub>2</sub> (green X), mean ± SD, n = 3. Error bars are in all cases existent but sometimes too small to be displayed

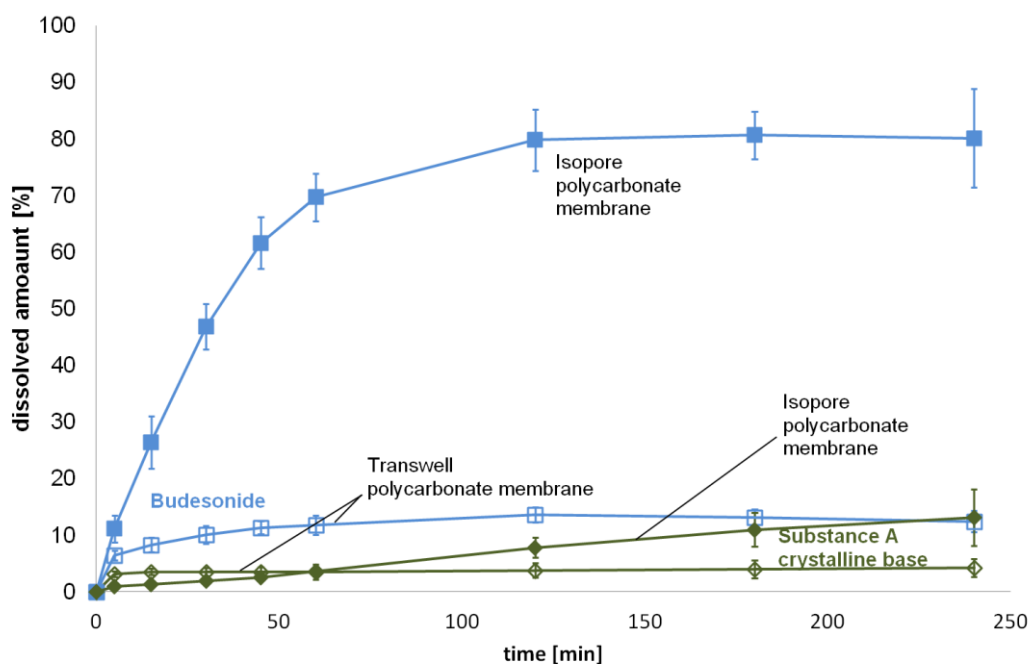


Figure 4.38: Dissolution profiles with the use of PC (open symbols) and IPC (full symbols) membrane, respectively. Set up was with stirring of the dissolution medium and without dissolution layer, Budesonide (blue squares), Substance A crystalline base (dark green rhombs), mean  $\pm$  SD,  $n = 3$ . Error bars are in all cases existent but sometimes too small to be displayed

Remarkable are the large differences between the polycarbonate membranes. But nevertheless, interestingly is also the high reproducibility of each dissolution profile for PC and IPC. IPC membranes show a higher permeability of dissolved substance than PC membranes for all used APIs. Bhagwat et al. also described problems with the PC membrane. They cut the membrane out and used instead a glass micro fiber filter [62]. Therefore, the differences between the membranes need to be identified. Both have a comparable pore number per  $\text{cm}^2$  (PC:  $1 \times 10^8$  pores /  $\text{cm}^2$ , IPC:  $1.5 \times 10^8$  pores /  $\text{cm}^2$ ) and SEM pictures show a similar appearance (Figure 4.39). Due to the substance specific differences in membrane permeation tests (chapter 4.1.4) and a larger difference in the dissolution profiles for all substances (Figure 4.37 and Figure 4.38), a direct comparison of the set ups between the two membranes for Budesonide (Figure 4.39) and contact angle measurements were performed. The results in Figure 4.39 support the already found differences in permeability and demonstrate that the results are not depending on the Transwell® set ups. For the IPC the modified insert with a sieve is used where the membrane is placed on, consequently there is a small gap between membrane and insert wall. This gap does not exist in the unmodified insert. For this reason, the PC membrane was cut out after dose collection and placed into the modified insert. A direct comparison of the profiles demonstrates again the large difference in between PC and IPC membrane (Figure 4.39) indicating the crucial role of the material. Additionally, an edge perforation of the Transwell® PC membrane was tested to avoid cutting but allow for an easier access of buffer onto the membrane. But with this set up no effect could be shown, too. The advanced contact angle measurement with water showed for PC membrane a con-

tact angle of  $63^\circ \pm 9^\circ$  and for IPC of  $57^\circ \pm 2^\circ$  (Table 4.10). These contact angles underline the hydrophilic character of both membranes, as described in the manufacturer information. But the higher variability for the PC membrane indicates that there might be hydrophilic and hydrophobic hot spots. The hot spots could be explained with the “tissue culture treatment” of PC membrane by the manufacturer. Due to this process the membrane surface becomes hydrophilic and especially negatively charged when medium is added [148]. Furthermore, the tissues culture treating agent might interact with the substances. Hence, substance dissolution through the PC membrane is hindered.

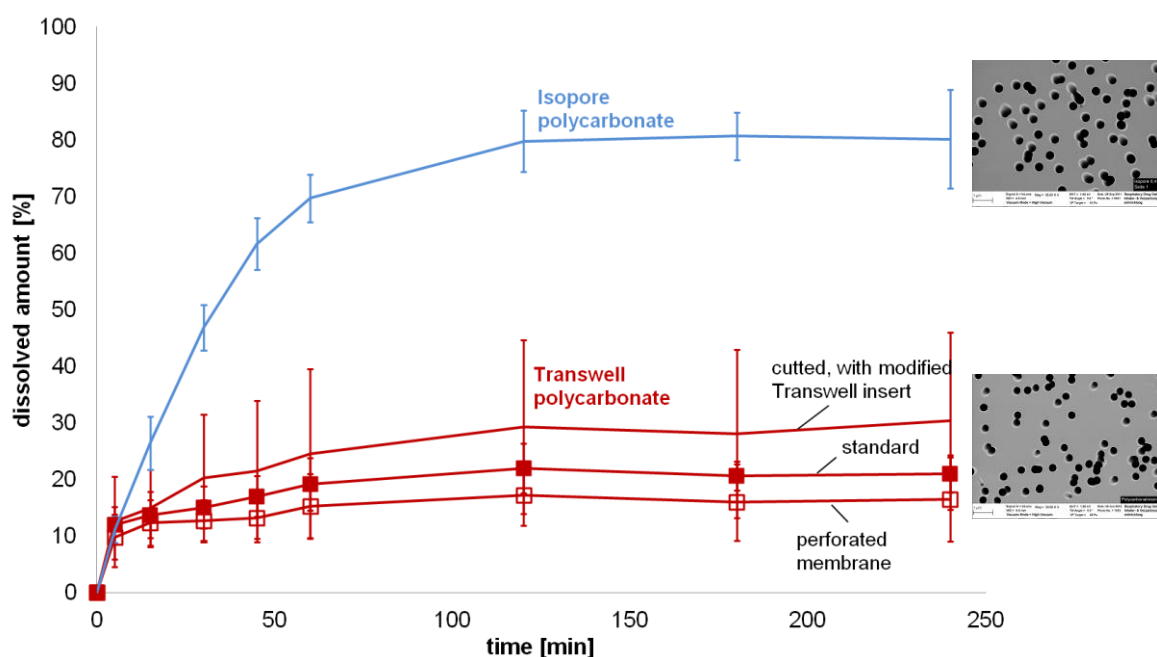


Figure 4.39: Budesonide dissolution profiles by the use of PC membrane and IPC membrane: IPC (blue line), PC Transwell® membrane cutted with modified Transwell® insert (red line), PC Transwell® insert (red square), PC Transwell® Insert perforated edge (open red square), mean  $\pm$  SD, n = 3 SEM pictures of IPC (up) and PC (down) membrane

#### 4.5.4. Surfactants

Figure 4.40 displays the influence of surfactants added to the dissolution medium in the Transwell® system on the dissolution using the IPC membrane. Table 4.13 (page 89) summarizes the MDTs and Table 4.14 (page 99) the results of dissolution profile comparison regarding fit factors. The IPC membrane was chosen due to the best results in the aforementioned dissolution tests.

For Substance A base the dissolution process is not significantly accelerated by the addition of DPPC to the dissolution medium. For Substance A dibromide and Budesonide the dissolution profiles indicate a slower dissolution process. For the dibromide this trend is not significant. The results of the visual comparison of the profiles are supported by test of similarity

with the fit factors. For the crystalline base there is a small increase of dissolution by the use of DPPC, but fit factors provide contradictory results.

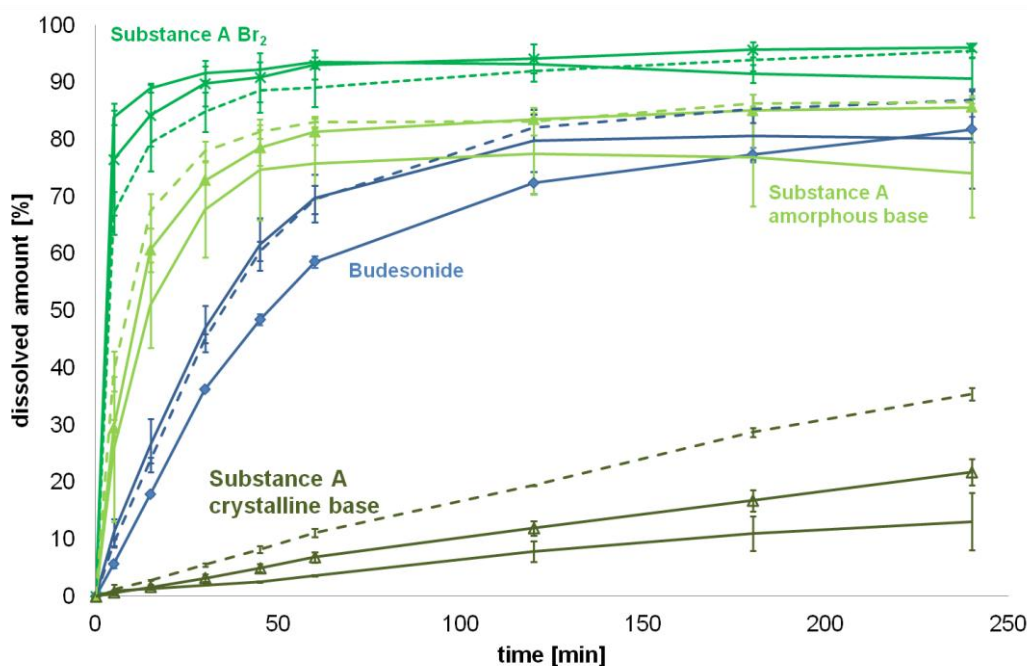


Figure 4.40: Comparison of dissolution profiles using surfactants 0.02% DPPC (symbol), 0.02% Alveofact (dashed line), buffer (no symbol), Substance A Br<sub>2</sub> (green X), Substance A amorphous base (light green triangle), Budesonide (blue square) and Substance A crystalline base (open dark green triangle), mean  $\pm$  SD, n = 3, error bars are in all cases existent but sometimes too small to be displayed

DPPC is a surface active substance and was used to improve the wettability of the used substances. Solubility tests show (Table 4.2) for Budesonide and Substance A crystalline base no or low improvement of the solubility, for Substance A amorphous base a decreased and for Substance A dibromide an increased solubility. The effect of wettability / solubility improvement depends strongly on the hydrophobic structures in the API molecules. Furthermore, the measurement of the micelle size for DPPC with dynamic light scattering showed a large micelle / object size (Table 4.3). As already shown by Son et al., these objects are too large for traveling through the pores with a diameter of 0.4  $\mu\text{m}$  [55]. But the micelles are only a reservoir for the remaining DPPC, in addition there are also free DPPC molecules [31] which could pass the membrane pores and increase wettability or solubility on the donor site. Alveofact® a medicine with 50.76 - 60.00 mg phospholipids (66  $\mu\text{mol}$ ) should show similar results to DPPC.

As displayed in Figure 4.40 addition of Alveofact® to the dissolution medium results in substance depending different dissolution profiles compared to PBS buffer. But the trends shown for DPPC, besides Budesonide, are similar. Therefore, the hypothesis of similar results for dissolution medium with DPPC and Alveofact® was achieved. With 0.02% addition of Alveofact® to the dissolution medium, for Substance A base dissolution is accelerated, for the

dibromide the dissolution process is slower. The effect of Alveofact® on the dissolution profile of Budesonide is contradictory to DPPC. The profile with Alveofact® and of pure buffer show similar dissolution profiles.

Table 4.14:  $f_1$  and  $f_2$  test results

<b>profiles similar</b>	<b><math>f_1</math> &lt; 15</b>	<b><math>f_2</math> 50-100</b>	<b>similarity?</b>
<b>Substanz A Br<sub>2</sub></b>			
normal vs. DPPC	7.0	64.3	yes
DPPC vs. Alveofact	7.7	61.3	yes
Alveofact vs. normal	18.0	47.5	no
<b>Substanz A amorphous base</b>			
normal vs. DPPC	9.4	61.0	yes
DPPC vs. Alveofact	5.7	65.5	yes
Alveofact vs. normal	13.4	50.1	yes
<b>Substanz A crystalline base</b>			
normal vs. DPPC	61.6	69.3	inconsistent
DPPC vs. Alveofact	66.1	58.0	inconsistent
Alveofact vs. normal	41.1	51.2	inconsistent
<b>Budesonide</b>			
normal vs. DPPC	13.5	54.5	yes
DPPC vs. Alveofact	18.7	53.9	inconsistent
Alveofact vs. normal	3.8	8.2	yes

Summarizing, adding of 0.02% DPPC or Alveofact® to the dissolution medium show a slight acceleration of dissolution process for Substance A base, although there is no effect on solubility, which provides the hypothesis of a better wettability. The wettability improvement for DPPC is underlined by the results of contact angle measurements of substance pellets (Table 4.7). For Substance A dibromide although solubility is increased, the dissolution rate decreases using these surfactants. These results are confirmed by the contact angle measurements. They show by the use of DPPC a better wettability of the substances, but are due to the high variability not meaningful.

The results for Budesonide are contradictory to those of Arora et al.. They showed for Budesonide a dissolved amount of 50 - 80% within 5 hours using the PE membrane with an additional dissolution layer [61]. In this thesis it was demonstrated that the PE membrane itself is hindering permeation of already dissolved Budesonide and therefore, the effect observed by Arora et al. is membrane and not substance depending.

It should be noted that before dissolution tests are started first a suitable membrane has to be chosen. Therefore, membrane permeation tests are mandatory. If this is considered, the modified Transwell® is a suitable dissolution test for powders of inhalation.

The usage of an additional dissolution layer is not beneficial but stirring of the acceptor medium is advantageous.

In future this *in vitro* test might be advanced for performing cell- and tissue based *in vitro* models as next step. As dose collection method for depositing the fine particles directly on the cell layer for example the PADD OCC system [149] could be used. A further step could be an *in vitro in vivo* correlation, as tried by Bhagwat et al. [62]. They used 0.5% SDS in the dissolution medium for improving solubility and therefore getting comparable results to pharmacokinetic studies. But the usage of SDS can be critical, due to a large improvement of solubility and therefore discrimination power between different substances could vanish.

## 4.6. Paddle Apparatus

### 4.6.1. Stirring speed

Figure 4.41 shows the dissolved amount of Budesonide in the paddle apparatus with membrane holder at different stirring speeds. MDT is summarized in Table 4.15. The profiles of 100 rpm and 140 rpm are similar (Table 4.16, page 118) but at 140 rpm the SD was smaller. 50 rpm showed as expected compared to 140 rpm the slowest dissolution profile due to an assumed correlation between stirring speed and dissolution rate [46]. With increasing stirring speed the diffused amount at the membrane is faster reduced and hence more dissolved substance could diffuse through the membrane. A stirring speed of more than 140 rpm was, however, not possible because the membrane holder was irregularly moving at higher speeds. Son et al. mentioned already a dead volume between membrane holder and bottom of the vessel and that circulation of dissolution medium is hindered between the holder and the vessel wall around the holder [55]. The lag time for reaching the dead volume of dissolved substance at a stirring speed of 100 rpm is approximately 3 minutes, for 140 rpm approximately 2 minutes. Hence, a higher stirring speed ensures a faster circulation in the dead volume. Therefore, 140 rpm was chosen for all other experiments with the Erweka paddle apparatus.

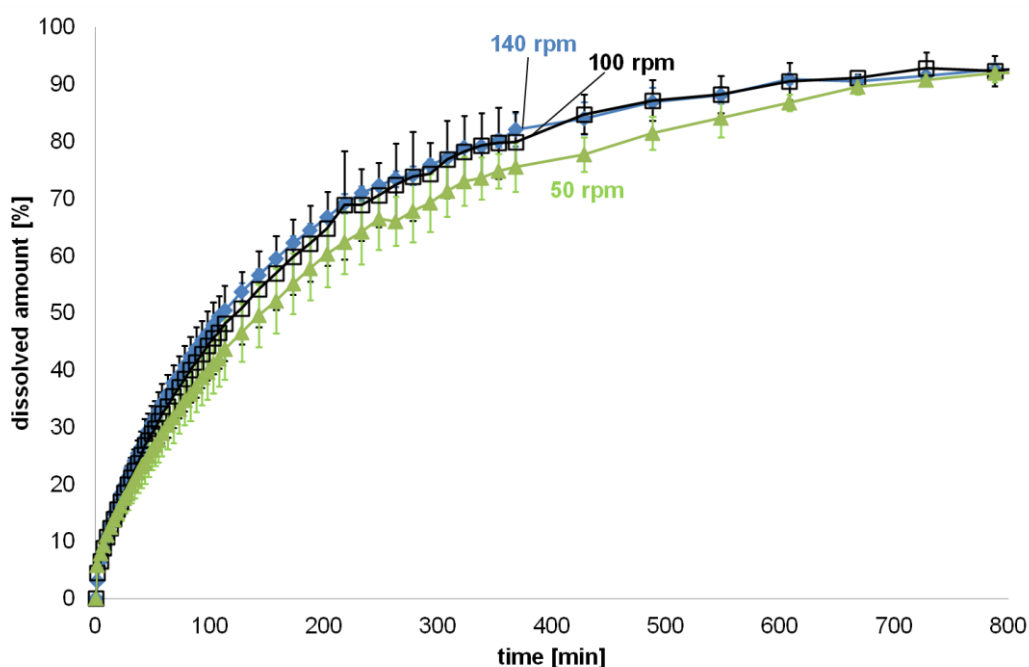


Figure 4.41: Influence of stirring speed on the dissolution profile of Budesonide RC membrane, aACI 140 rpm (blue rhomb), 100 rpm (black open square) and 50 rpm (green triangle), mean  $\pm$  SD, n = 3, error bars are in all cases existent, but sometimes too small to be displayed

#### 4.6.2. Influence of FPD on the dissolution process of Budesonide and Fenoterol

In Figure 4.42 the influence of fine particle mass on the membrane (Table 4.15, page 117) on the dissolution process in the paddle apparatus for Fenoterol and Budesonide is displayed. The MDTs are summarized in Table 4.15. As it can be seen in Figure 4.42 the dissolution for Fenoterol is much faster than for Budesonide due to the higher solubility (Table 4.2). For Budesonide it could be shown that the dissolution process depends on the fine particle dose on the membrane. The dissolution process for  $353 \mu\text{g} \pm 114 \mu\text{g}$  deposited mass is much faster than the process with a FPD of  $1892 \mu\text{g} \pm 126 \mu\text{g}$ . For Fenoterol the mass dependency ( $272.4 \mu\text{g} \pm 65.8 \mu\text{g}$  vs.  $1582 \mu\text{g} \pm 124 \mu\text{g}$ ) (Table 4.15, page 117) is not significant and the two profiles appear to be similar. Both Fenoterol dissolution profiles reach the 85% limit within 2 minutes. Hence, for fit factor tests the number of data points ( $n = 3$ ) is too small [120].

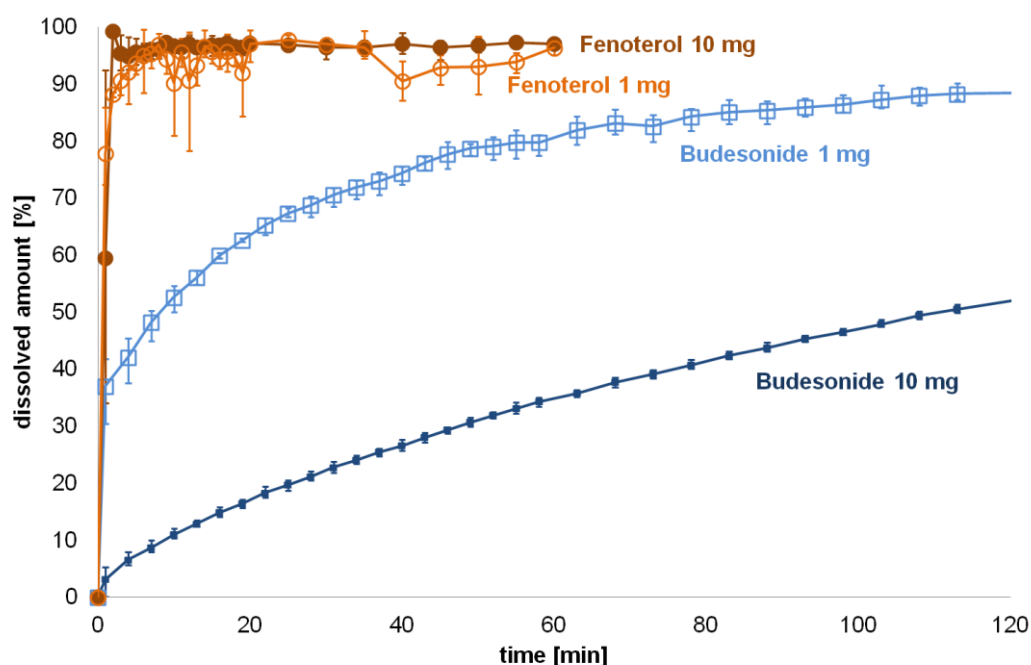


Figure 4.42: Influence of FPD on membrane for Budesonide and Fenoterol HBr RC membrane, aACI, Fenoterol HBr 1 mg (open orange dot), Fenoterol HBr 10 mg (dark orange dot), Budesonide 1 mg (open blue square) and Budesonide 10 mg (dark blue square), mean  $\pm$  SD,  $n = 3$ , error bars are in all cases existent but sometimes too small to be displayed

#### 4.6.3. Comparison of different membrane materials

In Figure 4.43 and Figure 4.44 the dissolution profiles and in Table 4.15 (page 117) the MDT for substances using RC and IPC membrane are shown. The rank order of dissolution profiles, due to solubility data, should be: Fenoterol – Substance A dibromide, Substance A amorphous base - Budesonide – Substance A crystalline base. In contrast to the Franz cell set up (Figure 4.22) for the RC membrane the rank order is as predicted by the solubility data and no similarity for the dissolution profiles could be shown (Table 4.16, page 118). Thus discrimination between all tested substances is possible.

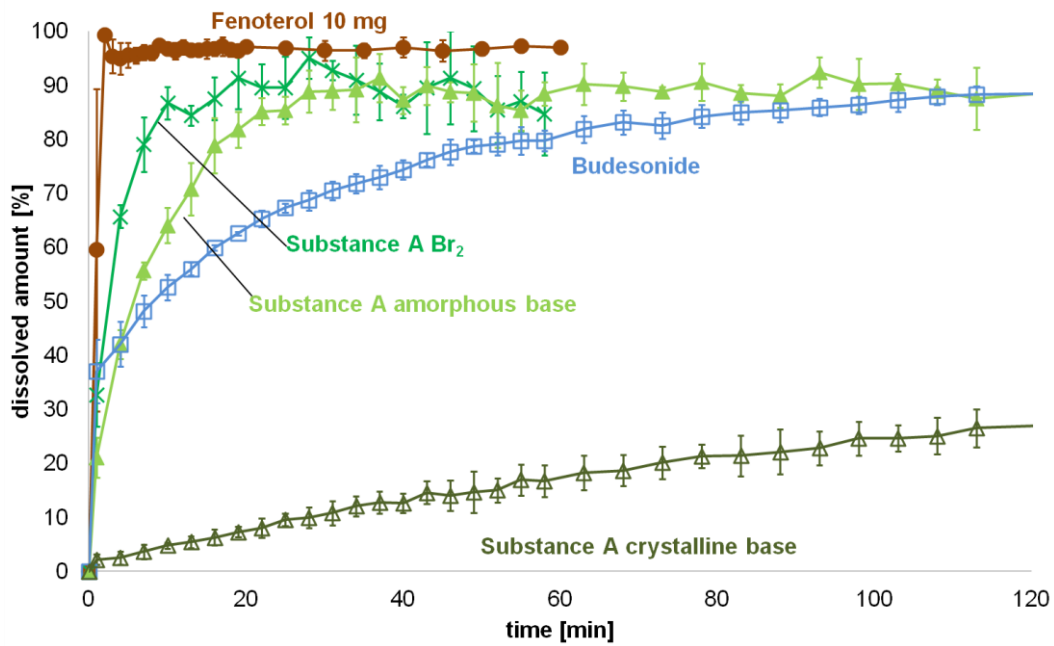


Figure 4.43: Dissolution profiles using the RC membrane aACI, Fenoterol HBr 10 mg (dark orange dot), Substance A Br<sub>2</sub> (green x), Substance A amorphous base (light green triangle), Budesonide 1 mg (open blue square) and Substance A crystalline base (open dark green triangle), mean ± SD, n = 3, error bars are in all cases existent but sometimes too small to be displayed

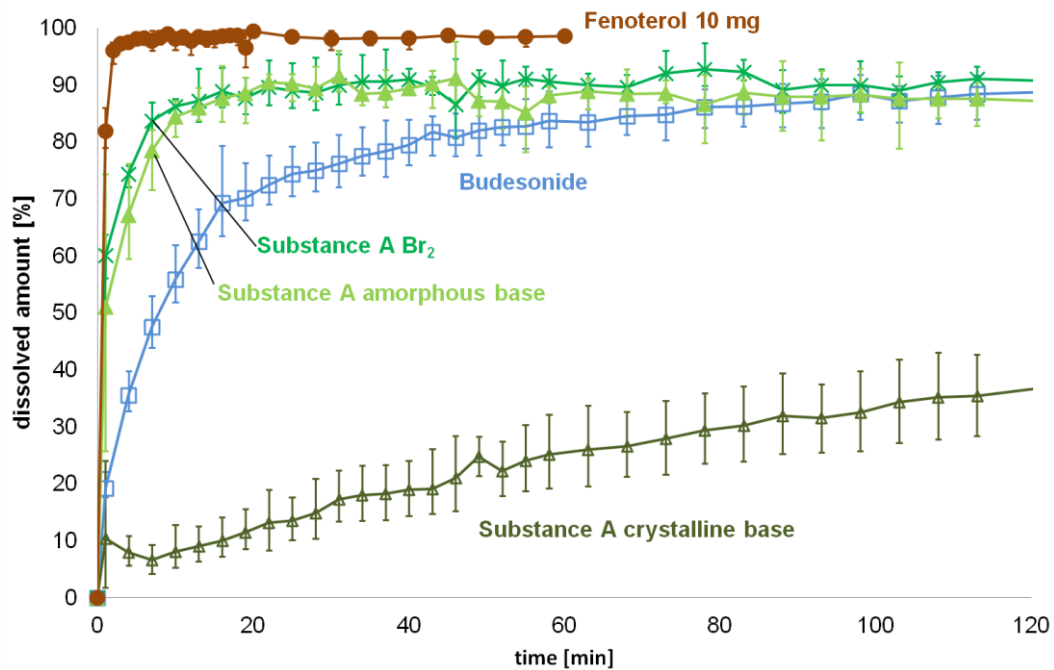


Figure 4.44: Dissolution profiles using the IPC membrane aACI, Fenoterol HBr 10 mg (dark orange dot), Substance A Br<sub>2</sub> (green x), Substance A amorphous base (light green triangle), Budesonide 1 mg (open blue square) and Substance A crystalline base (open dark green triangle), mean ± SD, n = 3, error bars are in all cases existent but sometimes too small to be displayed

For the IPC membrane as described for Franz cell there is no difference in dissolution profiles for Substance A dibromide and Substance A amorphous base ( $f_1 = 7.6$ ;  $f_2 = 61.8$  (Table 4.16, page 118)). This could be explained by the different structure of the membrane. The IPC membrane has, due to the defined pores a stronger retention effect than the RC membrane with the more spongy structure. Therefore, the particle size depending dissolution rate influence as already described for the Franz Cell (Figure 4.22) is stronger. The influence of particle size on the dissolution profile is supported by the results of the model calculation (chapter 4.7.5).

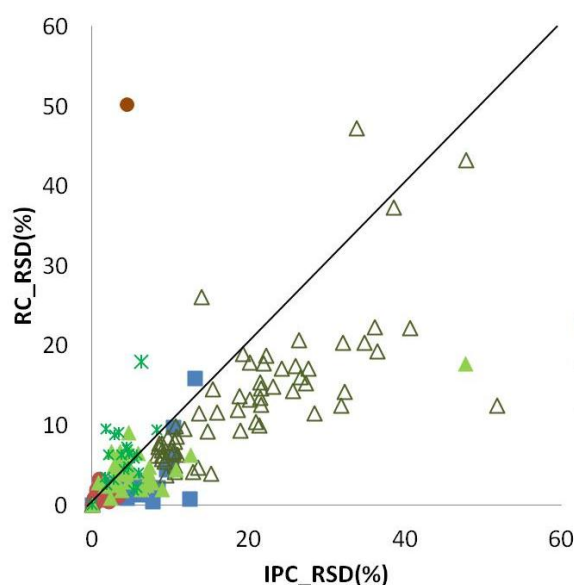


Figure 4.45: Comparison of reproducibility using IPC or RC membrane in paddle apparatus Budesonide 1 mg (blue square), substance A crystalline base (green, white triangle), substance A amorphous base (light green triangle), substance A Br<sub>2</sub> (green x), Fenoterol (dark orange dot), relative standard deviation (RSD) [%],  $n = 3$ , less symbols in the respective part above or below the bisecting line means less variability and higher reproducibility. Therefore, the RC is more suitable for dissolution testing in paddle apparatus than the IPC membrane.

In Figure 4.45 the mean relative standard deviations (RSD) of the two membrane types are plotted against each other. The reproducibility of data for the both membrane types are comparable except for Substance A crystalline base. In contrast to the Franz cell (Figure 4.24) the RC membrane is the most suitable membrane in the paddle apparatus. Beside the higher reproducibility, it has the better discrimination power and the more convenient handling and therefore was chosen for the following experiments.

The higher reproducibility using the RC membrane in paddle apparatus underlines the hypothesis of inhomogeneous wetting in the Franz cell due to the swelling dependent deformation of the clamped membrane (Figure 4.25). In contrast to the Franz cell in the mem-

brane holder of the paddle apparatus the membrane has the chance to stretch during the swelling process, because it is not clamped rigidly.

#### 4.6.4. Equipment change

Due to equipment change of dissolution apparatus from the Erweka to the Sotax apparatus comparison of the respective dissolution profiles was necessary. In the Sotax apparatus it is unfortunately not possible to use a higher stirring speed than 100 rpm. When the stirring speed is increased the membrane holder is moving irregularly. Therefore, a comparison of 100 rpm and 140 rpm stirring speed in the Sotax paddle apparatus was not possible. As already described above for the Erweka apparatus the dissolution profiles using either 140 rpm or 100 rpm are similar. But with the decreased stirring speed the SD increases and the lag time for circulation in the dead volume under the membrane holder is increased. To prevent this irregular movement a stirring speed of 100 rpm was used in the further experiments with the Sotax paddle apparatus.

Figure 4.46 and Table 4.18 show as expected similar profiles for the two dissolution tester. Remarkable are the different variability of the dissolution profiles. Astonishingly profiles of Budesonide in the Sotax apparatus show a higher reproducibility, probably due to different hydrodynamic conditions. The vessels have a deviating form and sampling in both apparatus is different as described above. In the Erweka apparatus sampling is performed through the shaft of the paddle. In the Sotax apparatus an additional small stable sleeve for sampling is placed in the vessel.

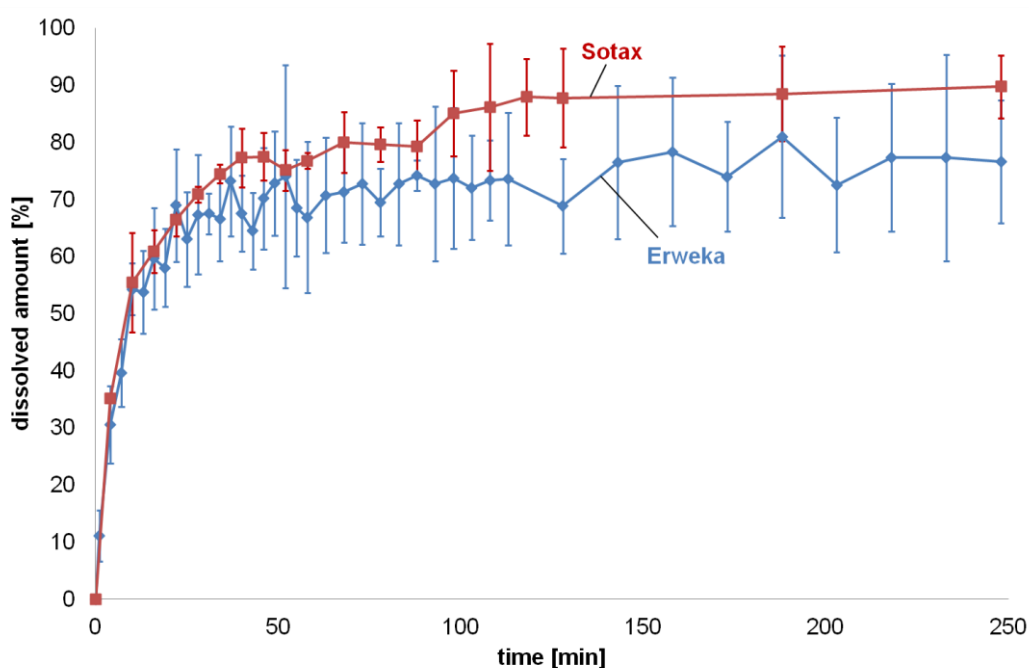


Figure 4.46: Comparison of Erweka paddle apparatus and Sotax paddle apparatus RC membrane, Budesonide, mean  $\pm$  SD, n = 3

#### 4.6.5. Best dose collection method

To overcome the problem of agglomerates on the membrane and therefore hindered dissolution the dose collection method had to be improved. The agglomerates are generated during dose collection with the aACI because the deagglomerated particles are impacted in line with the holes of the filter stage on the membrane. Hence, areas with a high amount of agglomerated particles occur.

As new approach spraying of substance on the membrane was tested as described in (chapter 3.3.2, 3.5.5.1). With similar masses on the membrane the SEM pictures (Figure 4.47) underline a more homogenous distribution with fewer agglomerates resulting similar dissolution profiles (Figure 4.47;  $f_1 = 9.2$ ;  $f_2 = 58.3$  (Table 4.16, page 118)). Beneficial is the ability of using not only micronized powders and to be independent of the aACI. But for reaching the same amount on the membrane, a higher amount of powder has to be weighed into the anti-solvent (chapter 3.3.2) which could be problematic if there is only a small amount of substance available. In addition, it is arguable if dichloromethane has any effect on substance properties.

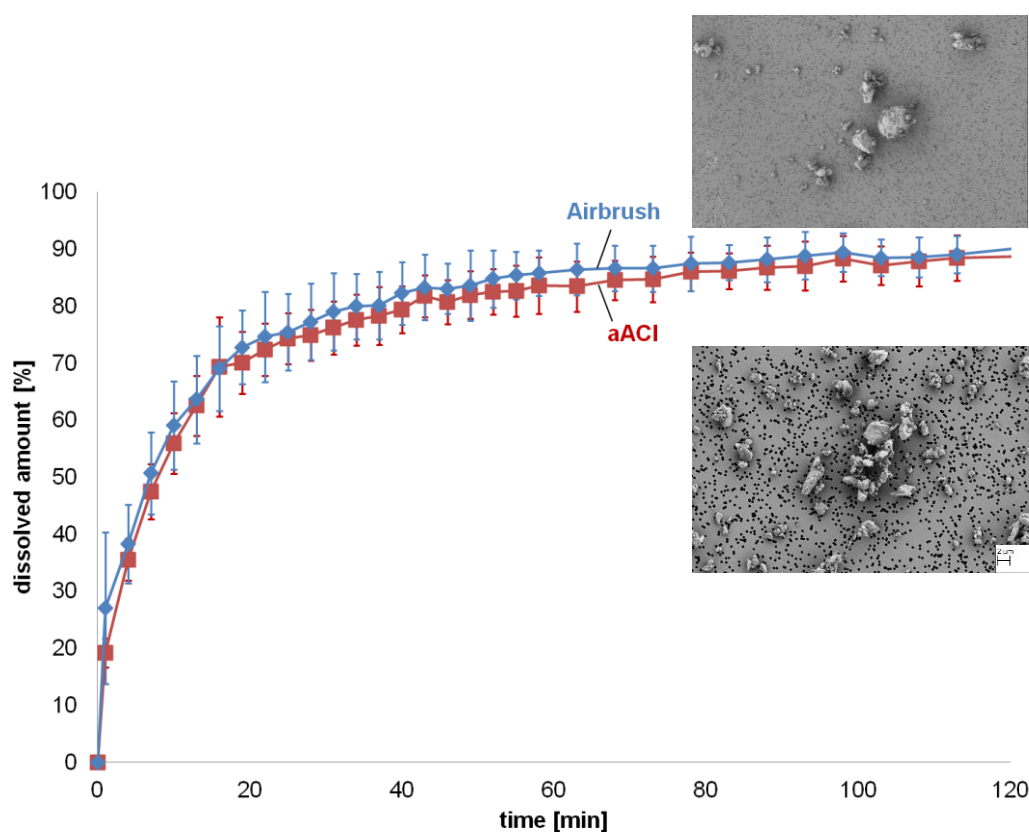


Figure 4.47: Comparison of dissolution profiles of Budesonide using the aACI or the airbrush for deposition. IPC membrane, aACI (red cube), airbrush (blue rhomb), mean  $\pm$  SD,  $n = 3$ , SEM pictures of Budesonide on IPC membrane above: after airbrush, down:aACI

Therefore, the dose collection method with the aACI was adapted and a stage extension is inserted to allow sedimentation of the particles instead of impaction.

Figure 4.48 demonstrates the impact of the dose collection method on the dissolution profile. The dissolution process is slower by using the aACI than by the use of mACI having the same particle mass on the filter. The SEM pictures (Figure 4.49) illustrate that using the mACI a more homogenous particle distribution on the filter is obtained compared to the aACI where dark areas are visible. These areas are in line with the holes of the filter stage and contain a high number of agglomerated particles. For the set up aACI + SE the dissolution profile is similar to the one with modified filter stage (mACI) ( $f_1 = 1.2$ ,  $f_2 = 92.1$  (Table 4.16, page 118)). For getting better SEM pictures the amount of FPD on membrane is increased (approximately 1 mg). Therefore, for the aACI + SE set up are also the holes of the filter stage in form of darker areas visible as for the aACI set up. Nevertheless, the shape is not as clearly defined as for the aACI SEM pictures. For that reason it could be supposed that with increasing FPD using the SE with normal filter stage the dissolution profile will approximate with the profiles of aACI.

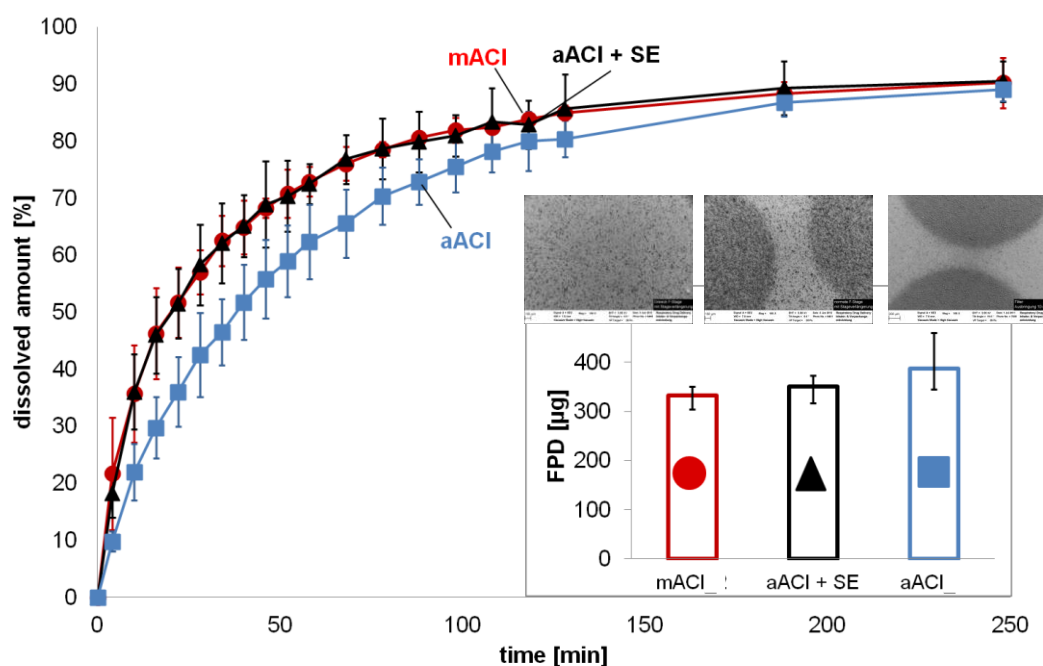


Figure 4.48: Dose collecting depending dissolution profiles of Budesonide mACI (red dot), aACI (blue squares) and aACI + SE (black triangle) mean  $\pm$  SD,  $n = 3$  with FPD on membrane mean  $\pm$  min/max with SEM pictures (for details see Figure 4.49)

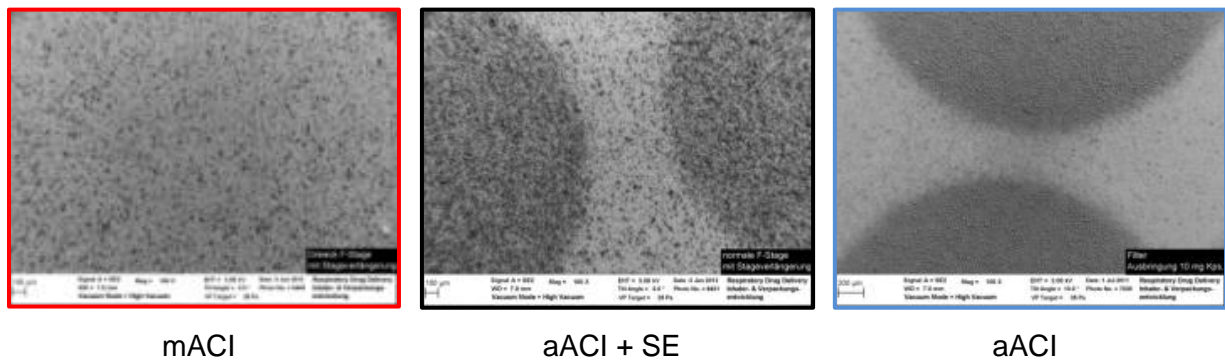


Figure 4.49: SEM pictures of regenerated cellulose with Budesonide after use of different dose collection methods (FPD on SEM picture membrane 1000 µg)

The impact of particle mass on the dissolution process is shown in Figure 4.50, the higher the mass of particles on the membrane, the slower the dissolution. Although mass differences for aACI are the same compared to mACI the differences in dissolution profiles for aACI are much larger than for the mACI. Fit factors ( $f_1 = 9.4$ ;  $f_2 = 59.1$  (Table 4.16, page 118)) confirm similarity of dissolution profiles for the mACI with different masses on the membrane. The fit factors show no similarity for the aACI profiles ( $f_1 = 34.9$ ;  $f_2 = 30.8$  (Table 4.16)). Additionally, MDT was calculated, but the trends displayed in the profile could not be shown clearly with the MDT (Table 4.15, page 117). In contrast to the dissolution profiles the MDT displays similarity of aACI set ups.

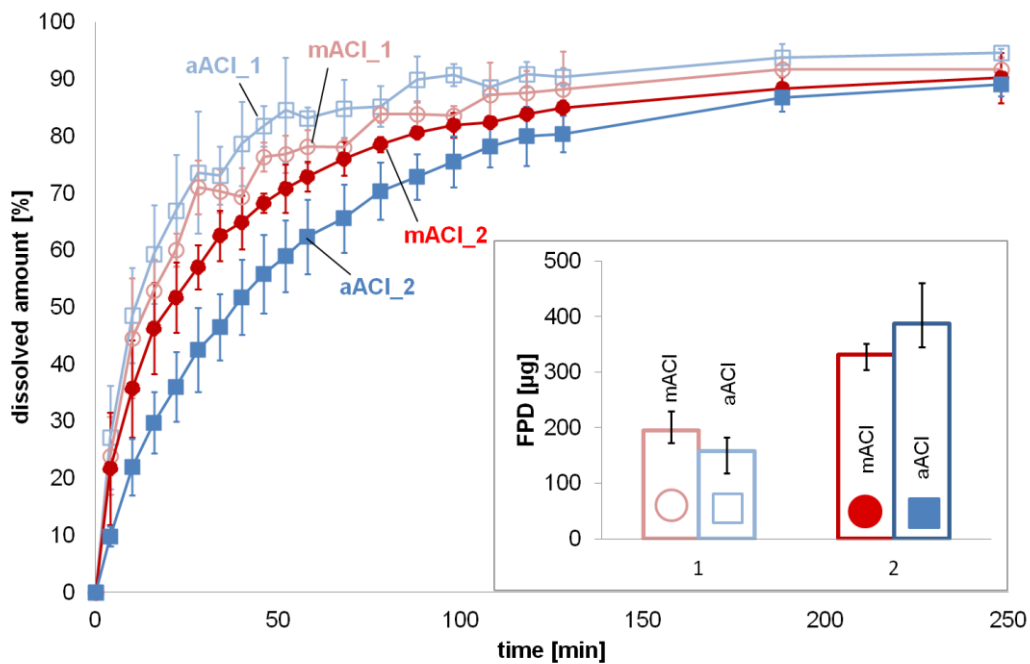


Figure 4.50: Mass dependent dissolution profile of Budesonide 200 µg FPD on membrane (open bright symbols), 400 µg on membrane (closed dark symbols), mACI (red dots), aACI (blue squares) mean ± SD, n = 3 with FPD on membrane mean ± min/max

Above with the Erweka apparatus an influence of particle mass (100  $\mu\text{g}$  vs. 1000  $\mu\text{g}$ ) on membrane onto the dissolution process and therefore on the dissolution profile was already demonstrated. In the modelling section (Figure 4.58) it could be demonstrated, that the FPD on the membrane has only a negligible influence on the dissolution profile assuming optimal conditions, especially no agglomerates and therefore no dissolution interaction between the particle and its neighbors. Figure 4.50 demonstrates for areas with a high amount of particles even changes of less than 200 $\mu\text{g}$  mass on the membrane strongly influence the dissolution process. The mACI guarantees a homogenous particle distribution on membrane, resulting in smaller mass dependency of the dissolution process.

In conclusion, a less mass depending dissolution profile is beneficial due to a reduced variability which indicates a higher robustness of the method. Although a higher weight of substance is necessary for mACI than for aACI, the amount is smaller than for the airbrush set up, furthermore the benefits of the new dose collection set up predominate this drawback. Consequently, mACI is a step to achieve optimum in vitro dissolution conditions.

#### 4.6.6. Comparison of different membrane holder types

Figure 4.51 shows no significant difference between the different membrane holder setups and the fit factors (Table 4.16, page 118) indicate similarity.

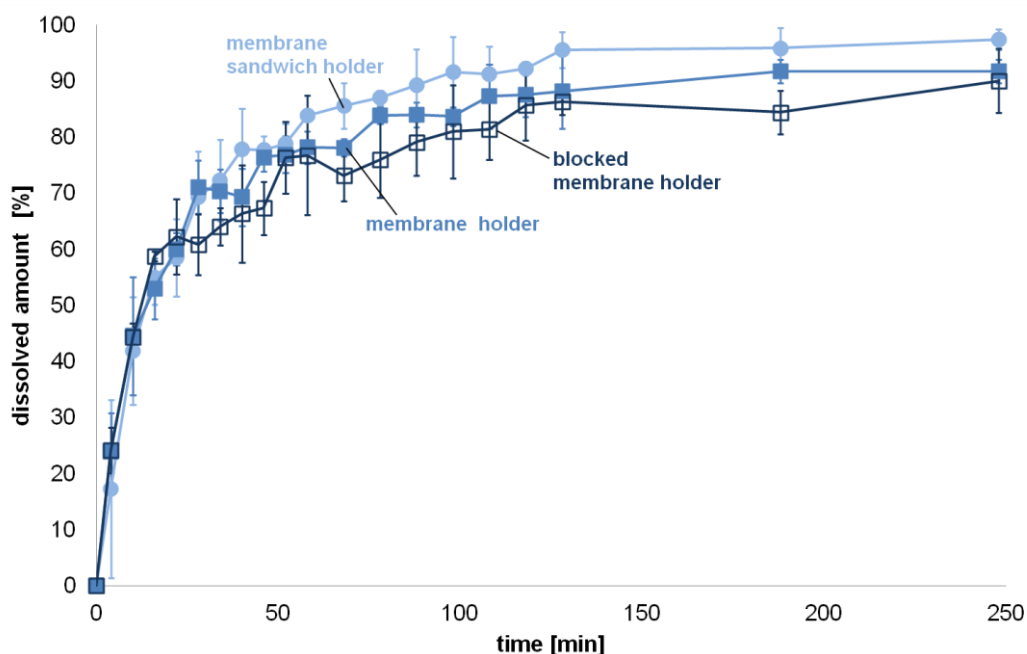


Figure 4.51: Dissolution profiles of Budesonide for different membrane holders mACI, membrane sandwich holder (light blue dots), membrane holder (blue squares), blocked membrane holder (blue open squares), mean  $\pm$  SD, n = 3

The blocked membrane holder was used to reduce the effect of diffusion over the edge of the membrane instead of diffusion direct through the membrane. Interestingly, with this set up an air liquid interface was created, too.

Due to the reduced diffusion pathways for the blocking set up slower dissolution profiles than without blocking were expected. This could not be shown for Budesonide (Figure 4.51). Hence, most of the dissolved amount diffuses through the membrane and not over the edge between membrane and membrane holder.

The idea behind the membrane sandwich holder was to reduce possible effects of the watch glass on the diffusion and therefore on the dissolution process. Comparison of the membrane holder set up and the membrane sandwich holder shows no difference between the dissolution profiles (Figure 4.51,  $f_1 = 5.8$ ,  $f_2 = 65.3$  (Table 4.16, page 118)). Hence, most of the solution diffuses through the upper membrane. The reason could be found in the constant movement of the paddle and thus low concentration of dissolved substance directly at the membrane. Consequently, the diffusion gradient is high and the dissolved substance moves faster through the upper membrane.

Beneath the watch glass the dissolution medium is almost unstirred and convection is relatively slow [55]. Changing the watch glass to another membrane like at the membrane sandwich holder, dissolution medium hydrodynamics on the lower part of the holder are the same. At the lower membrane the concentration of dissolved substance directly at the membrane is very high, but due to the low convection the diffusion gradient is small and substance pass the membrane at the upper sight.

Overall the “standard” membrane holder adapted form the transdermal patches is beneficial compared to other tested membrane holders (blocked and sandwich) and the system developed by Son et al. [55]. By the membrane holders used in this study the substance particles are directly placed on the membrane and the diffused dissolution medium has direct access to the particles for dissolving, possible air bubbles between watch glass and membrane have no impact on the dissolution process. Using the NGI dissolution cup the powder is on the plate, then a membrane is placed on top and the cassette is sealed. Hence, there is trapped air under the membrane, which could slow down or even hinder the access of dissolution medium to the API particles resulting in a reduced dissolution [17].

#### 4.6.7. Influence of temperature on the dissolution process

In Figure 4.52 the influence of temperature on dissolution profile is shown. As expected due to a better solubility of Budesonide at 37°C (21 µg/ml vs. 17 µg/ml at 22°C) the dissolution profile at 37°C is faster and standard deviation is smaller.

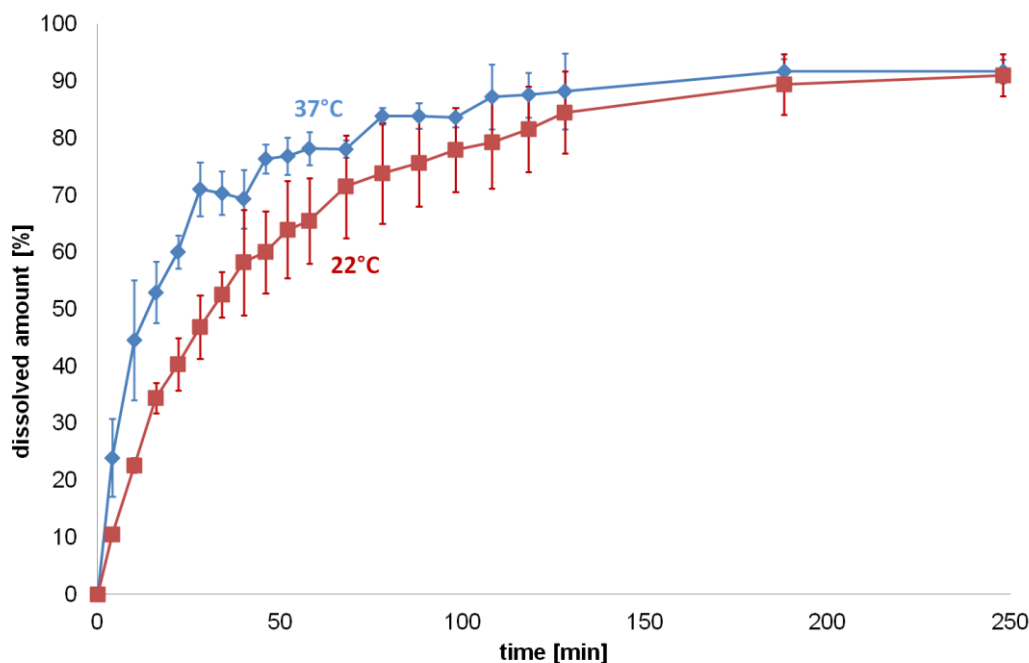


Figure 4.52: Dissolution profiles of Budesonide at different temperatures mACI, 37°C (blue rhomb), 22°C (red squares), mean  $\pm$  SD, n = 3, error bars are in all cases existent, but sometimes too small to be displayed

Therefore, temperature control during a dissolution test and between different dissolution tests is important. Furthermore, the temperature should be within a defined range, for avoiding any temperature influence on the solubility and hence on the dissolution process. The temperature for dissolution testing of powders for inhalation should be the same like the human body temperature, 37°C. This would be in accordance to the pharmacopoeias claims for dissolution testing of oral dosage forms (37°C  $\pm$  0.5°C [10,60]).

#### 4.6.8. Influence of lactose

As expected there is no difference in the dissolution process (Figure 4.53, MDT: Table 4.15, page 117) of micronized Budesonide and micronized Budesonide from a Respiritose blend ( $f_1 = 4.9$ ,  $f_2 = 71.9$  (Table 4.16, page 118)).

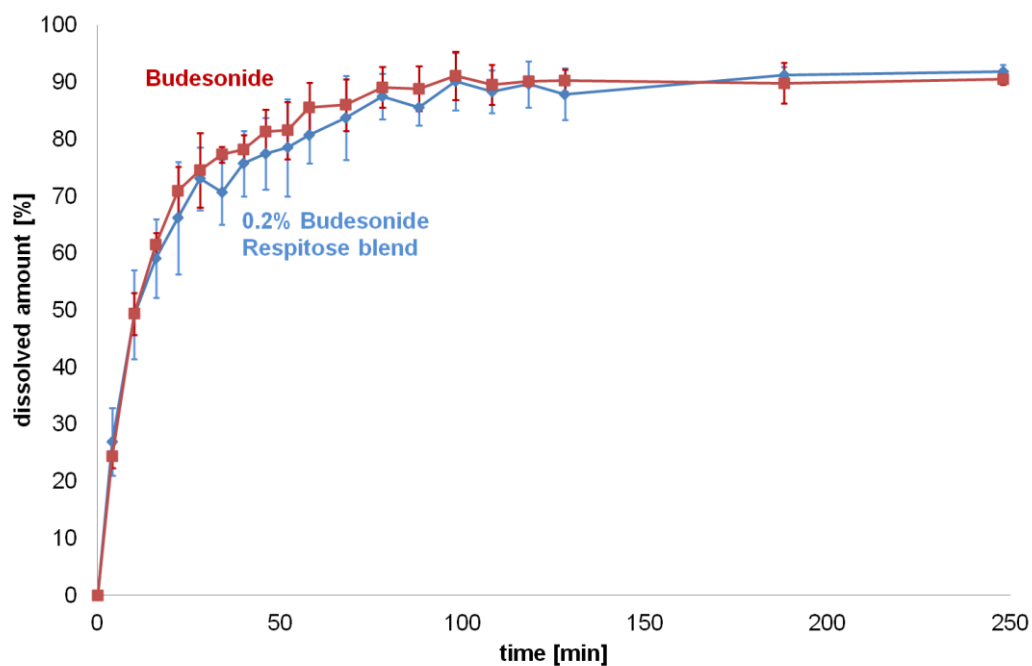


Figure 4.53: Dissolution profiles of Budesonide and Budesonide-Respitose blend mACI, bend (blue rhomb), micronized Budesonide (red squares), mean  $\pm$  SD, n = 3, error bars are in all cases existent, but sometimes too small to be displayed

#### 4.6.9. Dissolution medium containing surfactants

In Figure 4.54 influence of different surfactant on the dissolution process of Budesonide is shown. Due to the small micelle size (Table 4.3) the micelles of SDS and Tween® can pass the membrane and increase the wettability of Budesonide. The objects of DPPC are too large for passing the membrane [55], but as described above free DPPC molecules [31] can pass the membrane and increase the wettability. Due to the solubility data (Table 4.2) the rank order of dissolution profiles using surfactants expected is: SDS (fastest), Tween® 80, Tween® 20, DPPC, without surfactant (slowest).

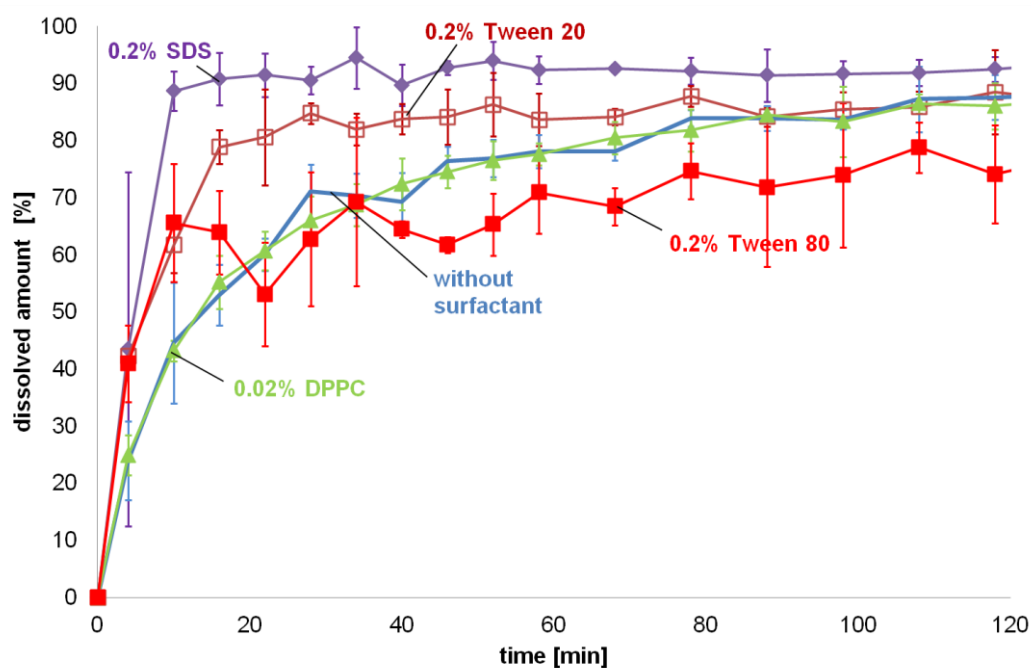


Figure 4.54: Dissolution profiles of Budesonide with use of different surfactants in the dissolution medium, mACI, 0.2% SDS (purple rhomb), 0.2% Tween® 20 (open red squares), 0.2% Tween® 80 (red squares), 0.02% DPPC (green triangle) and without surfactant (no symbol), mean  $\pm$  SD,  $n = 3$ , error bars are in all cases existent, but sometimes too small to be displayed

This expected rank order is not in all cases given. It is obvious that the dissolution profile of Budesonide using PBS buffer containing SDS has the fastest dissolution process, but at the beginning the profiles using Tween® 80 and 20 in dissolution medium show the same slope. In the further progress of dissolution Tween® 80 data variability highly increases and dissolution process slows compared to Tween® 20. The cause for this behavior might be found in HPLC handling problems if Tween® 80 is used. The profile by using DPPC is similar to the profile without surfactant (Table 4.18), but shows a more smooth behavior with higher reproducibility. Besides the SDS set up, MDT (Table 4.15) calculation provides contradictory results compared to the profiles. In chapter 5.1.1 a discussion of the MDT “problematic” will follow.

In Table 4.2 the solubility data of substances in PBS buffer with and without surfactants are compared to each other. In this thesis a comparison of dissolution profiles of different substance is aimed. Therefore, the use of the surfactant should increase the wettability of the substances but not increase the solubility, because a solubility increase might reduce the discrimination power. It is obvious that SDS and Tween® 20 strongly increase the solubility of Budesonide and Substance A base. Hence, these surfactants (SDS, Tween®) are not suitable and DPPC was chosen for further experiments.

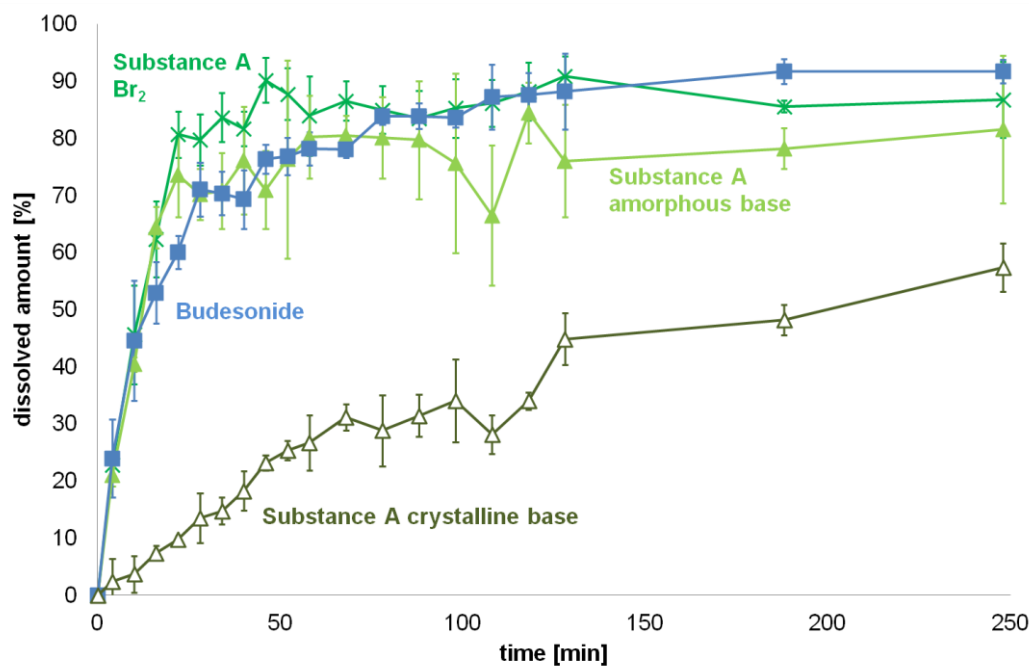


Figure 4.55: Dissolution profiles using the RC membrane mACI, Substance A Br<sub>2</sub> (green x), Substance A amorphous base (light green triangle), Budesonide (blue square) and Substance A crystalline base (open dark green triangle), mean  $\pm$  SD, n = 3, error bars are in all cases existent but sometimes too small to be displayed

Due to the low solubility of substance A crystalline base, the substance shows as expected the slowest dissolution process independent of dissolution medium or membrane holder (Figure 4.55 - Figure 4.57). In the following results description for Substance A crystalline base is not extra mentioned, because the dissolution process is always the slowest. From solubility results the rank order of dissolution profiles in buffer expected was Substance A dibromide, Substance A amorphous base, and Budesonide. The FPD on membrane for all substances is similar (Table 4.15). As Figure 4.55 displays the dissolution profiles are similar especially in the first 20 minutes and discrimination between the substances is not possible. Fit factor test (Table 4.16, page 118) underlines these results. The fit factors for comparison of dissolution profiles of the dibromide and Budesonide are not definite.

If PBS buffer with 0.02% DPPC as dissolution medium is used discrimination between all tested substances is possible (Figure 4.56, Table 4.16). Furthermore, for the tested sub-

stances except for the crystalline base the standard deviation of the dissolution profiles decreases with the use of 0.02% DPPC in the dissolution medium.

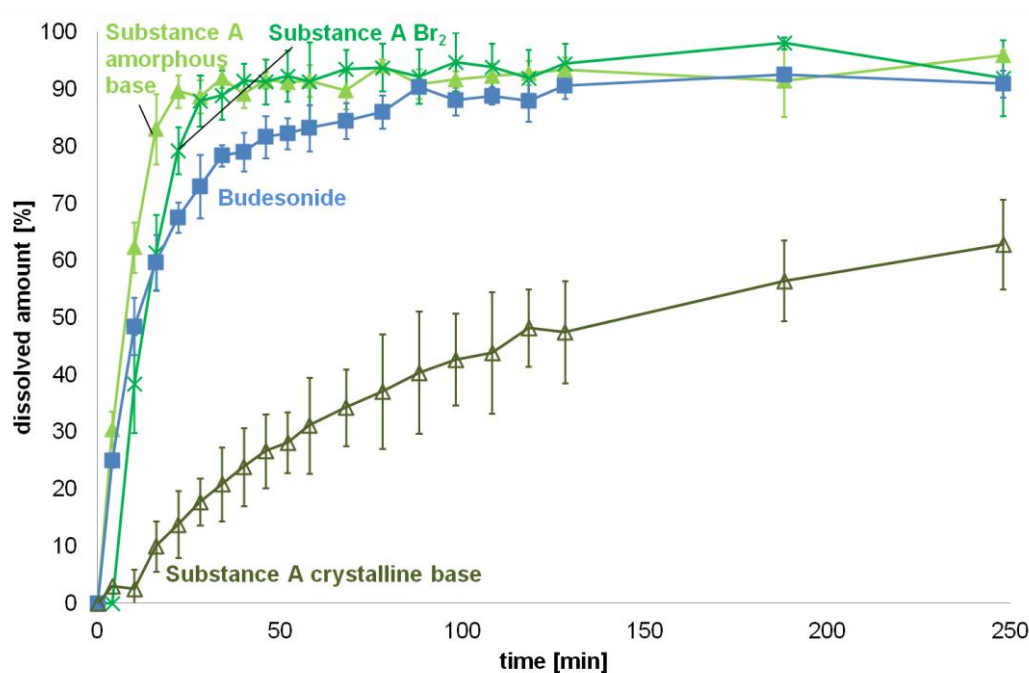


Figure 4.56: Dissolution medium containing 0.02% DPPC mACI, Substance A Br<sub>2</sub> (green x), Substance A amorphous base (light green triangle), Budesonide (blue square) and Substance A crystalline base (open dark green triangle), mean  $\pm$  SD, n = 3, error bars are in all cases existent but sometimes too small to be displayed

Amazingly in Figure 4.57, Budesonide shows a faster dissolution than Substances A dibromide and amorphous base.

However, discrimination between these two substances (amorphous base and dibromide) is not possible. The fit factors confirm these results (Table 4.16). As already described above blocking has no influence on the dissolution profiles of Budesonide. For Substance A dibromide and Substance A amorphous base the dissolution profile in the blocking set up is much slower, due to a reduced diffusion (Figure 4.56 compared to Figure 4.57). Substance A dibromide ( $c_s = 265 \mu\text{g/ml}$ ) and amorphous base ( $c_s = 211 \mu\text{g/ml}$ ) have both a more than 10 fold higher solubility than Budesonide ( $c_s = 17 \mu\text{g/ml}$ ), so the diffusion rate might be the rate limiting step and not the solubility. With hindering the diffusion over the membrane border, the rate-limiting step is more underlined.

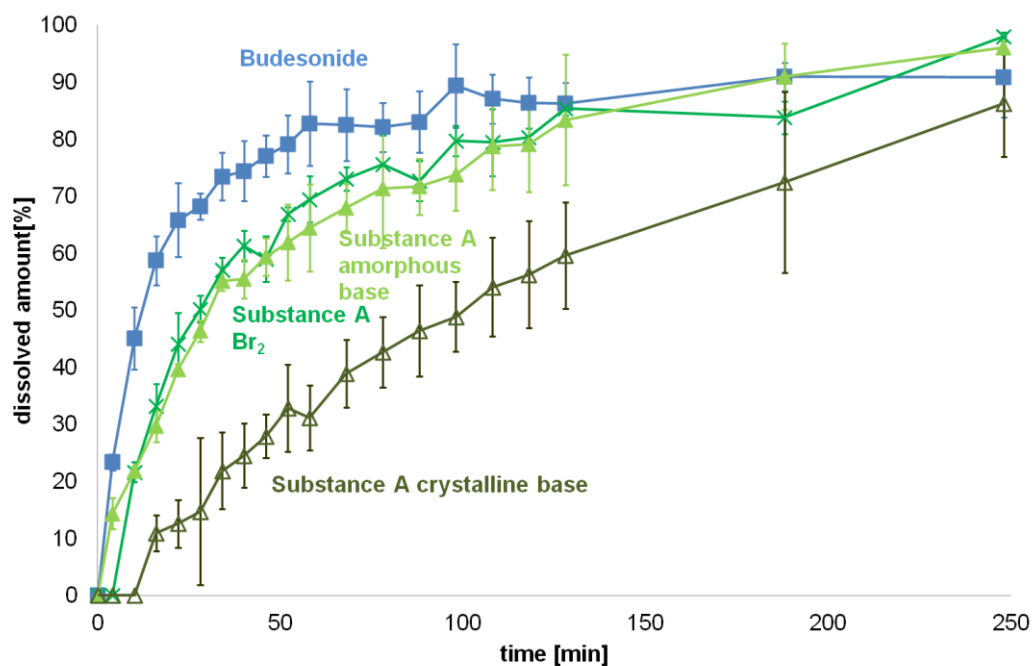


Figure 4.57: Dissolution medium containing 0.02% DPPC and blocked membrane holder mACI, Substance A Br<sub>2</sub> (green x), Substance A amorphous base (light green triangle), Budesonide (blue square) and Substance A crystalline base (open dark green triangle), mean  $\pm$  SD, n = 3, error bars are in all cases existent but sometimes too small to be displayed

Compared to the results with Erweka paddle apparatus it could be shown that by controlling the major influence factors, especially mass and distribution on membrane, Substance A amorphous base, Substance A dibromide and Budesonide show no discrimination (Figure 4.43 vs. Figure 4.55). By adding 0.02% DPPC to the dissolution medium, discrimination between the used substances (Figure 4.56) is possible.

Table 4.15. Summary of used substances and membrane material with corresponding dissolution set up, recalculated FPD on filter (mean  $\pm$  SD) and MDT (mean  $\pm$  SD), E = Erweka paddle apparatus, S = Sotax stirring speed always 100 rpm, Tw = Tween®

substance	mem- brane ma- terial	additional information	recalculated FPD on filter [ $\mu$ g] n = 3		MDT [min]	
			mean	$\pm$ SD	mean	$\pm$ SD
Budesonide	RC	E, aACI, 50rpm	1805.0	$\pm$ 264	204.6	$\pm$ 29.1
		E, aACI, 100rpm	1917.0	$\pm$ 442	174.9	$\pm$ 43.2
		E, aACI, 140rpm	1892.0	$\pm$ 126	160.3	$\pm$ 8.0
		E, aACI, 140rpm	353.0	$\pm$ 114	25.6	$\pm$ 1.3
	IPC	E, aACI, 140rpm	314.4	$\pm$ 22.7	21.6	$\pm$ 9.0
		E, Airbrush, 140rpm	211.8	$\pm$ 28.5	29.4	$\pm$ 5.6
	RC	S, mACI	194.8	$\pm$ 30.7	39.7	$\pm$ 11.1
		S, aACI, ,1	157.7	$\pm$ 34.5	49.7	$\pm$ 8.5
		S, aACI, 2	387.7	$\pm$ 63.4	45.9	$\pm$ 8.8
		S, aACI + SE, 2	350.2	$\pm$ 29.1	34.6	$\pm$ 5.1
		S, mACI, 1	194.7	$\pm$ 30.7	27.9	$\pm$ 1.6
		S, mACI, 2	331.9	$\pm$ 24.4	35.2	$\pm$ 9.7
		S, mACI, sandwich hold- er	78.2	$\pm$ 19.0	32.0	$\pm$ 4.6
		S, mACI, blocked holder	84.6	$\pm$ 8.7	23.1	$\pm$ 6.9
		S, mACI, 22°C	187.2	$\pm$ 15.6	45.0	$\pm$ 7.6
		S, mACI, 0.02% DPPC	129.5	$\pm$ 14.8	26.2	$\pm$ 2.8
	S, mACI, 0.2% Tw 20	176.2	$\pm$ 11.2	15.9	$\pm$ 2.3	
S, mACI, 0.2% Tw 80	157.1	$\pm$ 27.8	20.1	$\pm$ 12.5		
S, mACI, 0.2% SDS	184.4	$\pm$ 31.2	6.2	$\pm$ 1.4		
S, mACI, 0.02% DPPC, blocked holder	81.2	$\pm$ 16.2	27.7	$\pm$ 8.4		
Budesonide- Respitose	RC	S, mACI, 37°C	216.0	$\pm$ 2	25.0	$\pm$ 6.1
Substance A crystalline base	RC	E, aACI, 140rpm	447.0	$\pm$ 124	315.3	$\pm$ 7.6
		E, aACI, 140rpm	431.5	$\pm$ 42.0	243.9	$\pm$ 28.0
	IPC	S, mACI	103.2	$\pm$ 6.9	91.7	$\pm$ 1.3
		S, mACI, 0.02% DPPC	110.4	$\pm$ 11.3	81.1	$\pm$ 8.2
		S, mACI, 0.02% DPPC, blocked holder	59.3	$\pm$ 9.2	97.8	$\pm$ 10.3
Substance A amorphous base	RC	E, aACI, 140rpm	187.5	$\pm$ 14.3	9.8	$\pm$ 3.6
		E, aACI, 140rpm	153.7	$\pm$ 63.4	3.2	$\pm$ 1.0
	IPC	S, mACI	98.9	$\pm$ 10.6	23.9	$\pm$ 9.0
		S, mACI, 0.02% DPPC	98.6	$\pm$ 20.4	16.7	$\pm$ 7.5
		S, mACI, 0.02% DPPC, blocked holder	62.7	$\pm$ 12.9	55.9	$\pm$ 12.7
Substance A dibromide	RC	E, aACI, 140rpm	156.3	$\pm$ 64.4	4.6	$\pm$ 0.7
		E, aACI, 140rpm	167.4	$\pm$ 61.6	6.6	$\pm$ 5.7
	IPC	S, mACI	98.0	$\pm$ 16.9	21.7	$\pm$ 3.0
		S, mACI, 0.02% DPPC	77.2	$\pm$ 15.9	17.0	$\pm$ 0.8
		S, mACI, 0.02% DPPC, blocked holder	59.8	$\pm$ 10.4	59.4	$\pm$ 1.5
Fenoterol	RC	E, aACI, 140rpm	272.4	$\pm$ 65.8	0.8	$\pm$ 0.1
		E, aACI, 140rpm	1582.0	$\pm$ 124	0.9	$\pm$ 0.3
	IPC	E, aACI, 140rpm	2067.0	$\pm$ 447	0.7	$\pm$ 0.1

Table 4.16: Results of fit factor calculation

	$f_1$	$f_2$	Similar?
similar profiles	< 15	50-100	
<b>stirring speed</b>			
50 rpm vs. 100 rpm	7.8	63.3	yes
100 rpm vs. 140 rpm	3.1	85.4	yes
<b>PBS buffer aACI, RC membrane</b>			
Fenoterol vs. Substance A Br <sub>2</sub>	57.0	32.0	no
Substance A Br <sub>2</sub> vs. Substance A amorphous base	30.8	36.3	no
Substance A amorphous base vs. Budesonide	25.4	42.5	no
<b>PBS buffer aACI, IPC membrane</b>			
Fenoterol vs. Substance A Br <sub>2</sub>	37.2	24.4	no
Substance A Br <sub>2</sub> vs. Substance A amorphous base	7.6	61.8	yes
Substance A amorphous base vs. Budesonide	5.7	30.0	no
Airbrush vs. aACI	3.3	77.1	yes
Erweka vs. Sotax	9.2	58.3	yes
<b>dose collection method depending</b>			
aACI vs. aACI +SE	19.1	47.7	no
aACI vs. mACI	17.9	48.2	no
mACI vs. aACI +SE	1.2	92.1	yes
<b>mass and dose collection method depending</b>			
aACI 200µg vs. aACI 400µg	34.9	30.8	no
mACI 200µg vs. mACI 400µg	9.4	59.1	yes
aACI 200µg vs. mACI 200µg	7.2	63.2	yes
aACI 400µg vs. mACI 400µg	17.9	48.2	no
<b>different membrane holders</b>			
normal vs. blocked	5.6	64.8	yes
normal vs. sandwich	5.8	65.3	yes
blocked vs. sandwich	11.5	53.6	yes
Budesonid: without surfactant vs. 0.02% DPPC	4.6	71.4	yes
Budesonid: 22°C vs. 27°C	19.9	42.0	no
Budesonid vs Budesonid- Respirose blen	4.9	71.9	yes
<b>PBS buffer</b>			
Substance A Br <sub>2</sub> vs. Budesonide	14.7	47.6	inconsistent
Budesonide vs. Substance A amorphous base	8.4	55.4	yes
Substance A Br <sub>2</sub> vs. substance A amorphous base	11.6	52.0	yes
Substance A amorphous base vs. Substance A crystalline base	64.1	16.4	no
<b>PBS buffer with 0.02% DPPC</b>			
Substance A Br <sub>2</sub> vs. Budesonide	20.8	44.1	no
Budesonide vs. Substance A amorphous base	32.3	39.0	no
Substance A Br <sub>2</sub> vs. Substance A amorphous base	48.2	34.6	no
Substance A amorphous base vs Substance A crystalline base	89.0	12.8	no
<b>PBS buffer with 0.02% DPPC, blocking</b>			
Substance A Br <sub>2</sub> vs. Budesonide	28.9	39.4	no
Budesonide vs. Substance A amorphous base	25.6	37.0	no
Substance A Br <sub>2</sub> vs. Substance A amorphous base	6.4	65.1	yes
Substance A amorphous base vs Substance A crystalline base	44.1	29.3	no

## 4.7. Dissolution Model

### 4.7.1. Influence of particle mass on the membrane

For the model in Figure 4.58 FPD on the membrane was varied (10  $\mu\text{g}$ , 100  $\mu\text{g}$ , 250  $\mu\text{g}$ , 500  $\mu\text{g}$ , 750  $\mu\text{g}$ , and 1000  $\mu\text{g}$ ). The calculated models in Figure 4.58 show a minimal dependence of dissolution profile on the deposited mass on the membrane. In the first twenty minutes the profiles are identical. With increasing time the dissolution profiles diverge depending on particles on the membrane. The “fastest” dissolution is as expectable for the smallest amount (10  $\mu\text{g}$ ) the slowest for the highest deposited mass (1000  $\mu\text{g}$ ). Comparison of the profiles 10  $\mu\text{g}$  and 1000  $\mu\text{g}$  with fit factor test shows similar almost identical profiles ( $f_1 = 1.1$ ,  $f_2 = 95.7$  (Table 4.18, page 125)). The model is based on the assumption of optimal conditions, which means no agglomerates; no dissolution interaction between the particles, therefore the model is probably not sensitive on different masses, resulting in similar dissolution profiles.

The SEM pictures display a chronological order of the decrease of substance on the membrane associated with an increasing dissolution profile.

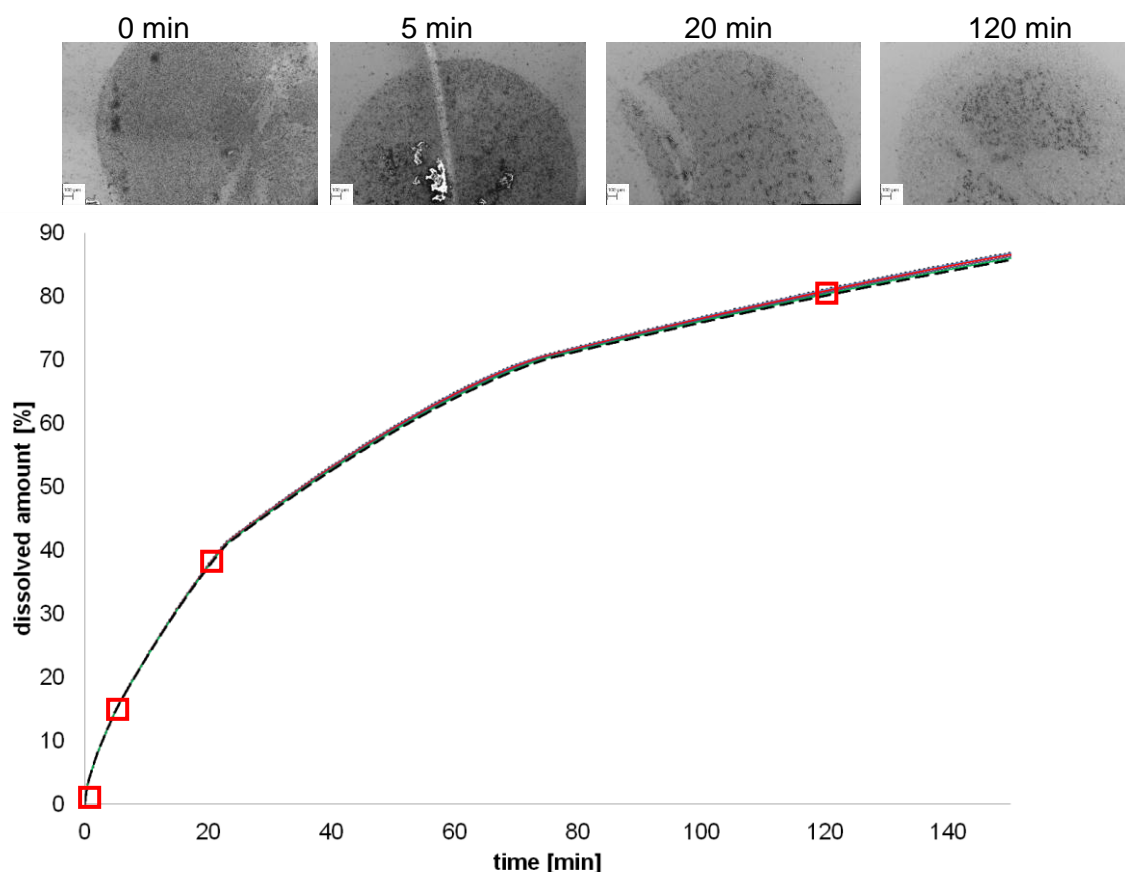


Figure 4.58: Graphs for calculated model for Budesonide with a different mass on the membrane (10  $\mu\text{g}$  (dotted line), 100  $\mu\text{g}$  (blue), 250  $\mu\text{g}$  (red), 500  $\mu\text{g}$  (purple) 750  $\mu\text{g}$  (green), 1000  $\mu\text{g}$  dashed line) with SEM pictures of a membrane with Budesonide at the time points 0 min, 5 min, 20 min, and 120 min. The SEM pictures display a more and more brighter “circle”. This illustrates the more and more decreasing particle mass on the membrane, shown by an increasing slope of dissolved amount

### 4.7.2. Influence of particle shape

The aerodynamic particle diameter was converted with Equation 3.11 in the geometric diameter using either the shape factor for spherical particles or for cubic ones.

In Figure 4.59 the dissolution profile by assumption of spherical particles is a little bit faster than for the cubic particles. However, the two profiles are similar ( $f_1 = 4.1$ ,  $f_2 = 79.7$  (Table 4.18, page 125)).

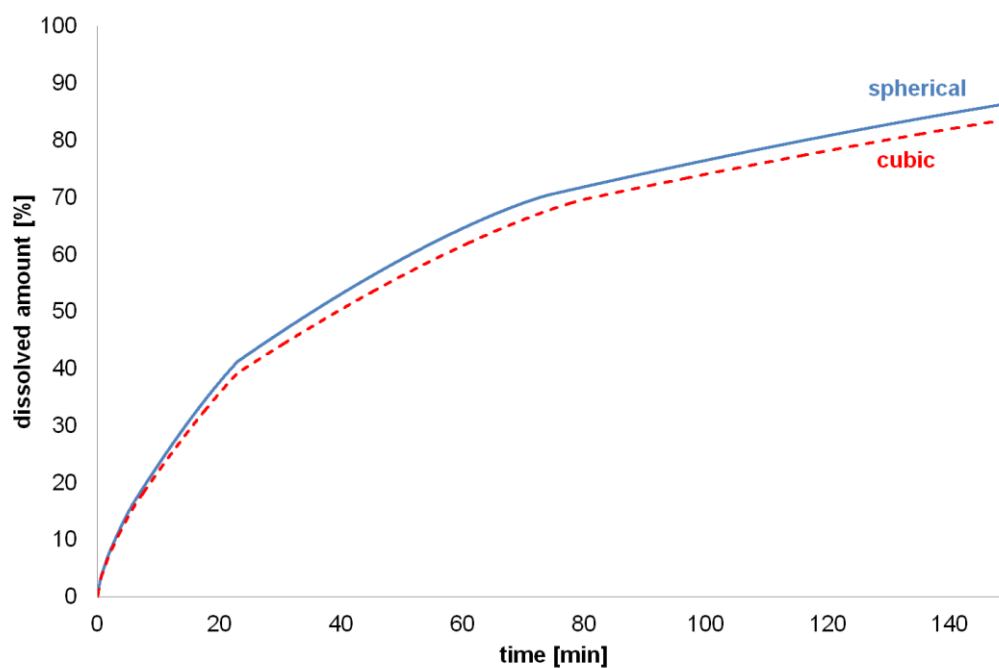


Figure 4.59: Graphs for calculated model of Budesonide with spherical (blue line) or cubic (red dashed line) particles

### 4.7.3. Influence of solubility

As expected dissolution profiles strongly depend on the solubility of the substance in the dissolution medium (Figure 4.60), the higher the solubility the faster the dissolution.

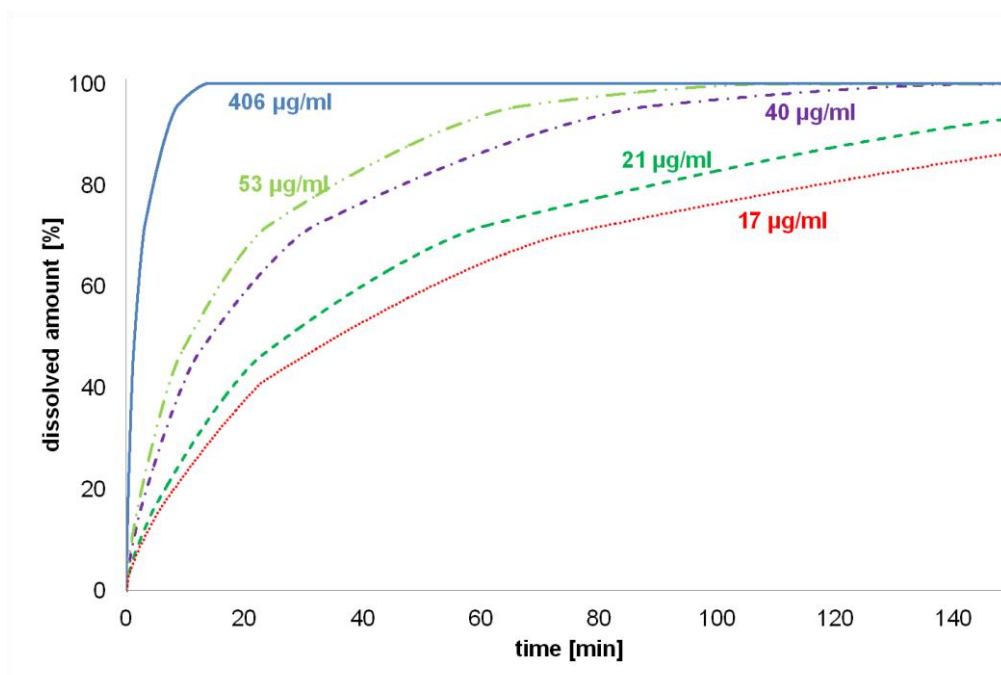


Figure 4.60: Graphs for calculated model of Budesonide with different solubility. The solubility data are based on the solubility measurement for budesonide in PBS buffer pH 7.4 with different surfactants (table 2).

### 4.7.4. Influence of diffusion layer thickness

Figure 4.61 demonstrates the influence of the diffusion layer thickness  $h$  on the dissolution profiles. The models A and D are based on the assumption that the diffusion layer thickness is directly depending on the radius of each particle size group. In model D the diffusion layer is shrinking with the particle, in model A the diffusion layer is staying constant while the particle is dissolving. At the beginning the models A and D are similar due to the same starting diffusion layer thickness, later the models diverge. At model A, the constant  $h$  results in a slower dissolution process, than for model D where  $h$  decreases with the particle size. The dissolution curves of the models B and C differ strongly from A and D. B and C are both models with a time independent diffusion layer and for the different particle size classes the diffusion layer thickness is equal. Model B is based on the assumption that the diffusion layer thickness for all groups correlates with the radius of the largest particles; in model C with the smallest. It is obvious that a too small diffusion layer thickness results in a very fast dissolution profile and an overall too large  $h$  in a too slow profile.

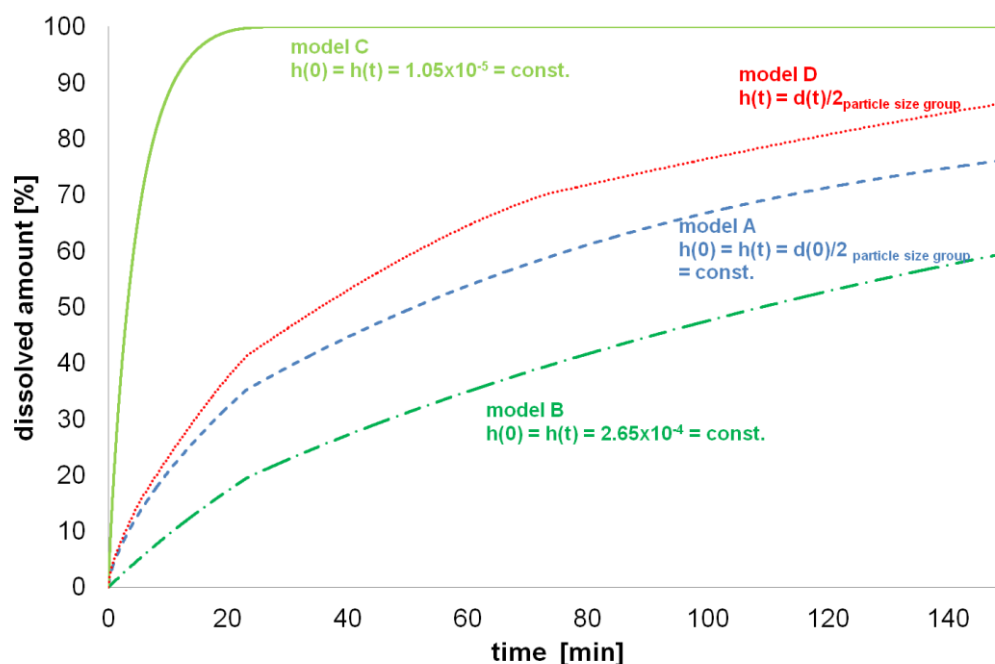


Figure 4.61: Graphs for calculated model of Budesonide with several assumptions for diffusion layer thickness  $h$

A:  $h(0) = h(t) = \text{const.} = d(0)/2_{\text{particle size group}}$  (blue dashed line)

B:  $h(0) = h(t) = \text{const.} = 2.65 \times 10^{-4}$  (dark green dashed dotted line)

C:  $h(0) = h(t) = \text{const.} = 1.05 \times 10^{-5}$  (green line)

D:  $h: 2.65 \times 10^{-4} \mu\text{m}, 2.08 \times 10^{-4} \mu\text{m}, 1.25 \times 10^{-4} \mu\text{m}, 7.65 \times 10^{-5} \mu\text{m}, 3.50 \times 10^{-5} \mu\text{m}, 2.05 \times 10^{-5} \mu\text{m}, 1.05 \times 10^{-5} \mu\text{m}$  and  $h(t) = d(t)/2_{\text{particle size group}}$  (red dotted line)

#### 4.7.5. Influence of particle size distribution

In Figure 4.62 the models for different particle sizes and particle size distributions on the membrane are compared with experimental data from Figure 4.50. Table 4.17 summarizes the different particle sizes for the model. As expected, with a higher percentage of smaller particles the dissolution results in faster dissolution profiles (b and a). The dissolution profiles of c and d are identical in the first 50 minutes, later the profiles diverge. The model with the largest particles (d) has the slowest dissolution profile. As already described, mACI shows a faster dissolution as aACI because of a more homogeneous distribution of particles on the membrane. The next step is comparison of the models with experimental data. The slower profile of aACI fits in the first 20 minutes with the model a, c and d. After approximate 50 minutes model d don't describe the experimental set up any longer and model a fits best. The results of fit factor test underlines the similarity, the rank order starting with the best fitting model is a, c, d, and b (Table 4.18, page 125). The models a, c and d have a higher amount of particles larger than  $4.16 \mu\text{m}$ . In contrast, the dissolution profile of mACI fits with model b, which has a higher amount of small particles and has no similarity with model d (Table 4.18).

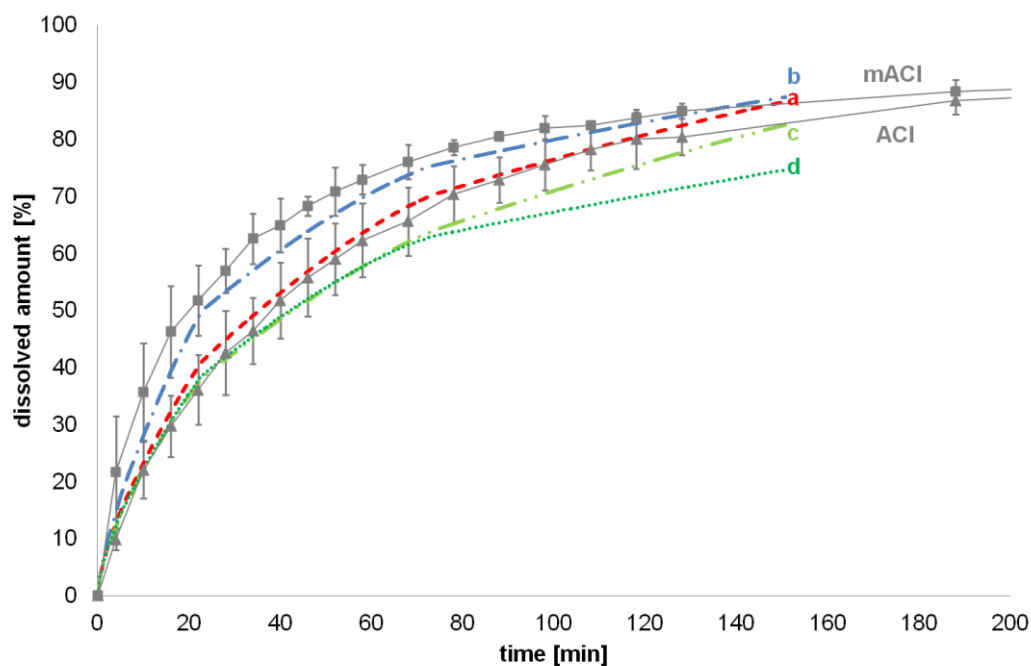


Figure 4.62: Comparison of various modeled profiles for Budesonide with different particle size distributions on the membrane compared to experimental data. mACI: square; aACI: triangle, for a- d see table 5

Table 4.17: Data for Figure 4.62

a) experimental data, b) and c) permutation of percentages (b) more small particle, c) more large particles), d) randomly chosen diameters for assumption of agglomerates

particle diameter [ $\mu\text{m}$ ]	a [%]	b [%]	c [%]	d	
	(red)	(blue)	(light green)	diameter [ $\mu\text{m}$ ]	[%]
5.29	18.8	18.8	29.7	8	18.8
4.16	29.7	18.1	27.4	5	29.7
2.49	27.4	27.4	18.8	2.49	27.4
1.53	18.1	29.7	18.1	1.53	18.1
0.70				3.2 %	
0.41				1.3 %	
0.21				1.5 %	

#### 4.7.6. Comparison of experimental and modeled data

Figure 4.63 compares experimental dissolution profiles with the associated model, in Table 4.18 results of fit factor test are summarized. For the model calculation solubility of substances in PBS buffer containing 0.02% DPPC (Table 4.2) and the data summarized in Table 3.12 were used. Furthermore, a time-dependent diffusion layer thickness was assumed. The

model for Substance A base and Budesonide describes the experimental data quite well. But the model for Substance A dibromide is really different from the experimental data.

In addition the model using solubility of substances in PBS buffer (dotted line) is inserted. Comparison of the two models show as expected for Budesonide and Substance A dibromide a slower dissolution profile, for Substance A amorphous base a faster profile and for Substance A crystalline base no difference.

It is obvious that the model with buffer data for Substance A dibromide also does not describe the experimental data well, but it is closer to the experimental data. The case of the dibromide demonstrates that there are further impact factors which are not fully considered through the model.

Nevertheless, this model is useful for the description of dissolution profiles for powders for inhalation, because trends of experimental data could be shown by the model.

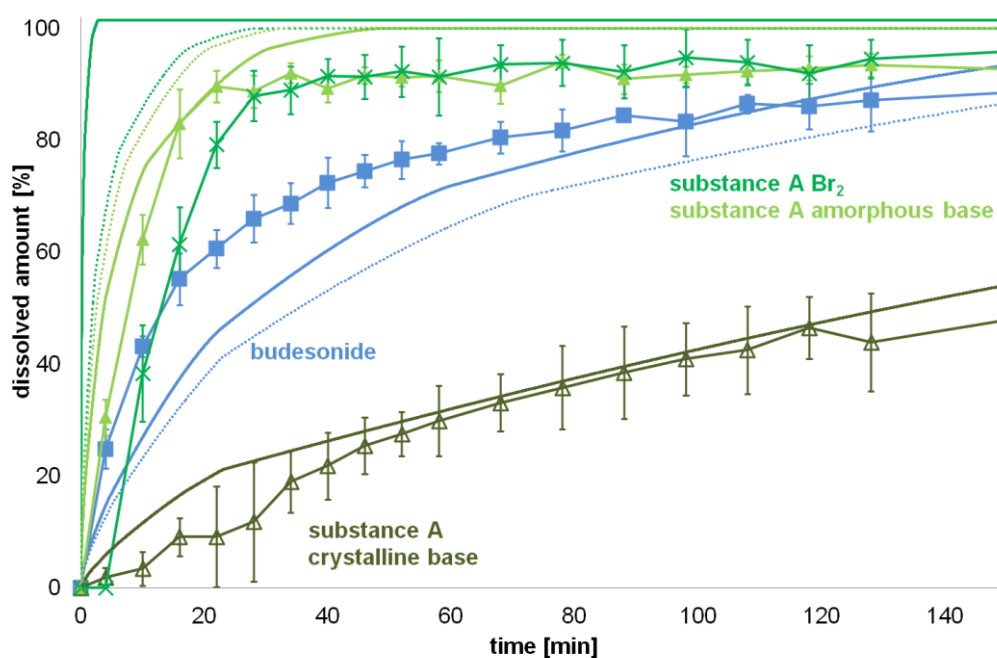


Figure 4.63: Comparison of model data (no symbols) with experimental data (symbols) of the tested substances (Substance A Dibromide green X; Substance A amorphous base light green triangle, Budesonide blue square, Substance A crystalline base open dark green triangle) set up: mACI and 0.02% DPPC in PBS buffer, mean  $\pm$  SD,  $n = 3$ , in addition dotted lines: model of substance in PBS buffer

Table 4.18: Results of fit factor calculation

	$f_1$	$f_2$	Similar?
similar profiles	< 15	50-100	
10 $\mu\text{g}$ vs. 1000 $\mu\text{g}$ (Figure 4.58)	1.1	95.7	yes
spherical vs. cubic (Figure 4.59)	4.1	79.7	yes
<b>particle size</b> (Figure 4.62)			
b vs. a	8.7	62.1	yes
b vs. c	15.7	50.2	inconsistent
b vs. d	17.7	47.8	no
a vs. c	7.7	66.5	yes
a vs. d	9.9	59.7	yes
c vs. d	3.0	78.7	yes
b vs. mACI	5.9	68.7	yes
d vs. mACI	28.7	42.1	no
c vs. aACI	6.1	71.7	yes
a vs. aACI	2.9	63.7	yes
b vs. aACI	11.3	56.5	yes
d vs. aACI	9.0	62.7	yes
<b>model vs. experimental data</b> (Figure 4.63)			
Substance A crystalline base	13.8	63.9	yes
Substance A amorphous base	11.1	48.1	inconsistent
Substance A Br <sub>2</sub>	-	-	no
Budesonide	13.6	50.1	yes



# Chapter 5

## General Discussion

This chapter focuses on general points and discusses and compares the different dissolution techniques.

## 5.1. General Points

### 5.1.1. Comparison of dissolution profiles with MDT and “fit factors”

The calculation of MDT itself is consistent. However, the results of MDT and the findings of the dissolution profiles are not in all cases concurrently. An important pre - requisite for calculation is reaching of a plateau phase where almost the whole substance is dissolved and the profile should not show any further increase [35,139] or variation. Due to the strong dependence of the MDT on this upper limit for each profile plateau phase deviations have to be averaged to one value introducing errors. Furthermore, for the crystalline base a MDT calculation could not be always performed, although the dissolution time was > 240 minutes, because the profile often does not reaches a plateau phase. Calculation of MDT without reaching plateau results in not significant values.

For getting a high statistical power of difference ( $f_1$ ) and similarity ( $f_2$ ) test EMA and FDA claim several requirements (chapter 3.6.2.2) e.g. strict borders for coefficient of variation (less than 20% for the first point and less than 10% for following points [21]) and 12 individual values for each time point [21,120].

In this thesis  $f_1$  and  $f_2$  test were used as additional factors for evaluating if two profiles are similar or not. Due to the limited amount of individual values ( $n = 3$ ) and in some cases a higher coefficient of variation than 20% the statistical power of the “fit factor” test is reduced. Especially if the variability of data is high and a low number of values is given the variance is increased. This could be shown at “border cases” where  $f_1$  test provides similarity and  $f_2$  test no similarity or vice versa.

### 5.1.2. Wettability and Dissolution

For increasing the dissolution rate of a substance the particle size could be decreased [31]. However, in the case of powders for inhalation this process has a reduced applicability because the micronized substances particles have already an aerodynamically particle size around or below 5  $\mu\text{m}$ .

In literature the use of surfactants is described for overcoming wetting problems [20]. For performing a dissolution test it is necessary to consider what the aim of the performed dissolution test is e.g. discrimination between different substances, *in vivo in vitro* correlation or dissolution test of one substance. As consequence of this consideration it needs to be decided which surfactant in which concentration is useful. Surfactants increase or decrease the wettability and / or solubility of one substance. In this thesis the focus lies more on discrimination between substances. Therefore, a large increase of solubility for example with SDS

was not suitable because the discrimination power between the substances was decreased. Hence, DPPC with a small effect on the solubility of substance (beside Substance A dibromide) was used.

Another very important point is the duration of the experiment, especially if an amorphous substance is used. An amorphous modification might recrystallize during the dissolution test in a more stable crystalline modification with a different solubility. Furthermore, the salt form of substances could change due to the amount of salts in the dissolution medium. Different salt forms of substance have a different solubility. Hence, the dissolution process could be influenced.

## **5.2. Is a comparison of the dissolution techniques possible?**

The used dissolution techniques have different advantages and disadvantages. For a comparison between the techniques first criteria need to be established. The criteria for comparison could be similarities, handling, duration of experiment, amount of dissolution medium, reproducibility, discrimination power, and validity on which the next subchapter will focus

### **5.2.1. Similarities**

According to the dissolution profiles all techniques can be used to differentiate between good (Fenoterol) and poorly soluble substances (Budesonide).

Furthermore, a large influence of the deposited mass of the substance on the membrane on the dissolution process was shown. A higher mass on the membrane results in a thicker powder layer. In a thicker powder layer the possibility of agglomerates is increased resulting in a released dissolution [55] due to a reduced wettability of all particles, especially in the “middle” or upper site of the agglomerates. Hence, a mono particle layer has to be preferred [55]. As the model calculation shows under ideal conditions – monolayer, no dissolution interaction between the particle and its neighbors - the dissolution profile in the tested range (10 µg -1000 µg) is almost independent of particle mass. By use of the newly developed modified Andersen cascade impactor a less mass dependent dissolution process could be shown. As the SEM pictures reveal (Figure 4.49) the new set up achieves an evenly distributed and almost a mono layer of particles on the membrane.

In addition, an influence of particle size classes might be expected [61] and the model describes the influence of particle size on the dissolution quite well (chapter 4.7.5). However, a more detailed focus on individual particle size classes in this thesis was not performed, because only the whole particle fraction with an aerodynamic diameter  $\leq 5 \mu\text{m}$  was of interest. Additionally, the membrane associated processes are based on a combined dissolution-diffusion process [59]. First the dissolution medium has to pass the membrane through the

pores, and then it dissolves the dispersed API. Second, after the dissolution the solution diffuses through the membrane into the bulk of dissolution medium. Consequently, the membrane material, its properties and possible membrane substance interactions play an important role for the dissolution process. If sink conditions are given the dissolution process depends stronger on membrane material and stirring speed, than on the amount of dissolution medium [54]. Important membrane properties listed in literature are: membrane thickness, pore size and pore tortuosity [59]. In this thesis it could be demonstrated, that membrane material has to be added to the list above. The membrane permeation tests show impressively large differences between the different materials. Interestingly, the test also displays a difference between two comparable membranes with comparable thickness, pore size and tortuosity from two different manufacturers (chapter 4.1.4). This indicates a possible impact of pre treatment that should be taken into account.

### 5.2.2. Handling

The  $\mu$ Diss® dissolution technique is very different from the other used set ups. Besides a different dose collection method, no membrane is used and the concentration measurements were performed online. Disadvantageous is the need of dose collection method which collects the FPD in a liquid. Due to a lag time for transferring the suspension the dissolution process starts before the measurement is started.

Regarding handling aspects the main problem by using the flow through cell is to achieve a fully closed system without leakage. In addition, in the set up used in thesis it is difficult to harmonize first droplet from the cell and starting of the auto sampler.

For the Franz cell and the paddle apparatus with membrane holder sampling is automated. The main difficulty by use of the Franz cell, is to avoid the already in literature described problem of air bubbles beneath the membrane [112,114,116]. Interestingly, the problem of air bubbles seems not existent in the Transwell® system. The handling at the Transwell® dissolution system is not as easy as at the paddle apparatus, because sampling must be done manually, but nevertheless the Transwell®s dissolution system is quite suitable. It is possible to use different membrane materials due to inserting a small mesh and compared to the Franz cell also regenerated cellulose membrane can be used. A further advantage of the Transwell® system is the possibility to use cells as *in vivo* model for dissolution testing in the future. An additional advantaged of the paddle apparatus is the possibility of seven simultaneously experiments and the easy handling of the membrane holder. The membrane is placed in the membrane holder and than in the vessel of the paddle apparatus.

### 5.2.3. Duration of experiment

Overall the duration of the experiment depends on the solubility of the used substances. Nevertheless, the duration of the experiments in the  $\mu$ Diss® and flow through cell is approximately 1 to 2h, in Franz Cell, Transwell® and paddle apparatus approximately 4 h. Furthermore, currently in the Transwell® dissolution system in the  $\mu$ Diss® six, and in the paddle apparatus with membrane holder seven experiments could be performed simultaneously.

### 5.2.4. Amount of dissolution medium

The amount of dissolution medium varies from a few milliliters in the Transwell® dissolution system and the  $\mu$ Diss® to 60 ml depending on duration (60 min) and flow rate (1ml/min) in the flow through cell up to 1l in the modified Franz Cell and paddle apparatus.

Additionally, the amount of dissolution medium depends on solubility of the substances. For ensuring sink conditions for extreme poorly water soluble substances larger amounts of dissolution medium are mandatory. If large amounts of dissolution medium are necessary of course costs for expensive buffers or surfactants increase.

### 5.2.5. Reproducibility, discrimination power and validity

The  $\mu$ Diss® might be useful at the beginning of substance and / or product development, when only small amounts of API are produced, especially for intrinsic dissolution tests. As dissolution test for powders for inhalation it is not useful, due the small discrimination power. Furthermore, the dissolution process can be influenced by using a suspension because particles could stick on the vessel wall, the optrode, float or sediment. However, no membrane is needed and thus no interaction between membrane material and substance can influence the dissolution and diffusion.

Mechanistically, compared to the other membrane based systems in the flow through cell besides diffusion the dissolution process is also influenced by the constant flow of the dissolution medium. In literature for flow through cell sink conditions are stated [20], but that is only true if an adequate flow rate depending on the solubility of the substance is used. Is the flow rate to low and the substance good soluble more substance could be dissolved and sink conditions are exceeded. The custom made flow through cell used in this thesis could not guarantee sink conditions over the whole experiment. The reason can be found in the “quench heads” which distribute the dissolution medium ideally. Therefore, the membrane is fully and homogeneous wetted. Thus, a lot of substance is initially dissolved and sink conditions are exceeded. However, for the non – sink conditions as well as for the sink conditions reproducibility and validity are poor. Hence, the flow through cell is not useful for dissolution testing of powders for inhalation.

In the Franz cell wetting of the particles on the membrane has a high experiment to experiment inconsistency resulting in an increased variability of data. An explanation can be found on the one side in the air bubbles beneath the membrane and on the other side in the membrane material. If regenerated cellulose as membrane material is used the clamped membrane is fluted due to the swelling of the cellulose. Thus, the wetting of the particles is inhomogeneous.

Comparing to the Franz Cell one could argue that reaching sink conditions in the strict definition (10% of saturation solubility) in the Transwell® dissolution system especially for poorly soluble substances like Budesonide ( $c_s = 17 \mu\text{g/ml}$ ) or Substance A crystalline base ( $c_s = 7 \mu\text{g/ml}$ ) (Table 4.2), respectively is not possible. However, due to sampling of 0.2 ml (8% of 2.5 ml dissolution medium, 5% of 3.85 ml, respectively), for the used FPD on membrane sink conditions are given over the whole experiment. A direct comparison of dissolution data for Transwell® and Franz cell for the IPC membrane shows similar dissolution profiles for Budesonide and Substance A crystalline base. In contrast to the Franz cell the Transwell® system can discriminate between Substances A amorphous base and dibromide. In the PhD thesis it could be shown that for better soluble substance the rate determining step of dissolved substance is diffusion through the membrane (chapter 4.4). Therefore, the different hydrodynamics in Franz cell and Transwell® influence the dissolution process. In the Transwell® as well as in the paddle apparatus the stirring hydrodynamics enforces the diffusion process through the membrane. In the paddle apparatus / Transwell® the diffusion layer at the membrane is quite small, because convection of the dissolution medium is high. Hence, concentration gradient is higher and more dissolved substance can pass the membrane. In the Franz cell stirring is performed on the bottom of the vessel, hence difference between this movement and membrane is high, and the convection at the membrane low (compared to Transwell® system the dissolution medium amount is 260 fold increased the membrane surface only 6 folds). Consequently, diffusion layer of diffused substance is larger and concentration difference between the two membrane sides low. Thus, diffusion through the membrane is slower compared to paddle apparatus / Transwell® and the rate determining step in the Franz cell for good soluble substances.

As already described the paddle apparatus is a widely used dissolution technique for solid and semi solid dosage forms and found suitable for dissolution testing of powders for inhalation in this thesis.

Compared to the Transwell® system, in the paddle apparatus a large volume of dissolution medium is used. But the focus of the thesis is on a useful *in vitro* dissolution test and not on mimicking *in vivo* conditions. Therefore, the paddle apparatus is suitable because of good reproducibility and validity.

Table 5.1 summarizes the results of the comparison between the different used dissolution techniques depending on different criteria.

Table 5.1 In this table for each technique the most suitable set up is taken into account  
+ good, 0 middle, - poor

Dissolution medium without addition of surfactants, dissolution medium is stirred

Franz cell and Transwell® dissolution system: IPC membrane, paddle apparatus: RC membrane, mACI

	μDiss®	modified flow through cell	modified Franz cell	Transwell® dissolution system	paddle apparatus with membrane holder
handling	0	0	0	0	+
duration of experiment	+	+	0	0	+
amount of dissolution medium	+	+	-	+	-
reproducibility	+	-	+	+	+
discrimination power	0	-	0	+	0
validity	0	-	0	+	+

Consequently, referred to the above mentioned reasons for dissolution testing of inhalation powders flow through cell is not appropriate, Franz cell and μDiss with limitations, and Transwell® and paddle apparatus should be used.



# Chapter 6

## Summary and Outlook

*In vitro* dissolution testing of solid and semi-solid dosage forms is a reliable tool for quality control testing and prediction of *in vivo* drug release [20]. Currently, for the *Ad hoc* advisory panel of the USP there is no need for dissolution testing of powders for inhalation [13] but the development of new APIs tend to poorly soluble substances [15]. For bioavailability of substances it is necessary that the APIs dissolve in the limited volume of aqueous fluid in the lung [13,14]. For understanding of the *in vivo* processes *in vitro* tests are not necessary, but the *in vitro* dissolution tests could be used as a selection tool for drug substances and formulations and as quality test. Currently, some work was already done but the research results in this field have not progressed far enough yet.

The aims of the presented work were to evaluate the most suitable dissolution technique for aerodynamic classified powders, to point out important impact factors and to evaluate a theoretical model for predicting dissolution profiles of powders for inhalation. Therefore, five different dissolution systems were tested.

In this thesis, it could be demonstrated that dose collection method as well as the used membrane material plays an important role on the dissolution tests. The modified Andersen cascade impactor emerged as the only dose collection technique which ensures an almost mono layer and homogeneous particle distribution on the membrane. As dissolution techniques paddle apparatus with membrane holder and modified Transwell system were most suitable. Both set ups have advantages and disadvantages and a decision which technique should be used depends on the specific aim of the user. Furthermore, a suitable theoretical model was developed.

However, it should be emphasized that the here presented findings are just the beginning to a standardized dissolution technique for powders for inhalation. Nevertheless, this thesis revealed important impact factors on the dissolution process of inhalation powders. Yet, there are still open questions which need to be answered in the future:

- In the dissolution testing of solid and semi solid dosage forms biorelevant dissolution media are used. A further step in dissolution testing of powders for inhalation could be the use of broncho alveolar lining fluid (BALF) or simulated lung fluid especially in the Transwell® system
- The *in vitro* measured data should be compared to *in vivo* data and an *in vitro in vivo* correlation should be performed.
- Currently, the dissolution tests focus on *in vitro* tests. In the future there might be an advanced *in vitro* dissolution model with lung cell lines.

# Chapter 7

## Appendix

**HPLC Methods**

eluent A	buffer pH3 / acetonitrile (90/10 Vol%) degased 4,9g KH <sub>2</sub> PO <sub>4</sub> + 1800ml Wasser,pH3 mit H <sub>3</sub> PO <sub>4</sub> (16%) +180ml ACN,
eluent B	acetonitrile, degased
column	LiChrosphor 60 RP select B, 60x4 mm
column temperature	40°C
sample temperature	37°C
injection volume	10 µl
needle wash	acetonitrile/water (50/50)

**Budesonide**

Gradient	60% A    40% B
flow rate	1,7 ml min <sup>-1</sup>
UV detection	280 nm

**Fenoterol HBr**

Gradient	90% A    10% B
flow rate	1 ml min <sup>-1</sup>
UV detection	280 nm

**Substance A**

Gradient	65% A    35%B
flow rate	1 ml min <sup>-1</sup>
UV detection	226 nm

# Chapter 8

## List of bibliography

- [1] R.U. Agu and M.I. Ugwoke, In vitro and in vivo testing methods for respiratory drug delivery, *Expert Opinion on Drug Delivery*, 8 (2011) 57-69.
- [2] J.S. Patton and P.R. Byron, Inhaling medicines: delivering drugs to the body through the lungs, *Nature Reviews Drug Discovery*, 6 (2007) 67-74.
- [3] R.O. Salama, D. Traini, H.K. Chan, and P.M. Young, Preparation and characterisation of controlled release co-spray dried drug-polymer microparticles for inhalation 2: Evaluation of in vitro release profiling methodologies for controlled release respiratory aerosols, *European Journal of Pharmaceutics and Biopharmaceutics*, 70 (2008) 145-152.
- [4] C.A. Ruge, J. Kirch, and C.-M. Lehr, Pulmonary drug delivery: from generating aerosols to overcoming biological barriers - therapeutic possibilities and technological challenges, *The Lancet Respiratory Medicine*, 1 (2013) 402-413.
- [5] K. Aktories, U. Förtsermann, F.B. Hofmann, and K. Starke, *Allgemeine und spezielle Pharmakologie und Toxikologie*, Urban und Fischer Verlage, Elsevier GmbH, München, 2005.
- [6] A. Henning, M. Schneider, M. Bur, F. Blank, P. Gehr, and C.M. Lehr, Embryonic chicken trachea as a new in vitro model for the investigation of mucociliary particle clearance in the airways, *AAPS PharmSciTech*, 9 (2008) 521-527.
- [7] B. Forbes, B. Asgharian, L.A. Dailey, D. Ferguson, P. Gerde, M. Gumbleton, L. Gustavsson, C. Hardy, D. Hassall, R. Jones, R. Lock, J. Maas, T. McGovern, G.R. Pitcairn, G. Somers, and R.K. Wolff, Challenges in inhaled product development and opportunities for open innovation, *Advanced Drug Delivery Reviews*, 63 (2011) 69-87.
- [8] M. Bur, H. Huwer, L. Muys, and C.M. Lehr, Drug transport across pulmonary epithelial cell monolayers: Effects of particle size, apical liquid volume, and deposition technique, *Journal of Aerosol Medicine and Pulmonary Drug Delivery*, 23 (2010) 119-127.
- [9] United States Pharmacopeial Convention, Aerosol, nasal sprays, metered dose inhalers, and dry powder inhaler, *United States Pharmacopeia and National Formulary*, Vol. USP35, NF30. Maryland, 2012.
- [10] *European Pharmacopoeia 7.7* online, 2013.
- [11] J.S. Patton, J.D. Brain, L.A. Davies, J. Fiegel, M. Gumbleton, K.J. Kim, M. Sakagami, R. Vanbever, and C. Ehrhardt, The particle has landed-characterizing the fate of inhaled pharmaceuticals, *Journal of Aerosol Medicine and Pulmonary Drug Delivery*, 23 (2010) S71-S87.
- [12] C.I. Grainger, L.L. Greenwell, G.P. Martin, and B. Forbes, The permeability of large molecular weight solutes following particle delivery to air-interfaced cells that model the respiratory mucosa, *European Journal of Pharmaceutics and Biopharmaceutics*, 71 (2009) 318-324.
- [13] V.A. Gray, A.J. Hickey, P. Balmer, N.M. Davies, C. Dunbar, T.S. Foster, B.L. Olsson, M. Sakagami, V.P. Shah, M.J. Smurthwaite, J.M. Veranth, and K. Zaidi, The Inhalation Ad Hoc Advisory Panel for the USP performance tests of inhalation dosage forms, *Pharmacopeial Forum*, 34 (2008) 1068-1074.
- [14] A. Henning, M. Schneider, N. Nafee, L. Muijs, E. Rytting, X. Wang, T. Kissel, D. Grafahrend, D. Klee, and C.M. Lehr, Influence of particle size and material properties on mucociliary clearance from the airways, *Journal of Aerosol Medicine and Pulmonary Drug Delivery*, 23 (2010) 233-241.
- [15] H.I. Labouta and M. Schneider, Tailor-made biofunctionalized nanoparticles using layer-by-layer technology, *International Journal of Pharmaceutics*, 395 (2010) 236-242.
- [16] C. Duret, N. Wauthoz, T. Sebti, F. Vanderbist, and K. Amighi, Solid dispersions of itraconazole for inhalation with enhanced dissolution, solubility and dispersion properties, *International Journal of Pharmaceutics*, 428 (2012) 103-113.
- [17] N. Wauthoz, P. Deleuze, A. Saumet, C. Duret, R. Kiss, and K. Amighi, Te-mozolomide-based dry powder formulations for lung tumor-related inhalation treatment, *Pharmaceutical Research*, 28 (2011) 762-775.

- [18] J.T. McConville, N. Patel, N. Ditchburn, M.J. Tobyn, J.N. Staniforth, and P. Woodcock, Use of a novel modified TSI for the evaluation of controlled-release aerosol formulations. I, *Drug Development and Industrial Pharmacy*, 26 (2000) 1191-1198.
- [19] N.M. Davies and M.R. Feddah, A novel method for assessing dissolution of aerosol inhaler products, *International Journal of Pharmaceutics*, 255 (2003) 175-187.
- [20] T. Riley, D. Christopher, J. Arp, A. Casazza, A. Colombani, A. Cooper, M. Dey, J. Maas, J. Mitchell, M. Reiners, N. Sigari, T. Tougas, and S. Lyapustina, Challenges with Developing In Vitro Dissolution Tests for Orally Inhaled Products (OIPs), *AAPS PharmSciTech*, 13 (2012) 978-989.
- [21] Food and Drug Administration, Guidance for Industry; Dissolution Testing of Immediate Release Solid Oral Dosage Forms, online, (1997).
- [22] J. Wang and D.R. Flanagan, General solution for diffusion-controlled dissolution of spherical particles. 2. Evaluation of experimental data, *Journal of Pharmaceutical Sciences*, 91 (2002) 534-542.
- [23] C.K. Brown, H.D. Friedel, A.R. Barker, L.F. Buhse, S. Keitel, T.L. Cecil, J. Kraemer, J.M. Morries, C. Reppas, M.P. Stickelmeyer, C. Yomota, and V.P. Shah, FIP / AAPS Joint Workshop Report: Dissolution / In Vitro Release Testing of Novel / Special Dosage Forms, *AAPS PharmSciTech*, 12 (2011) 782-794.
- [24] G. Thews, E. Mutschler, and P. Vaupel, *Anatomie, Physiologie, Pathophysiologie des Menschen*, Wissenschaftliche Verlagsgesellschaft, Stuttgart, 2007.
- [25] W.C. Hinds, *Aerosol technology: properties, behaviour, and measurement of airborne particles*, John Wiley & Sons Inc., 1999.
- [26] J. Todoroff and R. Vanbever, Fate of nanomedicines in the lung, *Current Opinion in Colloid and Interface Science*, 16 (2011) 246-254.
- [27] M. Sakagami, In vivo, in vitro and ex vivo models to assess pulmonary absorption and disposition of inhaled therapeutics for systemic delivery, *Advanced Drug Delivery Reviews*, 58 (2006) 1030-1060.
- [28] B. Forbes, Human airway epithelial cell lines for in vitro drug transport and metabolism studies, *Pharmaceutical Science and Technology Today*, 3 (2000) 18-27.
- [29] H. Fischer and J.H. Widdicombe, Mechanisms of acid and base secretion by the airway epithelium, *Journal of Membrane Biology*, 211 (2006) 139-150.
- [30] A.W. Ng, A. Bidani, and T.A. Heming, Innate host defense of the lung: Effects of lung-lining fluid pH, *Lung*, 182 (2004) 297-317.
- [31] R. Voigt, *Pharmazeutische Technologie*, Deutscher Apotheker Verlag, Stuttgart, 2006.
- [32] D. Köhler and W. Fleischer, *Theorie und Praxis der Inhalationstherapie*, Acris Verlag GmbH, München, 2000.
- [33] A.A. Andersen, New sampler for the collection, sizing, and enumeration of viable airborne particles, *Journal of Bacteriology*, 76 (1958) 471-481.
- [34] C. Weiler. Generierung leicht dispergierbarer Inhalationspulver mittels Sprühtrocknung. 2008. Johannes Gutenberg Universität.  
Ref Type: Thesis/Dissertation
- [35] Langguth, Fricker, and Wunderli-Allenspach, *Biopharmazie*, Wiley-VCH, Weinheim, 2004.
- [36] C.A. Ruge, U.F. Schaefer, J. Herrmann, J. Kirch, O. Canadas, M. Echaide, J. Perez-Gil, C. Casals, R. Müller, and C.M. Lehr, The interplay of lung surfactant proteins and lipids assimilates the macrophage clearance of nanoparticles, *PLoS ONE*, 7 (2012).
- [37] J. Kirch, M. Guenther, N. Doshi, U.F. Schaefer, M. Schneider, S. Mitragotri, and C.M. Lehr, Mucociliary clearance of micro- and nanoparticles is independent of size, shape and charge-an ex vivo and in silico approach, *Journal of Controlled Release*, 159 (2012) 128-134.
- [38] J. Kirch, M. Guenther, U.F. Schaefer, M. Schneider, and C.M. Lehr. Computational fluid dynamics of nanoparticle disposition in the airways: mucus interactions and mucociliary clearance. *Computing and Visualization in Science*. 2012.  
Ref Type: In Press

- [39] J. Kirch, A. Schneider, B. Abou, A. Hopf, U.F. Schaefer, M. Schneider, C. Schall, C. Wagner, and C.M. Lehr, Optical tweezers reveal relationship between microstructure and nanoparticle penetration of pulmonary mucus, *Proceedings of the National Academy of Sciences of the United States of America*, 109 (2012) 18355-18360.
- [40] P. Gehr, V. Im Hof, M. Geiser, and S. Schürch, The mucociliary transport system of the lungs and the role of surfactant, *Schweizerische Medizinische Wochenschrift*, 130 (2000) 691-698.
- [41] C.A. Ruge, J. Kirch, O. Canadas, M. Schneider, J. Perez-Gil, U.F. Schaefer, C. Casals, and C.M. Lehr, Uptake of nanoparticles by alveolar macrophages is triggered by surfactant protein A, *Nanomedicine: Nanotechnology, Biology, and Medicine*, 7 (2011) 690-693.
- [42] S. Schurch, P. Gehr, V. Im Hof, M. Geiser, and F. Green, Surfactant displaces particles toward the epithelium in airways and alveoli, *Respiration Physiology*, 80 (1990) 17-32.
- [43] International Agency for Research on Cancer. Asbestos (chrysotile, amosite, crocidolite, tremolite, actinolite and anthophyllite). <http://monographs.iarc.fr/ENG/Monographs/vol100C/mono100C-11.pdf> . 2013.  
Ref Type: Electronic Citation
- [44] Pharmaceutical Dissolution Testing, Informa Healthcare USA, 2009.
- [45] J. Wang and D.R. Flanagan, General solution for diffusion-controlled dissolution of spherical particles. 1. Theory, *Journal of Pharmaceutical Sciences*, 88 (1999) 731-738.
- [46] A. Dokoumetzidis and P. Macheras, A century of dissolution research: From Noyes and Whitney to the Biopharmaceutics Classification System, *International Journal of Pharmaceutics*, 321 (2006) 1-11.
- [47] T. Riley, A. Jones, M. Bogalo Huescar, and T. Roche, In Vitro Method for Determining the Dissolution Rate of Inhaled Aerosols, *Respiratory Drug Delivery*, 2008, pp. 541-544.
- [48] R.O. Cook, R.K. Pannu, and I.W. Kellaway, Novel sustained release microspheres for pulmonary drug delivery, *Journal of Controlled Release*, 104 (2005) 79-90.
- [49] M. Asada, H. Takahashi, H. Okamoto, H. Tanino, and K. Danjo, Theophylline particle design using chitosan by the spray drying, *International Journal of Pharmaceutics*, 270 (2004) 167-174.
- [50] S. Jaspert, P. Bertholet, G. Piel, J.M. Dogné, L. Delattre, and B. Evrard, Solid lipid microparticles as a sustained release system for pulmonary drug delivery, *European Journal of Pharmaceutics and Biopharmaceutics*, 65 (2007) 47-56.
- [51] T.P. Learoyd, J.L. Burrows, E. French, and P.C. Seville, Chitosan-based spray-dried respirable powders for sustained delivery of terbutaline sulfate, *European Journal of Pharmaceutics and Biopharmaceutics*, 68 (2008) 224-234.
- [52] J. Raula, A. Rahikkala, T. Halkola, J. Pessi, L. Peltonen, J. Hirvonen, K. Järvinen, T. Laaksonen, and E.I. Kauppinen, Coated particle assemblies for the concomitant pulmonary administration of budesonide and salbutamol sulphate, *International Journal of Pharmaceutics*, 441 (2013) 248-254.
- [53] J. Siepmann and N.A. Peppas, Higuchi equation: Derivation, applications, use and misuse, *International Journal of Pharmaceutics*, 418 (2011) 6-12.
- [54] Y.J. Son and J.T. McConville, Development of a standardized dissolution test method for inhaled pharmaceutical formulations, *International Journal of Pharmaceutics*, 382 (2009) 15-22.
- [55] Y.J. Son, M. Horng, M. Copley, and J.T. McConville, Optimization of an in vitro dissolution test method for inhalation formulations, *Dissolution Technologies*, 17 (2010) 6-13.
- [56] G. Pilcer, R. Rosière, K. Traina, T. Sebti, F. Vanderbist, and K. Amighi, New co-spray-dried tobramycin nanoparticles-clarithromycin inhaled powder systems for lung infection therapy in cystic fibrosis patients, *Journal of Pharmaceutical Sciences*, 102 (2013) 1836-1846.

- [57] C. Duret, N. Wauthoz, T. Sebti, F. Vanderbist, and K. Amighi, New respirable and fast dissolving itraconazole dry powder composition for the treatment of invasive pulmonary aspergillosis, *Pharmaceutical Research*, 29 (2012) 2845-2859.
- [58] J. Mees, C. Fulton, S. Wilson, N. Bramwell, M. Lucius, and A. Cooper. Development of Dissolution Methodology for Dry Powder Inhalation Aerosols. IPAC-RS 2011 Conference, Bethesda, MD . 2011.  
Ref Type: Abstract
- [59] Y.J. Son and J.T. McConville, Development of a Standardized Dissolution Test for Inhalable Formulations, 2008.
- [60] United States Pharmacopeial Convention, Dissolution, United States Pharmacopeia and National Formulary, Vol. USP 36; NF 31. Rockville, 2013.
- [61] D. Arora, K.A. Shah, M.S. Halquist, and M. Sakagami, In Vitro aqueous fluid-capacity-limited dissolution testing of respirable aerosol drug particles generated from inhaler products, *Pharmaceutical Research*, 27 (2010) 786-795.
- [62] S. Bhagwat, M. Rohrschneider, S. Alfadahl, and G. Hochhaus. Development of an in vitro test method for dissolution of inhaled corticosteroids. ISAM Conference . 2013.  
Ref Type: Abstract
- [63] M. Sakagami and D. Arora Lakhani, Understanding Dissolution in the Presence of competing cellular uptake and absorption in the airways, Dalby, R.N.; Byron, P.R.; Peart, J.; Suman, J.D.; Farr, S.J.; Young, P.M, 2012, pp. 185-192.
- [64] M. Haghi, D. Traini, M. Bebawy, and P.M. Young, Deposition, diffusion and transport mechanism of dry powder microparticulate salbutamol, at the respiratory epithelia, *Molecular Pharmaceutics*, 9 (2012) 1717-1726.
- [65] United States Pharmacopeial Convention, The dissolution procedure: development and validation, United States Pharmacopeia and National Formulary, Vol. USP 34; NF 29. Rockville, 2011.
- [66] Hunnius Pharmazeutisches Wörterbuch, Walter de Gruyter, 2004.
- [67] E. Mutschler, G. Geisslinger, H.K. Kroemer, and M. Schäfer-Korting, Mutschler Arzneimittelwirkung, Wissenschaftliche Verlagsgesellschaft, Stuttgart, 2001.
- [68] Klinische Pharmakologie, Thieme, 2005.
- [69] R. Buhl, D. Berdel, C.P. Criée, A. Gillissen, P. Kardos, C. Kroegel, W. Leupold, H. Lindemann, H. Magnussen, D. Nowak, D. Pfeiffer-Kascha, K. Rabe, M. Rolke, C. Schultze-Werninghaus, H. Sitter, D. Ukena, C. Vogelmeier, T. Welte, R. Wettengel, and H. Worth, Guidelines for diagnosis and treatment of asthma patients. German Airway League and German Respiratory Society, *Pneumologie*, 60 (2006) 139-177.
- [70] Römpp Lexikon der Chemie. <http://www.roempp.com/prod/> [3.29]. 2012. Thieme Verlag online Version. 25-2-2013.  
Ref Type: Electronic Citation
- [71] H. Petersen, A. Kullberg, S. Edsbäcker, and L. Greiff, Nasal retention of budesonide and fluticasone in man: Formation of airway mucosal budesonide-esters in vivo, *British Journal of Clinical Pharmacology*, 51 (2001) 159-163.
- [72] F. Yoshida and J.G. Topliss, QSAR model for drug human oral bioavailability, *Journal of Medicinal Chemistry*, 43 (2000) 2575-2585.
- [73] R. Veldhuizen, K. Nag, S. Orgeig, and F. Possmayer, The role of lipids in pulmonary surfactant, *Biochimica et Biophysica Acta - Molecular Basis of Disease*, 1408 (1998) 90-108.
- [74] Sigma Aldrich Online Katalog. [www.sigmaaldrich.com](http://www.sigmaaldrich.com) . 26-2-2013.  
Ref Type: Electronic Citation
- [75] Inactive Ingredient Search for Approved Drug Products.  
<http://www.accessdata.fda.gov/scripts/cder/iig/getiigWEB.cfm> . 2013. 11-6-2013.  
Ref Type: Electronic Citation
- [76] Technical Resource: Remove detergent from protein samples. Pierce.  
[http://www.fishersci.ca/uploadedFiles/Whats\\_New/pierce\\_detergent.pdf](http://www.fishersci.ca/uploadedFiles/Whats_New/pierce_detergent.pdf) . 2013.  
Ref Type: Electronic Citation
- [77] Product Information Avanti.  
[http://avantilipids.com/index.php?option=com\\_content&view=article&id=216&Itemid=](http://avantilipids.com/index.php?option=com_content&view=article&id=216&Itemid=)

- 206&catnumber=850355 . 26-2-2013. Avanti Polar Lipids.  
Ref Type: Electronic Citation
- [78] International Conference on Harmonisation of Technical Requirements for Registration of Pharmaceuticals for Human Use (ICH). Validation of analytical procedures: Text and Methodology Q2(R1).  
<http://www.ich.org/products/guidelines/quality/article/quality-guidelines.html> . 2013. 21-2-2013.  
Ref Type: Electronic Citation
- [79] Encyclopaedia Britannica, 2013.
- [80] G.L. Amidon, H. Lennernas, V.P. Shah, and J.R. Crison, A theoretical basis for a biopharmaceutical drug classification: The correlation of in vitro drug product dissolution and in vivo bioavailability, *Pharmaceutical Research*, 12 (1995) 413-420.
- [81] A. Avdeef and O. Tsinman, Miniaturized rotating disk intrinsic dissolution rate measurement: Effects of buffer capacity in comparisons to traditional wood's apparatus, *Pharmaceutical Research*, 25 (2008) 2613-2627.
- [82] C. Wähling, W. Seeger, and A. Hanefeld, Flow-through cell method and IVIVR for poorly soluble drugs, *Dissolution Technologies*, 18 (2011) 15-25.
- [83] A. Jouyban, *Handbook of Solubility Data for Pharmaceuticals*, CRC Press, Taylor and Francis Group, 2010.
- [84] P.F. Schmidt, *Praxis der Rasterelektronenmikroskopie und Mikroberichtsanalyse*, expert verlag, Renningen-Malmsheim, 1994.
- [85] J. Goldstein, D. Newbury, D. Joy, C. Lyman, P. Echlin, E. Lifshin, L. Sawyer, and J. Michael, *Scanning Electron Microscopy and X-Ray Microanalysis*, Kluwer Academic / Plenum Publishers, New York, 2003.
- [86] C.M. Keck and R.H. Müller, *Moderne Pharmazeutische Technologie*, Online, 2009.
- [87] Y. Mori, H. Yoshida, and H. Masuda, Characterization of reference particles of transparent glass by laser diffraction method, *Particle and Particle Systems Characterization*, 24 (2007) 91-96.
- [88] Sympatec laser diffraction: Overview and Concept.  
<http://www.sympatec.com/DE/LaserDiffraction/LaserDiffraction.html> . 9-7-2012.  
Ref Type: Electronic Citation
- [89] Statische Laserlichtstreuung. <http://www.retsch-technology.de/de/rt/applikationen/technische-grundlagen/statische-laserlichtstreuung/> . 11-7-2012.  
Ref Type: Electronic Citation
- [90] S.C. Nichols, Calibration and mensuration issues for the standard and modified andersen cascade impactor, *Pharmacopeial Forum*, 26 (2000) 1466-1467.
- [91] K.H. Bauer, K.-H. Frömming, and C. Führer, *Lehrbuch der Pharmazeutischen Technologie*, Wissenschaftliche Verlagsgesellschaft, Stuttgart, 2006.
- [92] *Handbook of surface and colloid chemistry*, CRC Press, New York, 1997.
- [93] E.L. Decker, B. Frank, Y. Suo, and S. Garoff, Physics of contact angle measurement, *Colloids and Surfaces A: Physicochemical and Engineering Aspects*, 156 (1999) 177-189.
- [94] G. Brezesinski and H.-J. Mögel, *Grenzflächen und Kolloide, physikalisch - chemische Grundlagen*, Spektrum akademischer Verlag, Heidelberg, 1993.
- [95] D.Y. Kwok and A.W. Neumann, Contact angle measurement and contact angle interpretation, *Advances in Colloid and Interface Science*, 81 (1999) 167-249.
- [96] T. Young, An Essay on the Cohesion of Fluids, *Philosophical Transactions of the Royal Society of London*, (1805) 65-87.
- [97] A. Avdeef, K. Tsinman, O. Tsinman, N. Sun, and D. Voloboy, Miniaturization of powder dissolution measurement and estimation of particle size, *Chemistry and Biodiversity*, 6 (2009) 1796-1811.
- [98] K. Tsinman, A. Avdeef, O. Tsinman, and D. Voloboy, Powder dissolution method for estimating rotating disk intrinsic dissolution rates of low solubility drugs, *Pharmaceutical Research*, 26 (2009) 2093-2100.

- [99] K.C. Bynum and E. Kraft, A new technique in dissolution testing, *Pharmaceutical Technology*, 23 (1999) 42-44.
- [100] I. Nir, B.D. Johnson, J. Johansson, and C. Schatz, Application of fiber-optic dissolution testing for actual products, *Pharmaceutical Technology North America*, 25 (2001) 33-40.
- [101] K.C. Bynum, K. Roinestad, A. Kassis, J. Pocreva, L. Gehrlein, F. Cheng, and P. Palermo, Analytical Performance of a fiber optic probe dissolution system, *Dissolution Technologies*, 8 (2001).
- [102] X. Lu, R. Lozano, and P. Shah, In-situ dissolution testing using different UV-fiber optic probes and instruments, *Dissolution Technologies*, 10 (2003).
- [103] L. Liu, G. Fitzgerald, M. Embry, R. Cantu, and B. Pack, Technical Evaluation of a fiber-optic probe dissolution system, *Dissolution Technologies*, 15 (2008).
- [104] B. Jensen, M. Reiners, M. Wolkenhauer, P. Ritzheim, S. May, M. Schneider, and C.-M. Lehr, *Dissolution Testing for Inhaled Products*, 2011, pp. 303-308.
- [105] F. Langenbucher, D. Benz, W. Kürth, H. Möller, and M. Otz, Standardized Flow-cell Method as an Alternative to Existing Pharmacopoeial Dissolution Testing, *Pharmaceutical Industrie*, 51 (1989) 1276-1281.
- [106] J.W. Eaton, D. Tran, W.W. Hauck, and E.S. Stippler, Development of a Performance Verification Test for USP Apparatus 4, *Pharmaceutical Research*, 29 (2012) 345-351.
- [107] United States Pharmacopeial Convention, *Dissolution, United States Pharmacopeia and National Formulary, Vol. USP 34; NF 29*. Rockville, 2011.
- [108] N. Fotaki, Flow-through cell apparatus (USP Apparatus 4): Operation and features, *Dissolution Technologies*, 18 (2011) 46-49.
- [109] E.S. Stippler, Review of research paper: Development of a performance verification test for USP apparatus 4, *Dissolution Technologies*, 18 (2011) 44.
- [110] S.N. Bhattachar, J.A. Wesley, A. Fioritto, P.J. Martin, and S.R. Babu, Dissolution testing of a poorly soluble compound using the flow-through cell dissolution apparatus, *International Journal of Pharmaceutics*, 236 (2002) 135-143.
- [111] T.J. Franz, Percutaneous absorption. On the relevance of in vitro data, *Journal of Investigative Dermatology*, 64 (1975) 190-195.
- [112] Food and Drug Administration, *Guidance for Industry; nonsterile semisolid dosage forms*, online, (1997).
- [113] A. Melero, T.M. Garrigues, M. Alós, K.H. Kostka, C.M. Lehr, and U.F. Schaefer, Nortriptyline for smoking cessation: Release and human skin diffusion from patches, *International Journal of Pharmaceutics*, 378 (2009) 101-107.
- [114] S.-F. Ng, J.J. Rouse, F.D. Sanderson, V. Meidan, and G.M. Eccleston, Validation of a Static Franz Diffusion Cell System for in vitro Permeation Studies, *AAPS PharmSciTech*, 11 (2010) 1432-1441.
- [115] V.P. Shah, S.W. Shaw, D.D. Norton, J. Elkins, G. Deng, Eaton.J., J. Hajoay, S. Nie, and J. Wang, In vitro release: Collaborative Study Using the Vertical Diffusion Cell, *Pharmacopeial Forum*, 32 (2006) 1590-1596.
- [116] S.C. Chattaraj, J. Swarbrick, and I. Kanfer, A simple diffusion cell to monitor drug release from semi-solid dosage forms, *International Journal of Pharmaceutics*, 120 (1995) 119-124.
- [117] P.M. Young, D. Traini, and R. Salama, In vitro Techniques equipées to study clinically relevant controlled release products, *Respiratory Drug Delivery Europe*, (2011) 79-88.
- [118] H. Adi, P.M. Young, H.K. Chan, R. Salama, and D. Traini, Controlled release antibiotics for dry powder lung delivery, *Drug Development and Industrial Pharmacy*, 36 (2010) 119-126.
- [119] R. Cartier and M. Krüger. Nano-Carrier mit zeitlich und örtlich gesteuerter Freisetzung von Wirkstoffen zur Inhalation, Akronym: Nanolnhale: Abschlussbericht. Boehringer Ingelheim, Technische Informationsbibliothek und Universitätsbibliothek . 2009. Ref Type: Electronic Citation
- [120] European Medicines Agency, *Guideline on the investigation of bioequivalence*, online, (2008).

- [121] United States Pharmacopeial Convention, Drug release, United States Pharmacopeia and National Formulary, Vol. USP 36, NF 31. Rockville, 2013.
- [122] Quality solutions for Inhaler Testing Edition 2012.  
<http://www.copleyscientific.com/editorials.asp?d=11> , 77. 19-6-2013.  
Ref Type: Electronic Citation
- [123] B.I. Zentrale Mechaniker Werkstatt. Technische Zeichnung. 2011.  
Ref Type: Data File
- [124] A.T.K. Lu, M.E. Frisella, and K.C. Johnson, Dissolution modeling: Factors affecting the dissolution rates of polydisperse powders, *Pharmaceutical Research*, 10 (1993) 1308-1314.
- [125] G. Sertsou, Analytical derivation of time required for dissolution of monodisperse drug particles, *Journal of Pharmaceutical Sciences*, 93 (2004) 1941-1944.
- [126] P. Lansky and M. Weiss, Does the dose-solubility ratio affect the mean dissolution time of drugs?, *Pharmaceutical Research*, 16 (1999) 1470-1476.
- [127] A. Dokoumetzidis, V. Papadopoulou, and P. Macheras, Analysis of dissolution data using modified versions of Noyes-Whitney equation and the Weibull function, *Pharmaceutical Research*, 23 (2006) 256-261.
- [128] A. Okazaki, T. Mano, and K. Sugano, Theoretical dissolution model of poly-disperse drug particles in biorelevant media, *Journal of Pharmaceutical Sciences*, 97 (2008) 1843-1852.
- [129] J.J. Sheng, P.J. Sirois, J.B. Dressman, and G.L. Amidon, Particle diffusional layer thickness in a USP dissolution apparatus II: a combined function of particle size and paddle speed, *J. Pharm. Sci.*, 97 (2008) 4815-4829.
- [130] W.-L. Hsu, M.-J. Lin, and J.-P. Hsu, Dissolution of Solid Particle in Liquids: A Shrinking Core Model, *World Academy of Science, Engineering and Technology*, 53 (2009) 913-918.
- [131] S. May, B. Jensen, M. Wolkenhauer, M. Schneider, and C.M. Lehr, Dissolution Techniques for In Vitro Testing of Dry Powders for Inhalation, *Pharmaceutical Research*, 29 (2012) 2157-2166.
- [132] W. Hayduk and H. Laudie, Prediction of diffusion coefficients for nonelectrolytes in dilute aqueous solutions, *AIChE*, 20 (1974) 611-615.
- [133] M. Bisrat and C. Nystrom, Physicochemical aspects of drug release. VIII. The relation between particle size and surface specific dissolution rate in agitated suspensions, *International Journal of Pharmaceutics*, 47 (1988) 223-231.
- [134] R.J. Hintz and K.C. Johnson, The effect of particle size distribution on dissolution rate and oral absorption, *International Journal of Pharmaceutics*, 51 (1989) 9-17.
- [135] K. Sugano, Theoretical comparison of hydrodynamic diffusion layer models used for dissolution simulation in drug discovery and development, *International Journal of Pharmaceutics*, 363 (2008) 73-77.
- [136] C.N. Davies, Particle-fluid interaction, *Journal of Aerosol Science*, 10 (1979) 477-513.
- [137] <http://www.guidechem.com/dictionary/de/51333-22-3.html> . 2013.  
Ref Type: Electronic Citation
- [138] J.C. Butcher, S. Garg, D. Kim, and P. Sharma, A modified approach to predict dissolution and absorption of polydisperse powders, *Pharmaceutical Research*, 25 (2008) 2309-2311.
- [139] F.O. Costa, J.J.S. Sousa, A.A.C.C. Pais, and S.J. Formosinho, Comparison of dissolution profiles of Ibuprofen pellets, *Journal of Controlled Release*, 89 (2003) 199-212.
- [140] J.E. Polli, G.S. Rekhi, L.L. Augsburger, and V.P. Shah, Methods to compare dissolution profiles and a rationale for wide dissolution specifications for metoprolol tartrate tablets, *Journal of Pharmaceutical Sciences*, 86 (1997) 690-700.
- [141] I.M. Helbling, J.C.D. Ibarra, and J.A. Luna, Application of the Refined Integral Method in the mathematical modeling of drug delivery from one-layer torus-shaped devices, *International Journal of Pharmaceutics*, 423 (2012) 240-246.
- [142] J.W. Moore and H.H. Flanner, Mathematical Comparison of Dissolution Profiles, *Pharmaceutical Technology*, 20 (1996) 64-74.

- [143] J.H. Duan, K. Riviere, and P. Marroum, In Vivo Bioequivalence and in Vitro Similarity Factor ( $f_2$ ) for Dissolution Profile Comparisons of Extended Release Formulations: How and When do they match?, *Pharmaceutical Research*, 28 (2011) 1144-1156.
- [144] J.D. Gomez-Mantilla, V.G. Casabo, U.F. Schaefer, and C.M. Lehr, Permutation Test (PT) and Tolerated Difference Test (TDT): Two new, robust and powerful nonparametric tests for statistical comparison of dissolution profiles, *International Journal of Pharmaceutics*, 441 (2013) 458-467.
- [145] gravitational settling. <https://sakai.unc.edu/access/content/group/e64cd41d-8ddd-4001-aca7-356227cd8a54/public/001/Settling.pdf> . 2013.  
Ref Type: Electronic Citation
- [146] X.M. Zeng, G.P. Martin, and C. Marriott, *Particulate interactions in dry powder formulations for inhalation*, Taylor and Francis, London, 2001.
- [147] A. Barth, *Physik, Kurzlehrbuch und Prüfungsfragen für Pharmazeuten*, Deutscher Apotheker Verlag, Stuttgart, 2005.
- [148] Corning Cell Culture Surface.  
[http://www.corning.com/lifesciences/us\\_canada/en/technical\\_resources/surfaces/culture/stc\\_treated\\_polystyrene.aspx](http://www.corning.com/lifesciences/us_canada/en/technical_resources/surfaces/culture/stc_treated_polystyrene.aspx) . 10-4-0013.  
Ref Type: Electronic Citation
- [149] S. Hein, M. Bur, U.F. Schaefer, and C.M. Lehr, A new Pharmaceutical Aerosol Deposition Device on Cell Cultures (PADD OCC) to evaluate pulmonary drug absorption for metered dose dry powder formulations, *European Journal of Pharmaceutics and Biopharmaceutics*, 77 (2011) 132-138.



## **Scientific output**

The research of this PhD thesis has led to the following publications:

### **Publications:**

**May S.**, Jensen B., Wolkenhauer M., Schneider M., Lehr C.-M. (2012): Dissolution Techniques for *In Vitro* Testing of Dry Powders for Inhalation, *Pharmaceutical Research*, 29, 2157-2166

**May S.**, Kind, S., Jensen B., Wolkenhauer M., Schneider M., Lehr C.-M. (2013): *In vitro* dissolution testing of powder for inhalation in miniature, in preparation

**May S.**, Jensen B., Weiler, C., Wolkenhauer M., Schneider M., Lehr C.-M. (2013): Influence of Particle Deposition and Modeling of Dissolution Profiles, in preparation

### **Conference proceeding:**

- 12/2013      Drug Delivery to the Lungs 24, Edinburgh, Scotland, United Kingdom  
                  “*In vitro* Dissolution Techniques for Inhalation Powders” submitted
- 05/2013      Respiratory Drug Delivery Europe, Berlin, Germany  
                  “Impact of Deposition and the Presence of Surfactants on *In Vitro* Dissolution of Inhalation Powders”
- 05/2012      Respiratory Drug Delivery, Phoenix, Arizona, U.S.A.  
                  “Comparison of two dissolution tests for inhaled products”

### **Poster presentation:**

- 07/2013      40<sup>th</sup> Annual Meeting and Exposition of the Controlled Release Society, Honolulu, Hawaii, U.S.A.  
                  “Quo vadis Dissolution Testing for Inhalation Powders?”
- 03/2012      Controlled Release Society Germany Local Chapter, Würzburg, Germany  
                  “Franz diffusion cell set up for powder dissolution profiles”
- 03/2012      9<sup>th</sup> International Conference and Workshop on Biological Barriers – *in vitro* Tools, Nanotoxicology, and Nanomedicine, Saarbrücken, Germany  
                  “Testing of fine particles in Franz diffusion cell”

### **Invited lecture:**

- 12/2013      JPAG mini – symposium at DDL 24, Edinburgh, Scotland, United Kingdom  
                  “*In vitro* Dissolution Techniques for Inhalation Powders”

## **Curriculum vitae**

### **Personal Information**

Name	Sabine Erika May
Date of birth	May, 9 <sup>th</sup> 1985
Place of birth	Koblenz
Nationality	German

### **Doctoral Thesis**

10/2010 – 09/2013	PharmBio Tec GmbH, Saarland University, Saarbrücken experiments performed at Boehringer Ingelheim Pharma GmbH & Co KG, Ingelheim
-------------------	--

### **Undergraduate Study**

05/2010	Certification as pharmacist
10/2004 – 04/2009	Pharmaceutical studies, Johannes Gutenberg University, Mainz

### **Internships and practical experiences**

09/2012	Workshop: project management for the pharmaceutical industry, ETH Zürich (Switzerland)
06/2010 – 08/2010	Pharmacist, Mercator Apotheke, Mainz
11/2009 – 04/2010	Practical Training for pharmacists, Mercator Apotheke, Mainz
05/2009 – 10/2009	Practical Training for pharmacists, Boehringer Ingelheim Pharma GmbH & Co KG, Ingelheim
06/2008	Research internship Department of Pharmacology and Toxicology, Johannes Gutenberg University, Mainz Supervisor: Prof. Bernd Epe
03/2008	Research internship Department of Pharmacology and Toxicology, Johannes Gutenberg University, Mainz Supervisor: Prof. Bernd Epe

## **Acknowledgements**

An erster Stelle bedanke ich mich bei dem Unternehmen Boehringer Ingelheim Pharma GmbH & Co. KG, das mir die Doktorarbeit ermöglicht hat.

Meinem Doktorvater Prof. Dr. Claus-Michael Lehr danke ich herzlich für die gute Betreuung, die Förderung und Unterstützung meine Ergebnisse auf nationalen und internationalen Tagungen präsentieren zu dürfen. Auch wenn ich als externer Doktorand nicht immer vor Ort war, hatte er stets ein offenes Ohr für mich.

Dr. Birte Jensen (Boehringer) und Prof. Dr. Marc Schneider (Uni Saarbrücken), meinen Betreuern im wissenschaftlichen Alltag, danke ich für die Diskussionsbereitschaft und Unterstützung bei Fragen aller Art. Beide waren für meine wissenschaftlichen und organisatorischen Anliegen offen und haben stets versucht, anstehende Probleme schnellstmöglich zu klären.

Dr. Markus Wolkenhauer danke ich für die unzähligen konstruktiven Diskussionen über das Verhalten von Partikeln, seine wertvollen Hinweise, wie ich meine Präsentationen verbessern konnte, die Unterstützung bei allem, was mit Programmiersprachen zu tun hat und der mathematischen Überprüfung des Dissolutionmodells.

Dr. Claudius Weiler danke ich für die Idee, das Thema Dissolution auch einmal mehr von der theoretischen Seite zu betrachten und der Unterstützung bei den ersten Gehversuchen.

Meinen Kollegen bei Boehringer Ingelheim, insbesondere dem A8 und dem A4, danke ich für den Blick über den Dissolution - Tellerrand, die Einarbeitung in alle relevanten Techniken und die freundschaftliche Atmosphäre. Danke sage ich auch meiner Pharmaziepraktikantin Saskia Kind, die einen Großteil der Transwellversuche während ihres Praktikums durchgeführt hat.

Folgenden Kollegen möchte ich für die Unterstützung bei der ein oder anderen Messung danken: Susanne Bröder ( $\mu$ Diss), Nicole Feuerbach (Durchflusszelle), Mathias Munz (Laserdiffraktometrie), Michelle Seckler (Franz Zelle, ACI), den Laboren Dr. Holger Wagner und Dr. Peter Häbel (Berechnung der van der Waals Volumina).

Danke sage ich auch der zentralen Mechaniker Werkstatt, vor allem Rene Blass für die Umsetzung und den Bau meiner Ideen und der zentralen Elektroniker Werkstatt, insbesondere

Michael Bauß und Hubert Winkler, die spontan das eine oder andere Problem beheben konnten und auch Sonderwünsche angefertigt haben.

Wolfgang Bootz und Dr. Bernhard Meier danke ich für die Aufnahmen mit dem Rasterelektronenmikroskop und der Hilfe bei der Interpretation.

Des Weiteren bedanke ich mich bei Dr. Bettina Berner, Dr. Holger Memmesheimer, Dr. Maria Reiners, Dr. Marc Rohrschneider und Dr. Jörg Schiewe für die angeregten Diskussionen.

Ein Dank gilt auch meinen Freunden, die während der vergangenen 3 Jahre für die nötige Abwechslung vom wissenschaftlichen Alltag gesorgt haben.

Und last but not least danke ich meinen Eltern herzlich für die bedingungslose Unterstützung während meines Studiums und meiner Dissertation.